1972

Computerized enhancement of ultrasonic echograms

Charles Raymond Meyer
Iowa State University

INFORMATION TO USERS

This dissertation was produced from a microfilm copy of the original document. While the most advanced technological means to photograph and reproduce this document have been used, the quality is heavily dependent upon the quality of the original submitted.

The following explanation of techniques is provided to help you understand markings or patterns which may appear on this reproduction.

1. The sign or "target" for pages apparently lacking from the document photographed is "Missing Page(s)". If it was possible to obtain the missing page(s) or section, they are spliced into the film along with adjacent pages. This may have necessitated cutting thru an image and duplicating adjacent pages to insure you complete continuity.

2. When an image on the film is obliterated with a large round black mark, it is an indication that the photographer suspected that the copy may have moved during exposure and thus cause a blurred image. You will find a good image of the page in the adjacent frame.

3. When a map, drawing or chart, etc., was part of the material being photographed the photographer followed a definite method in "sectioning" the material. It is customary to begin photoing at the upper left hand corner of a large sheet and to continue photoing from left to right in equal sections with a small overlap. If necessary, sectioning is continued again — beginning below the first row and continuing on until complete.

4. The majority of users indicate that the textual content is of greatest value, however, a somewhat higher quality reproduction could be made from "photographs" if essential to the understanding of the dissertation. Silver prints of "photographs" may be ordered at additional charge by writing the Order Department, giving the catalog number, title, author and specific pages you wish reproduced.

University Microfilms

300 North Zeeb Road
Ann Arbor, Michigan 48106

A Xerox Education Company

Computerized enhancement of ultrasonic echograms

by

Charles Raymond Meyer

A Dissertation Submitted to the
Graduate Faculty in Partial Fulfillment of
The Requirements for the Degree of
DOCTOR OF PHILOSOPHY
Major: Biomedical Engineering

Approved:

Signature was redacted for privacy.
In Charge of Major Work

Signature was redacted for privacy.
For the Major Department

Signature was redacted for privacy.
For the Graduate College

Iowa State University
Ames, Iowa

1972

TABLE OF CONTENTS

TABLE OF CONTENTS (continued)

I. INTRODUCTION

In the field of medicine there exists a definite mandate for development of diagnostic procedures that are not harmful or destructive to the human organism. While it is well known that X-band radiation is damaging to organisms, the information obtained from X-rays concerning size, shape and position of internal organs is invaluable to the physician. It is desirable then to have a means of obtaining the size, shape and position of organs without damaging the organism. In this regard the area of non-destructive testing in the field of ultrasonics has much to offer. To date, no one has demonstrated a single harmful effect to biological organisms from low-energy, pulsed ultrasound (1). For this reason work has gone into the development of medical imaging devices using low-energy ultrasonics. There is some variation in the types of devices and their methods of operation that are used to obtain the desired information of size, shape and position of organs. Two methods of using ultrasound - high frequency pressure waves - for locating the position of changes in acoustical properties are presently in use: continuous and pulsed ultrasound.

Continuous ultrasound involves the continual electronic driving of the acoustic generator at a fundamental frequency equal to the natural mechanical frequency of the generator to produce standing pressure waves in the acoustic medium. In the area of continuous ultrasound there are several methods which allow detection and visualization of acoustic discontinuities in the medium. Image converters modulate the current in a scanning electron beam incident on the face of a cathode ray tube (CRT) depending upon the acoustic energy incident on each corresponding point of the face of the

converter (2). Another method in the area of continuous ultrasound is that of acoustical holography. Acoustical holography is a direct analog to laser holography. Reflected pressure waves from acoustic discontinuities are mixed with a reference beam split from the incident beam to form an interference pattern which is then illuminated by visible laser radiation to produce a smaller but visible representation of the acoustic discontinuity (3, 4). In addition, illumination of the acoustic interference pattern by two laser sources whose wavelengths differ by an amount equal to the wavelength of the acoustic generator allows visualization of the acoustic discontinuity without reduction of size (5).

Pulsed ultrasound involves the electronic pulsing of the ultrasonic transducer at a rate much lower than the transducer's natural resonant frequency. It may be helpful to note that the basic principles of radar and pulsed ultrasound are analogous. The acoustic transducer acts as a bilateral converter of acoustical and electrical energy. When the transducer is shock-excited by an electric pulse, the transducer generates a short, traveling pressure wave in the acoustic medium. The wave propagates along a straight line in a uniform medium. When the traveling wave strikes an acoustic discontinuity in the medium, part of the wave is reflected back to the transducer (6). The time taken for the echo to return to the transducer is used to determine the range of the acoustic discontinuity from the transducer. The direction of the discontinuity from the transducer is approximated by the traveling wave's direction of propagation. However, since the outgoing pressure wave has a finite width, the exact direction of the discontinuity from the transducer cannot be determined. The region that exists within the traveling wave's path such that a test object

placed in that region produces a detectable echo at the transducer is called the ultrasonic beam for the system. Echoes originating from the test object placed outside this beam have insufficient intensity to be detected. The width of this beam measured perpendicularly to the traveling wave's direction of propagation varies with the range from the transducer and is simply referred to as the beamwidth. In the region close to the cylindrical transducer the beamwidth is approximately equal to the diameter of the transducer. This region is known as the near field of the transducer. At distances further from the transducer the beamwidth begins to increase gradually and then at the furthest point it decreases rapidly to zero and vanishes (7).

In the area of pulsed ultrasound there are also some variations in the application of the basic principles. The A-scan method is used primarily to detect lateral shifts of the Falx Cerebri within the cranial cavity in order to help diagnose the presence of brain tumors or hematomas in the larger, lateral half of the brain. The equipment used for the A-scan method consists of an acoustic transducer, cathode ray tube, and controlling electronics. The transducer is hand-held against the head and the direction of the beam is estimated by the operator. In the A-scan method the distance from the transducer to acoustic discontinuities lying in the beam is determined by the time taken for the reflected traveling wave to return to the transducer. The time of return of an echo is indicated to the technician by the vertical deflection of a horizontally sweeping electron beam on the CRT. The horizontal sweep begins when the transducer is pulsed and the outgoing wave initiated. The distance to acoustic discontinuities from the generator in a medium of nearly constant propagation velocity is repre-

sented by the distance along the abscissa on the face of the cathode ray tube to the vertical traces (8). However, no information is obtained about the shape of the acoustic discontinuity.

Acoustical synthetic aperture is a method in the area of pulsed ultrasound to locate and describe the shape of acoustical discontinuities in the medium. In this method the generator is moved at constant speed and in a constant direction in the acoustic medium. The beamwidth of the system is relatively wide and the center line of the beam is directed perpendicular to the direction of travel of the generator. The returning echoes are mixed with a reference oscillator, and the interference pattern for different target distances recorded on photographic film for one position of the generator. This process is repeated as the position of the generator changes and the interference patterns are stored in succession on moving film. The film then contains a one-dimensional hologram for each given target distance. Illumination of the photographic film by a laser and the appropriate system of lenses gives a high quality, visual reproduction of the acoustic discontinuities of the medium (9, 10, 11).

At present one method in the area of pulsed ultrasound that has gained some acceptance in medical diagnostic procedures is the compound scanning (C-scan) method (8). This method is used to obtain a cross-sectional view of the boundaries of the internal organs within an organism. The display generated by this diagnostic device is referred to as an echogram and is used to aid in medical diagnosis of tumors, hemotomas, organ enlargements and fetal growth. The C-scan method utilizes a transducer, a mechanical scanning system, an image display and storage (via photographic film or a long persistance CRT) system, and a electronic controlling and processing

system. The transducer is moved in a compound scanning pattern in an acoustic coupling medium (usually water since it has nearly the same acoustic properties as living tissue) which surrounds the body of the organism. Compound scanning means that the direction of the transducer is varied over a $\pm 20^{\circ}$ range while the position of the transducer slowly moves in a large arc around the body with the result that a particular point within the organism that lies in the plane of the scan is viewed from many different positions and directions by the transducer (12). The position of the targets are repetitively calculated from many different positions surrounding the targets using each echo's trip-time and the ultrasonic beam's direction at the time of the echo's return. The results of the scans are triangulated to more closely locate the position of the targets within the organism.

The diagnostic device performs the triangulation by displaying the position of the reflecting organs and objects as the corresponding positions of visually intense dots on the face of the display tube (12). The coordinates on the face of the tube correspond on a one-to-one basis to the coordinates of the scanned plane containing the cross-section of the organism. The display is created by sweeping a blanked electron beam across the face of the tube in a direction corresponding to the direction of the center line of the transducer. The positions of small objects within the beampath that have surfaces normal to the incident wave of the transducer and that give rise to echoes of sufficient intensity are represented as intensified points along the center line of the transducer's beam. As the direction of the transducer is varied in compound scanning an arc of points is intensified for each reflecting object. And as the

position of the transducer is changed and its direction is again varied, a new set of points lying on new arcs is intensified. The most likely positions of the reflecting objects are at the intersections of the two sets of arcs. The points at the intersections of the arcs are more intense than the other intensified points on the face of the display tube since the points at the intersections have been intensified twice.

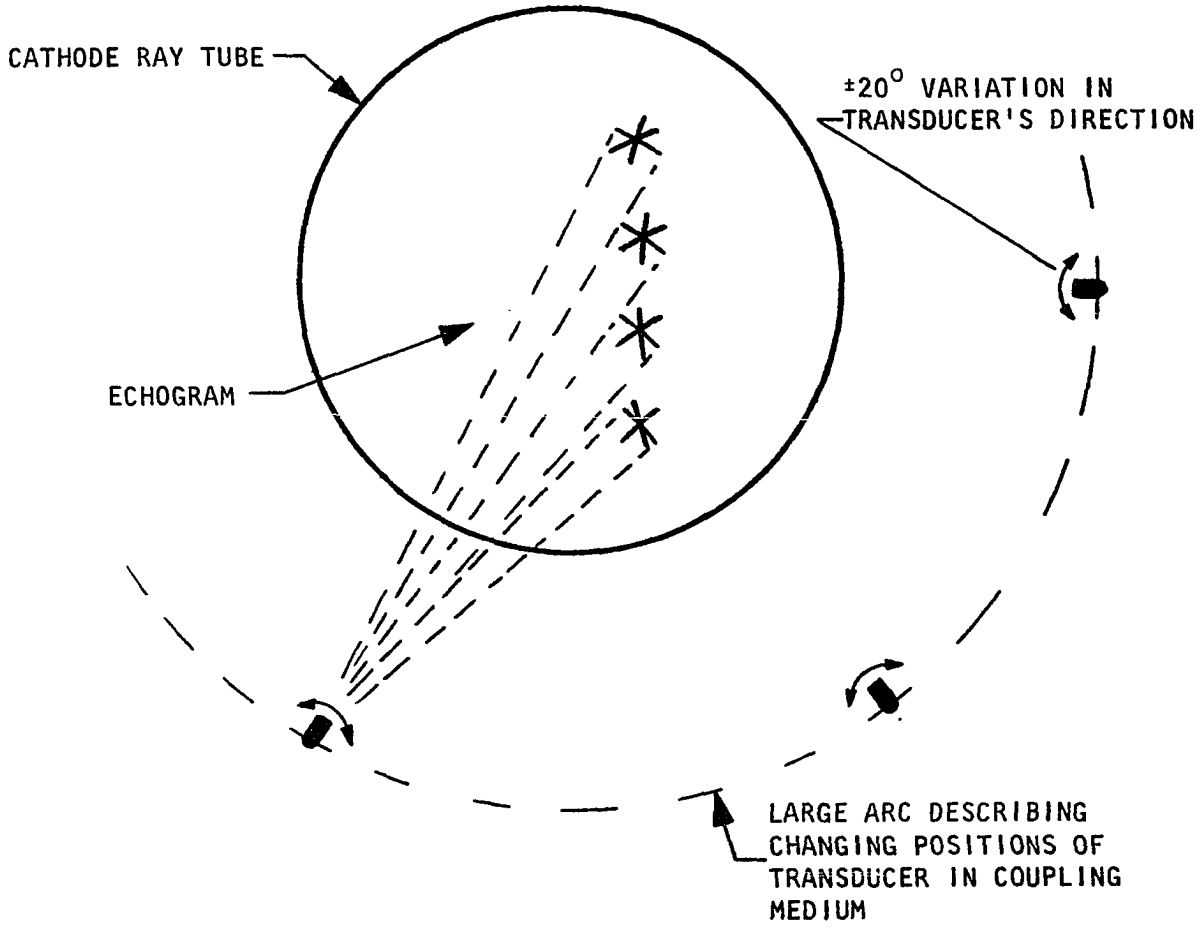

Figure 1. Construction of echogram on CRT display using compound scanning method.

Continuation of the compound scanning process causes a small reflecting object within the organism to appear on the display tube as bright disk whose broad center region is more intense than the outside rim. The most

likely position of the small object is at the position corresponding to the point of greatest intensity on the display. Larger reflecting objects appear as thick, whiskered lines outlining the shape of the object (13).

To an objective viewer the resulting echograms of this device are very crude representations of the tissues and structures within the organism. As previously mentioned small objects are displayed as larger disks and the boundaries of larger internal organs are displayed by thick, whiskered lines. Ideally, smooth tissue boundaries should be shown as smooth, thin lines and very small objects should be shown as singular points in the display. A source of error that degrades the resulting echogram is the beamwidth of the ultrasonic beam. Although compound scanning improves the effects of ultrasonic beamwidth, it aggravates the problem of image saturation. Image saturation is a state that occurs in display tubes in which further illumination of a previously brightened point fails to cause an increase in the intensity of the point (14). In compound scanning the degrading effect of image saturation causes the whole circular region surrounding the location of a small object to have an intensity approximately equal to the intensity of the object's actual location. However, if the effect of image saturation could be removed, the echogram would be a two-dimensional likelihood distribution on the face of the display tube where the brightness of a particular point on the face of the display corresponds to the likelihood that the associated position in the organism is a location of an acoustic discontinuity. Without image saturation the echogram generated by compound scanning would be greatly improved. The location of a small object would be displayed as a very small, visually intense point and the intensity of the circular region surrounding the point created by

the effect of beamwidth would be much reduced in comparison with the intense center. Thus, it is desirable to develop an ultrasonic diagnostic system where the two-dimensional likelihood function is generated in a medium that is not easily saturated.

The digital computer offers a more permanent, non-saturable memory scheme, where the address of a word within the memory can correspond to a small, two-dimensional region in the acoustic medium. For each point in the acoustic medium that causes an echo to return, the contents of the word at the appropriate address are incremented. Using FORTRAN IV as a programming language in conjunction with the IBM System/360 computer, a word in memory may be any value from zero to 2,147,483,647 (15). Such magnitude essentially removes all possibility of saturation. After the likelihood distribution is generated and stored in the memory of the computer, numerical methods can then be used to plot on a processed echogram only those points in the distribution that are the most likely positions of reflecting points. In this way the processed echogram closely resembles the tissues and structures within the organism. If it is desired, the two-dimensional likelihood distribution itself can be plotted. By eliminating the effect of image saturation in current diagnostic devices this proposed system can fully benefit from the process of compound scanning.

II. LITERATURE REVIEW

This is a short review of some of the problems encountered by other investigators in the compound scanning method of pulsed ultrasound and some of their attempted solutions to these problems. Robinson, Kossoff and Garrett have published a complete treatment of these errors and the following summary is taken from their article (13).

The axial resolution of the compound scanning system is defined as the minimum spacing between two small targets lying on the center line of the beam such that the system can detect the presence of two separate points. A transducer that is not highly damped produces a long wave train and contributes to poor axial resolution of the system because an echo from an object closer to the transducer has not sufficiently damped out before another echo from a further object returns. The electronics following the amplifier is not able to distinguish the presence of two echoes unless the reflecting objects are separated even further. An electronic amplifier with a narrow frequency bandwidth tends to oscillate longer than the pulse duration and also contributes to poor resolution for the same reason.

Azimuthal resolution is defined as the minimum spacing between two small targets lying on a line perpendicular to the center line of the ultrasonic beam, such that the system can detect the presence of two separate targets by varying only the direction of the beam. Thus, azimuthal resolution is equal to the system's beamwidth at any particular target range.

Multiple reflections between the target and transducer also contribute to artifacts. Consider the case where a generated wave leaves the transducer, strikes the target and is reflected to the transducer, strikes the

target and is reflected to the transducer, strikes the transducer and is reflected back towards the target, and repeats this sequence several times before the intensity of the wave diminishes below the detection threshold in a low-loss medium such as water. This case causes the system to correctly detect the position of the target, but generates pseudo-targets at distances equal to integral multiples of the correct distance.

The shadowing of a distant object by a object nearer the transducer which either totally absorbs or reflects the incident wave causes a loss of information in the echogram. Also, reflection of the incident wave by a smooth surface that is not normal to the center line of the beam causes the returning echo to miss the transducer. The return of an echo that has been refracted also causes error in determining the position of the object because the object is simply assumed to lie in a straight line along the center line of the transducer. The position of objects in a heterogenous medium cannot be correctly determined because the propagation velocity of the wave changes in each subdivision of the medium. In practice only one propagation velocity is assumed in determining the position of the objects from the time data. And, as already mentioned, image saturation also contributes to a loss of information.

Some methods of processing information have been proposed to reduce the effect of specific errors. The degrading effect of image saturation is reduced by video inversion, scanned deflection modulation, deflection-intensity modulation, or by use of a positionally incremented timebase display. In video inversion the scan across the face of the CRT is unblanked. Blanking occurs when an echo returns to the transducer, and the degree of

blanking depends on the amplitude of the echo. This method makes use of the linear portion of the relationship between intensity and blanking grid voltage for the CRT (16). In scanned deflection modulation no intensity modulation of the scanning electron beam in the CRT is used. During the scan the return of an echo causes the momentary vertical deflection of the electron beam. The direction of the beam of the acoustic transducer remains constant while the position is incremented in a direction normal to the beam. The process amounts to superimposing the results of many positionally incremented A-scans on a storage tube (16). A further modification of this process is called deflection-intensity modulation in which process the scanning electron beam is blanked until an echo returns. Upon reception of a echo the beam is both unblanked and momentarily deflected (16). A positionally incremented timebase display described by A. J. Hall reduces image saturation in conventional compound scanning methods by pulsing the transducer only when the direction of the transducer changes by some given amount - e.g. two degrees (17).

There are also methods for compensating for poor azimuthal resolution. A transducer with a variable focal point described by Thurstone and McKinney can be used where only those echoes that return from the region of the focal point are used to determine positions of target objects (18). All other echoes before and after that time period are ignored. Another method of azimuthal compensation is the use of an array of receiving transducers arranged in a circular pattern about the generating transducer. The output to the visual display from the array processor is a signal equal to the product (multiplication) of all the signals from each receiving transducer (19). Thus, a zero output from the processor exists any time one of the

receiving transducers is inactive. The wavefront of the returning echo must be incident on all of the receiving transducers at the same time to produce an output from the array processor.

III. THEORY

Assume that the ultrasonic beam has a large beamwidth and that the system has the axial resolution of d. For calculation purposes an object such as P anywhere within the beamwidth of the transducer which causes an echo to return is simply considered to lie on the center line of the beam as in Fig. 2. Figure 3 demonstrates the effect on the generation of the

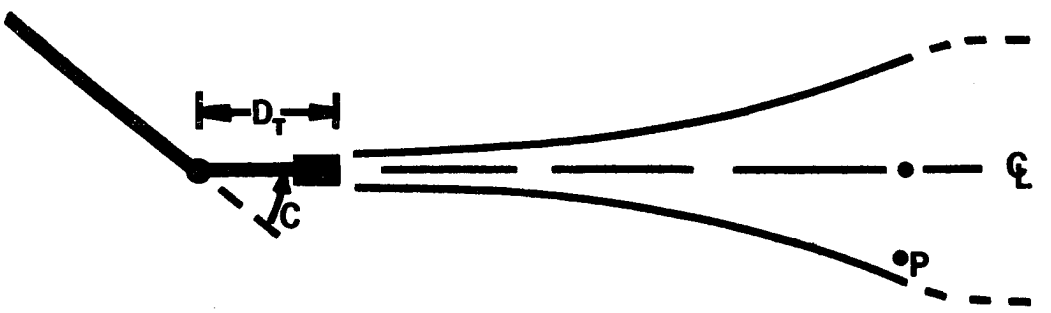

Figure 2. Effect of acoustic generator's beamwidth.

likelihood function by compound scanning with these two sources of error, beamwidth and finite axial resolution. When the transducer is in region F, increasing angle C causes points within the vertically hatched region to be calculated as the location of P. Note that if C is uniformly increased, each point within the vertically hatched region has an equal chance of being calculated. The same argument holds true when the transducer is in the region of G. Points within the horizontally hatched region have an equal chance of being calculated. Note that all points within the cross-hatched region have an equal chance of being calculated twice. As a matter of definition the term likelihood distribution will be the name given to

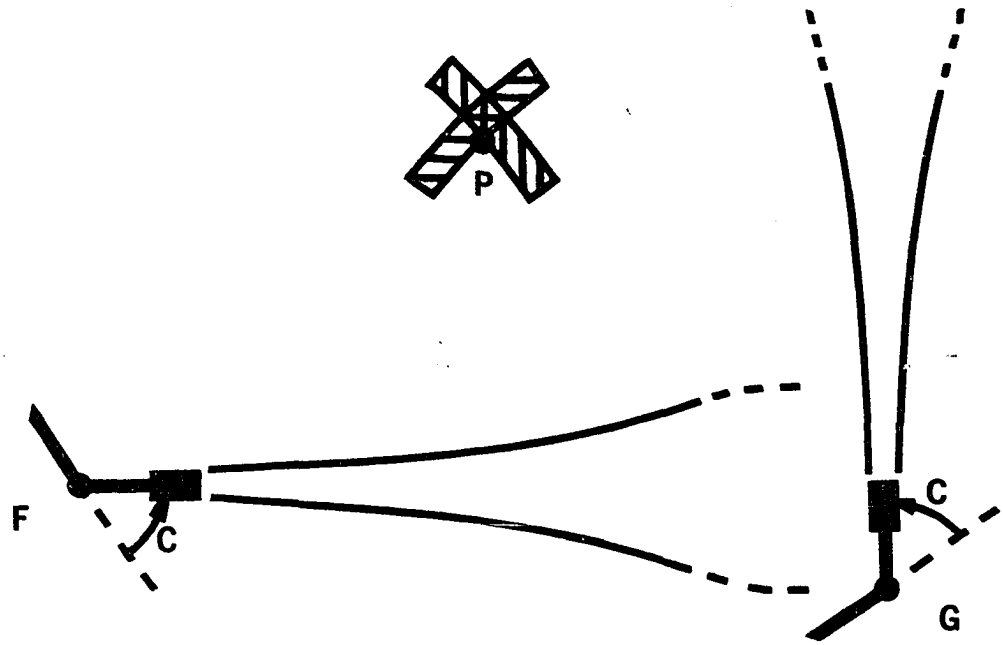

Figure 3. Effect of compound scanning.

the distribution constructed by experimentally sampling the acoustic medium and incrementing the calculated points. The term probability distribution will refer to the distribution obtained by theoretically constructing a likelihood distribution using a infinite number of samples.

Now consider the idealized case where a transducer with a very large beamwidth travels in a uniform manner along a very large circle about the position of an infinitesimally small target, P. Since the distance between the transducer and the target is very large, variations in the angle C during the compound scanning process produce a region of calculated points bounded by straight lines as shown in Fig. 4. As ϕ, the angle from the target to the region of the transducer, varies from 0 to ϕ_1, the point P_x is one of the points equally likely to be calculated and incremented in

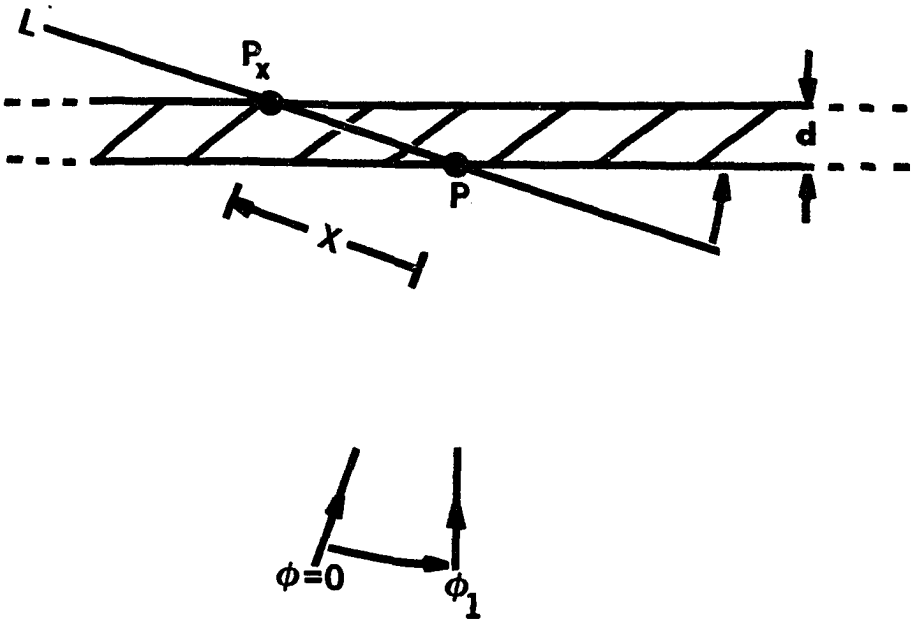

Figure 4. Construction of probability distribution for an infinitesimally small target.

the construction of the likelihood function for each value of ϕ in that range, where

$$\phi_1 = \text{Arcsin } (\frac{d}{X})$$

and where d is the axial resolution of the system. As ϕ varies from 0 to π, the point P_x is one of the points equally likely to be incremented for each value of ϕ if P_x is a point such that $X \leq d$. The resulting probability distribution, p(X), along line L that the point P_x will be calculated to be the position of the target is formed then by summing the number of times the point P_x is likely to be calculated for each ϕ, while varying ϕ over the range such that $0 \leq \phi < 2\pi$. Thus, in the limit

$$p(X) = \begin{cases} \frac{1}{H}\int_{-\phi_1}^{\phi_1} d\phi = \frac{2}{H}\int_{0}^{\mathrm{Arcsin}(\frac{d}{X})} d\phi = \frac{2}{H}\,\mathrm{Arcsin}(\frac{d}{X}) & \text{for } X \geq d \\ \frac{1}{H}\int_{0}^{\pi} d\phi = \frac{\pi}{H} & \text{for } X \leq d \end{cases}$$

where H is a constant chosen such that $\int_{-\infty}^{\infty} p(X)\, dX = 1$. Obviously p(X) is an even function since the same effects occur for negative values of X.

Then

$$p(X) = \begin{cases} \frac{2}{H}\,|\mathrm{Arcsin}(\frac{d}{X})| & \text{for } |X| \geq d \\ \frac{\pi}{H} & \text{for } |X| \leq d \end{cases}$$

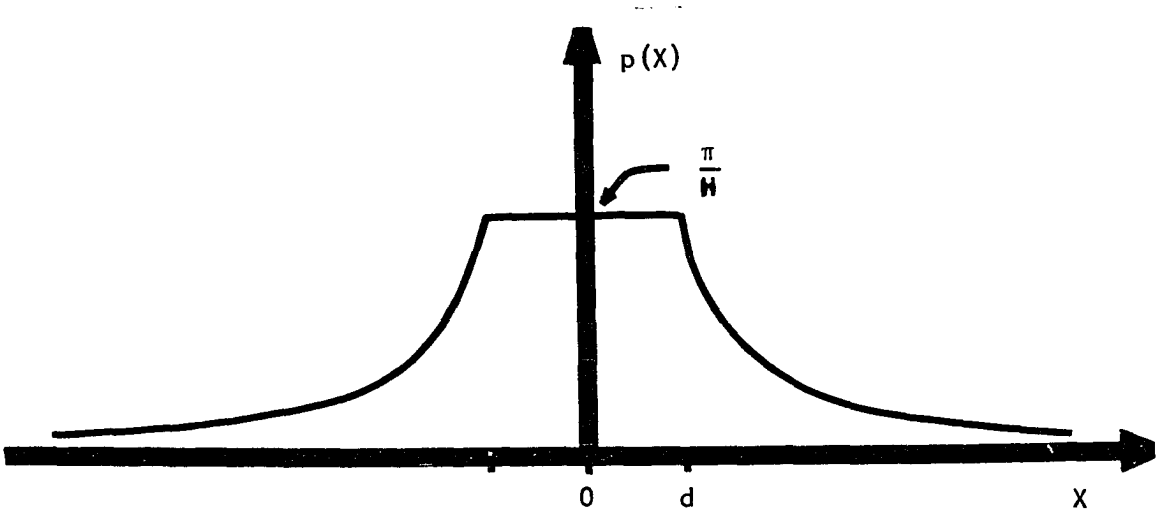

Figure 5. Continuous probability distribution for an infinitesimally small target.

Fig. 5 shows the ideal probability distribution along a line L through point P that the point X will be calculated to be the position of the target from experimental data acquired by uniform compound scanning of an infinitesimally small target at point P, using a system with axial resolution of d and a transducer with very large beamwidth. Since any line could be drawn through point P and the same argument repeated, the two-dimensional distribution p(X, Y) is obtained by rotating the one-dimensional distribution through 2π radians about the vertical axis.

In the process of constructing the likelihood function in the computer locations of reflecting points are calculated to have X- and Y-coordinates that lie on the continuous, real number line which consists of an infinite number of points. Since the computer does not have an infinite amount of storage, the real number line for both the X- and Y-axis must be quantized into a finite number of points. The discrete probability distribution $p(J_n)$, is derived by quantizing the X-axis of the continuous probability distribution, p(X). Given that the discrete number axis has points evenly separated by an interval, K, then

$$p(J_n) = \frac{1}{K} \int_{J_n - \frac{K}{2}}^{J_n + \frac{K}{2}} p(X)\, dX$$

where $$J_n = X_1 + nK$$

and where $$n = 0, \pm 1, \pm 2, \ldots$$

and X_1 is any real number such that

$$-K/2 < X_1 \leq K/2$$

Quantizing the X-axis of the zero centered continuous distribution of Fig. 5 with $X_1 = 0$, d = 1.85 mm and K = 2 mm (actual experimental values for d and K) results in the discrete probability distribution of Fig. 6, which has been magnitude normalized. Note that variations in X_1 change the appearance of the discrete distribution by shifting the position of

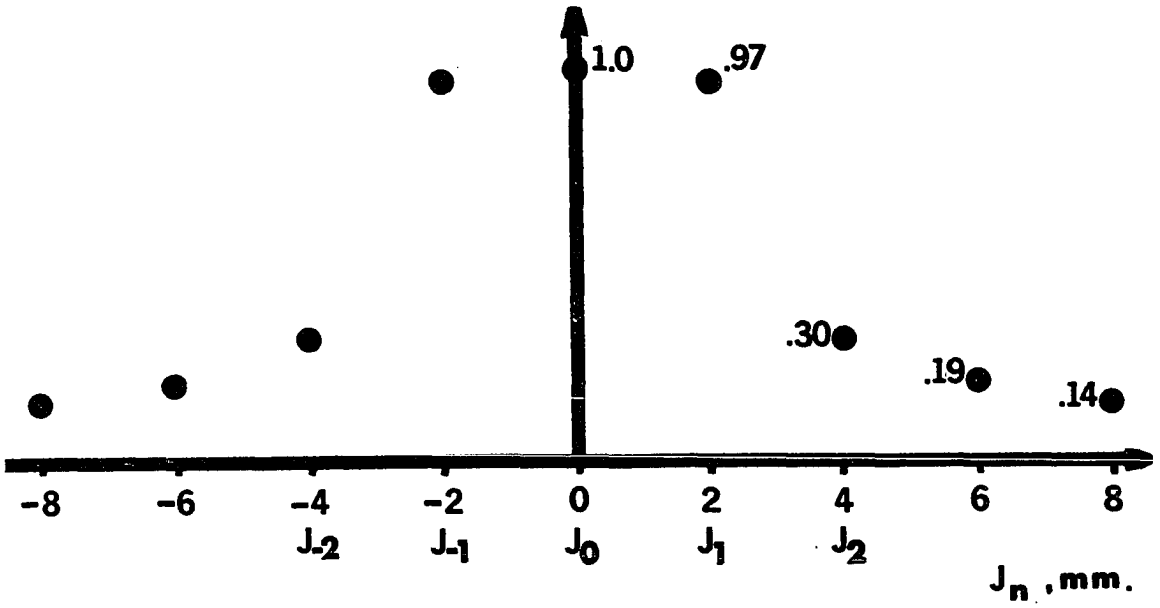

Figure 6. Discrete probability distribution for an infinitesimally small target where $X_1 = 0$, K = 2 mm, and d = 1.85 mm.

the peak and by loss of symmetry. At the extreme variation of X_1 where $X_1 = K/2$, symmetry is restored to the discrete distribution but two points, J_o and J_{-1}, have the same maximum ordinate value as shown in Fig. 7. Figure 7 has also been magnitude normalized where $X_1 = K/2 = 1$.

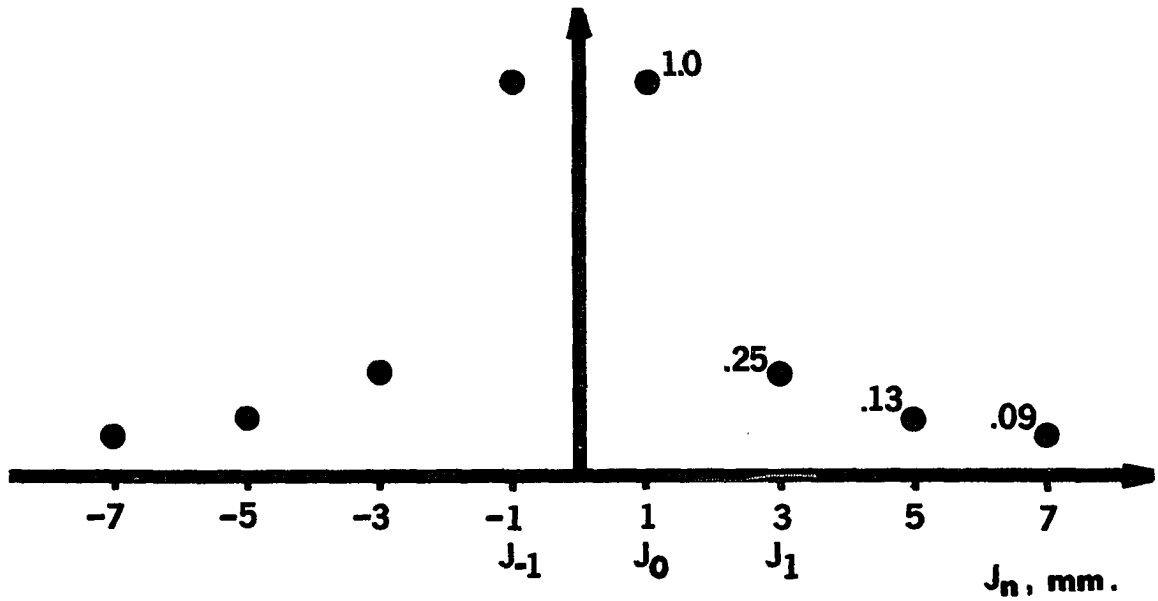

Figure 7. Discrete probability distribution for an infinitesimally small target where X_1 = 1 mm, K = 2 mm, and d = 1.85 mm.

Now using a small, homogeneous cylinder or rod of radius r as a target in the water bath, the one-dimensional distribution is developed showing the probability that a point which lies on a straight line, L, passing through the center coordinate of the rod will be calculated as the rod's center position. This distribution is generated from experimental data obtained by uniform compound scanning of the target with a system having a very large beamwidth and an axial resolution of d, where $d/2 \lesssim r \lesssim d$.

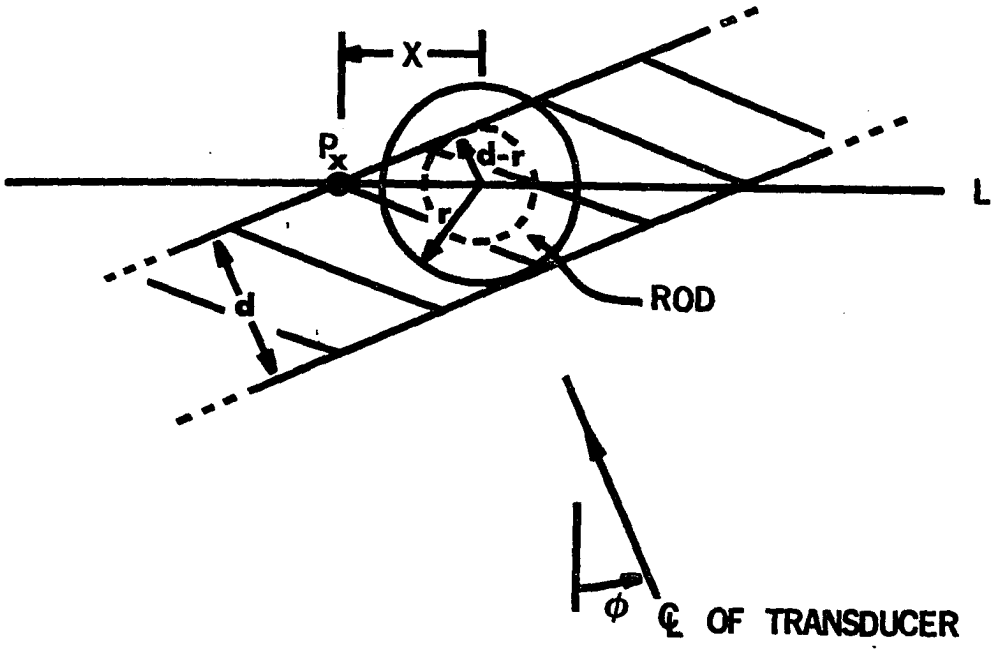

Figure 8. Construction of probability distribution for a rod of radius r, where $\frac{r}{2} \leq d \leq r$.

For positive X as ϕ varies for 0 to 2π radians:

$$p(X) = \begin{cases} \frac{1}{H}\int_0^{2\pi} d\phi & \text{for } 0 \leq X \leq d-r \\ \frac{2}{H}\int_0^{\text{Arcsin}(\frac{d-r}{X})} d\phi + \frac{1}{H}\int_{\pi}^{2\pi} d\phi & \text{for } d-r \leq X \leq r \\ \frac{2}{H}\int_0^{\text{Arcsin}(\frac{d-r}{X})} d\phi + \frac{2}{H}\int_0^{\text{Arcsin}(\frac{r}{X})} d\phi & \text{for } r \leq X \end{cases}$$

Then for all values of x:

$$p(X) = \begin{cases} \frac{2\pi}{H} & \text{for } |X| \leq (d-r) \\ \frac{2}{H}\left(\left|\text{Arcsin}\left(\frac{d-r}{X}\right)\right| + \frac{\pi}{2} \right) & \text{for } (d-r) \leq |X| \leq r \\ \frac{2}{H}\left(\left|\text{Arcsin}\left(\frac{d-r}{X}\right)\right| + \left|\text{Arcsin}\left(\frac{r}{X}\right)\right| \right) & \text{for } r \leq |X| \end{cases}$$

where H is a constant chosen such that $\int_{-\infty}^{\infty} p(X)\, dX = 1$. As before, the two-dimensional probability distribution for all points in the region of a single rod located at (0, 0) is obtained by rotating Fig. 9 through 2π radians about its vertical axis.

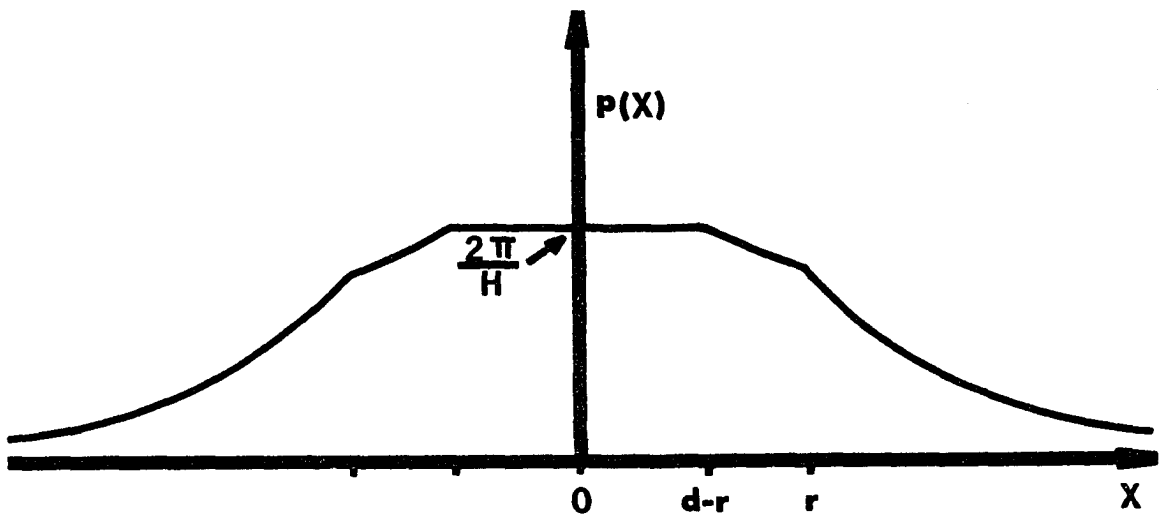

Figure 9. Continuous probability distribution for a rod of radius r, where $r/2 \leq d \leq r$.

The discrete distribution shown in Fig. 10 is obtained by quantizing the abscissa of Fig. 9 into a discrete number line of points separated

evenly by the interval K. The discrete distribution shown in Fig. 10 is obtained for the case of the rod where r = 1.19 mm (or 3/64 in.), d = 1.85 mm, K = 2 mm and X_1 = 0. Of course variations in the value of X_1

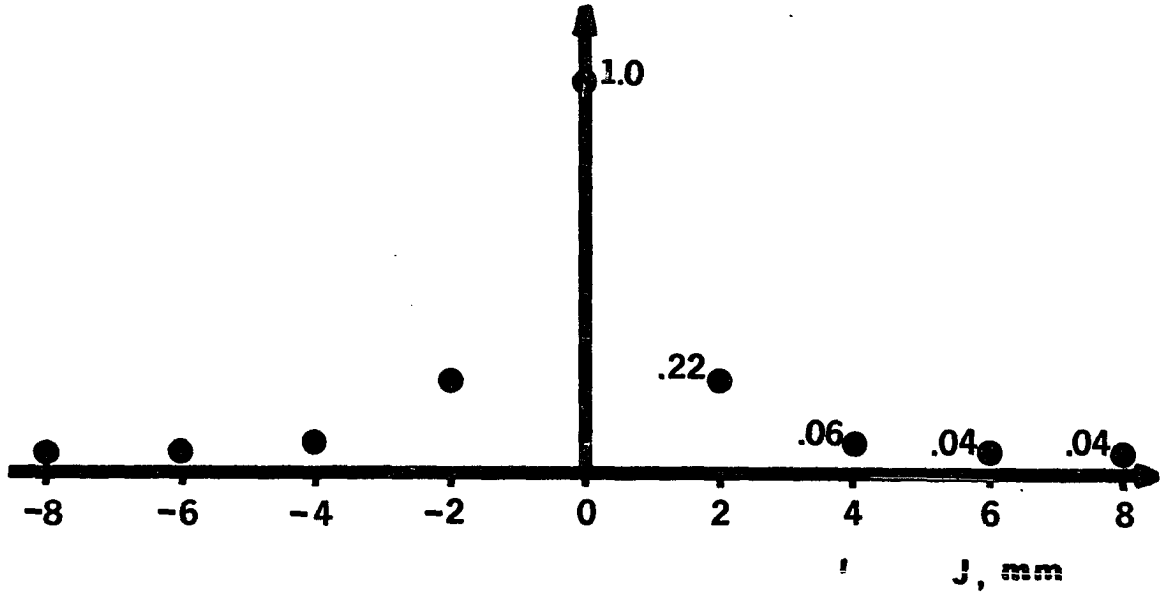

Figure 10. Discrete probability distribution for rod.

will alter the shape of Fig. 10, but as before, the position of the maximum of the discrete distribution will be located at the quantized coordinate closest to the center of the continuous distribution.

Thus far only the effects of beamwidth, time uncertainty in detection of returning echoes, and spacial quantization have been considered in developing models of the likelihood distributions. Another serious source of error is that which is due to the quantization of the angular positions of the arms by the analog-to-digital converter. In addition, shadowing of distant portions of the target by portions nearer the transducer and system non-linearities are other sources of error. Since these errors of angular quantization, shadowing, and non-linearities appear to be random, their

ability to introduce erroneous peaks can be removed by digital smoothing of the experimentally obtained, discrete likelihood distribution. Assume the maximum error introduced due to these effects is $|e_m|$. Then instead of incrementing the discrete distribution only at the position of the calculated point, X_p, increment the distribution at all of the points within the interval $\underline{II}$ where $\underline{II} = \{(X)\left|X_p - |e_m| < X < X_p + |e_m|\right.\}$. This results is a spacially smoothed likelihood distribution with few large, extraneous peaks. A model of the experimental likelihood distribution is obtained by smoothing the distribution of the incomplete model. Fig. 11 is the result of smoothing the distribution of Fig. 6 by incrementing all points in the interval $\underline{II}$, where $|e_m| = 2$ mm. Similarly the distribution of Fig. 12

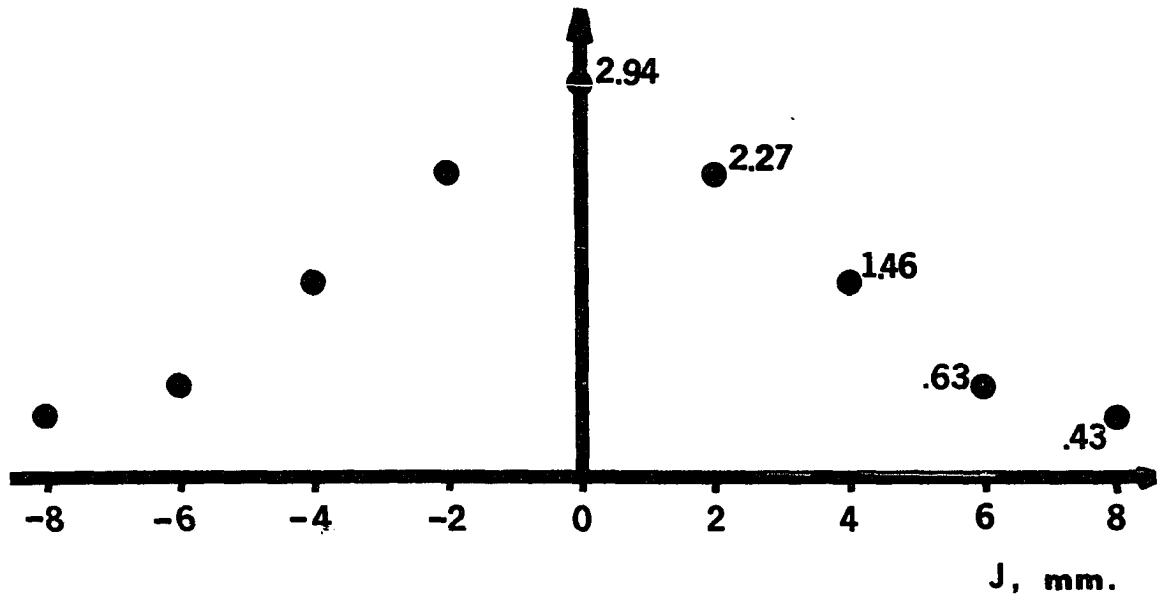

Figure 11. Smoothed discrete probability distribution for infinitesimally small target.

is the result of smoothing the distribution of Fig. 10 for the case of the rod.

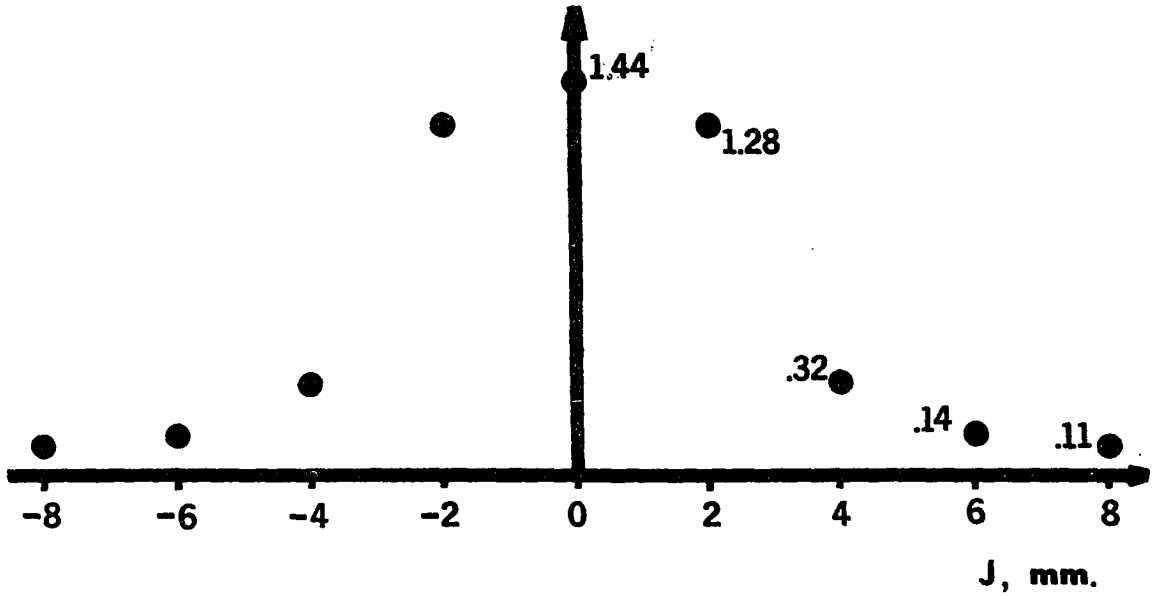

Figure 12. Smoothed discrete probability distribution for rod.

Now the general shape of the likelihood distributions are modeled for specific targets. After the experimental likelihood distribution for the total complex target is calculated and stored in the computer the next step in the process is to determine the cross-sectional conformation of the complex target from this distribution and to plot the shape on the final, processed, two-dimensional echogram.

Based on the axial resolution, d, of the data acquisition system, objects within complex targets fall into two general categories: small and large. Small objects whose mean diameter is less than 2d give rise to inverted conical peaks in the two-dimensional likelihood function. Larger objects in the complex target whose mean diameter is greater than twice the axial resolution of the system generate two-dimensional likelihood distributions that appear as ridges over regions as in Fig. 13. The magnitude of the ridge may vary considerably due to non-uniform scanning, shadowing

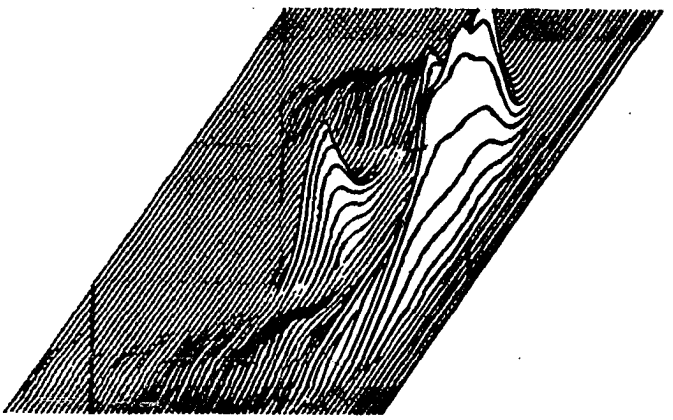

Figure 13. Two-dimensional likelihood distribution which forms ridges.

and object orientation. Regardless of the size of targets in the water bath, only those points in the likelihood function that have values above some threshold value should be considered in determining whether any of those points are the location of a small object or of part of a large object. The setting of this threshold can eliminate the plotting of positions of pseudo-targets generated by multiple reflections of ultrasonic waves between the transducer and a single object or generated by random noise from electrical sources. The threshold value is set quite low so that all significant points are considered. Typically the threshold is dependent on the maximum of the likelihood distribution, f_m, so that if the sampling process with the transducer is longer, the value of the threshold is higher.

If there is prior knowledge that the target in the water bath consists of only small objects, then the decision function that is used should detect and plot only the positions of significant peaks in the two-dimensional distribution. The decision process to locate the position of a significant peak in a smooth distribution is rather simple. If any point, (I, J), in the distribution has a value above threshold (e.g. $f(I, J) > f_m/3$) and that value, f(I, J), is greater than the value of the distribution evaluated at each of the 8 nearest neighboring points, then that point is the location of a significant peak and should be plotted as a point in the processed echogram. Each point in the likelihood distribution is checked to see if it satisfies these two conditions.

On the other hand if there is no such prior knowledge about the structure of the target, the decision function that is used should detect the position of crests in the distribution since most targets are large in comparison with the system's axial resolution. To determine the location of a point whose value lies on the crest a significant ridge in the distribution is more difficult. For the point (I, J) to be the position of a crest, f(I, J) should be above a threshold value which is much lower than the threshold used in peak detection, since shadowing from larger targets can reduce the number of times a significant position is calculated (e.g. $f(I, J) > f_m/32$). Each point in the likelihood distribution whose value, f(I, J), is above threshold should then be checked to see if f(I, J) lies on a crest. To determine if f(I, J) is on the crest of a ridge in the distribution, first find the direction of the line through the point (I, J) such that the distribution's average absolute slope over a small range along that line is maximized. This is equivalent to finding the direction

of the maximum gradient for the distribution at (I, J). Note that the direction of this line is always perpendicular to the direction of the ridge. Then if f(I, J) is greater than the values of the distribution evaluated at either of the two nearest neighboring points which lie on that line, f(I, J) is on the summit of that ridge. In the actual computerized decision process only the four directions shown in Fig. 14 are checked to find the maximum gradient. It almost goes without saying that if f(I, J) is on a summit of a significant ridge, then the point (I, J) is plotted in the processed echogram.

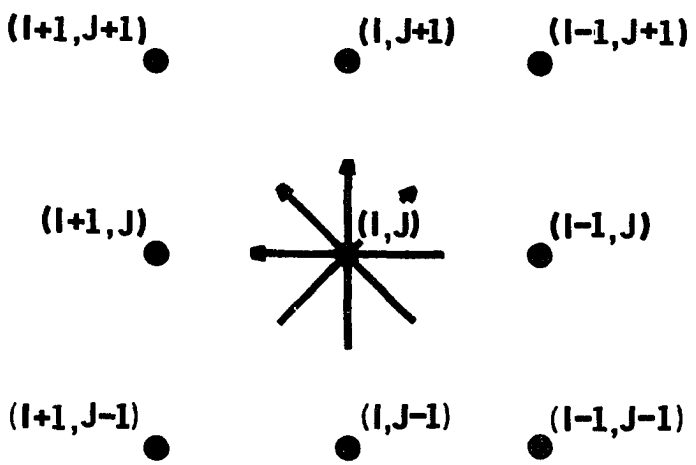

Figure 14. Two-dimensional orientation of matrix points for f(I, J).

Now that the decision theory has been discussed it is possible to discuss the system's resolution. Again, resolution is the minimum distance between two small objects such that the system can still determine the position of both targets. The distribution for an infinitesimally small object is shown in Fig. 5. Observe that the closest spacing between

two such objects that still results in a total distribution with two separate peaks is approximately 2d, where d is the axial resolution of the data acquisition system. The distribution for the two objects is derived by simple linear superposition of the two single distributions since none of the principles used in deriving the single-object distribution are changed. In particular, shadowing has no effect since the objects are infinitesimally small. Superposition of the distributions of two objects separated by a distance less than 2d would result in a distribution with a single maximum. Since the decision theory is based on the detection of maxima in the distribution, the positions of the two objects could not be determined. On this basis the system's ideal resolution for a target consisting of two infinitesimally small objects in the plane of the scanning transducer is 2d. The minimum resolvable distance may increase in the actual system if spacial smoothing of the distribution is used to reduce the effects of random noise such as shadowing and quantizing error. The actual resolution depends on the smoothing function used. It is worth noting that the minimum resolvable distance between two infinitesimally small objects based on Fig. 11, which is a smoothed distribution, is still 8 mm and corresponds to 4.33d since d = 1.85 mm in constructing the distribution. The performance of the system in determining the separation between larger objects in the plane of the scanning transducer is more difficult to theoretically obtain. Since refraction and shadowing of the remainder of the target by large interfaces may occur, it is impossible to use linear superposition of the distributions for each of the objects to obtain a combined distribution for the total target. Because of this complexity, the system's resolution is defined only on the basis of infinitesimally small objects

and ideally approaches the limit of 2d, where d is the data acquisition system's axial resolution. Note that the total system resolution is independent of the data acquisition system's azimuthal resolution, since all of the distributions are derived using a beamwidth that is much, much larger than the size of the target objects.

IV. EXPERIMENTAL APPARATUS AND PROCEDURES

A. Introduction

The total system can be divided into three main divisions: data acquisition, data storage and transfer, and data processing. The physical appearance of the data acquisition system is shown in Fig. 15. The transducer, which is restricted to motion in one plane by a supporting arm, was moved by hand in a water-filled tank. Water was used in the tank as an acoustic coupling medium because very little attenuation of the propagating pressure wave occurs. The supporting arm is used to electrically monitor the position and direction of the transducer. Three linear potentiometers are mounted at the pivots of the supporting arm so that the direction of each section of the arm is electrically monitored. The lengths of each section of the arm were measured. By the application of trignometric relations, the orientation of the transducer is known. The rectilinear coordinate system was chosen as shown in Fig. 16. Let P be a point located at (X, Y) which is viewed by the transducer in the acoustic medium. The transducer is located on the end of the arm, D_t. The arrow heads indicate the polarity of rotation for each angle. Then

$$X = D \cos(A) + D \cos(A+B) + (D_t+S) \cos(A+B+C) \quad (1)$$

$$Y = D \sin(A) + D \sin(A+B) + (D_t+S) \sin(A+B+C) \quad (2)$$

where

$$S = vT/2, \text{ distance from transducer to target.} \quad (3)$$

$v = 1.5\ 10^6$ mm/sec., the acoustic velocity of longitudinal pressure waves in water.

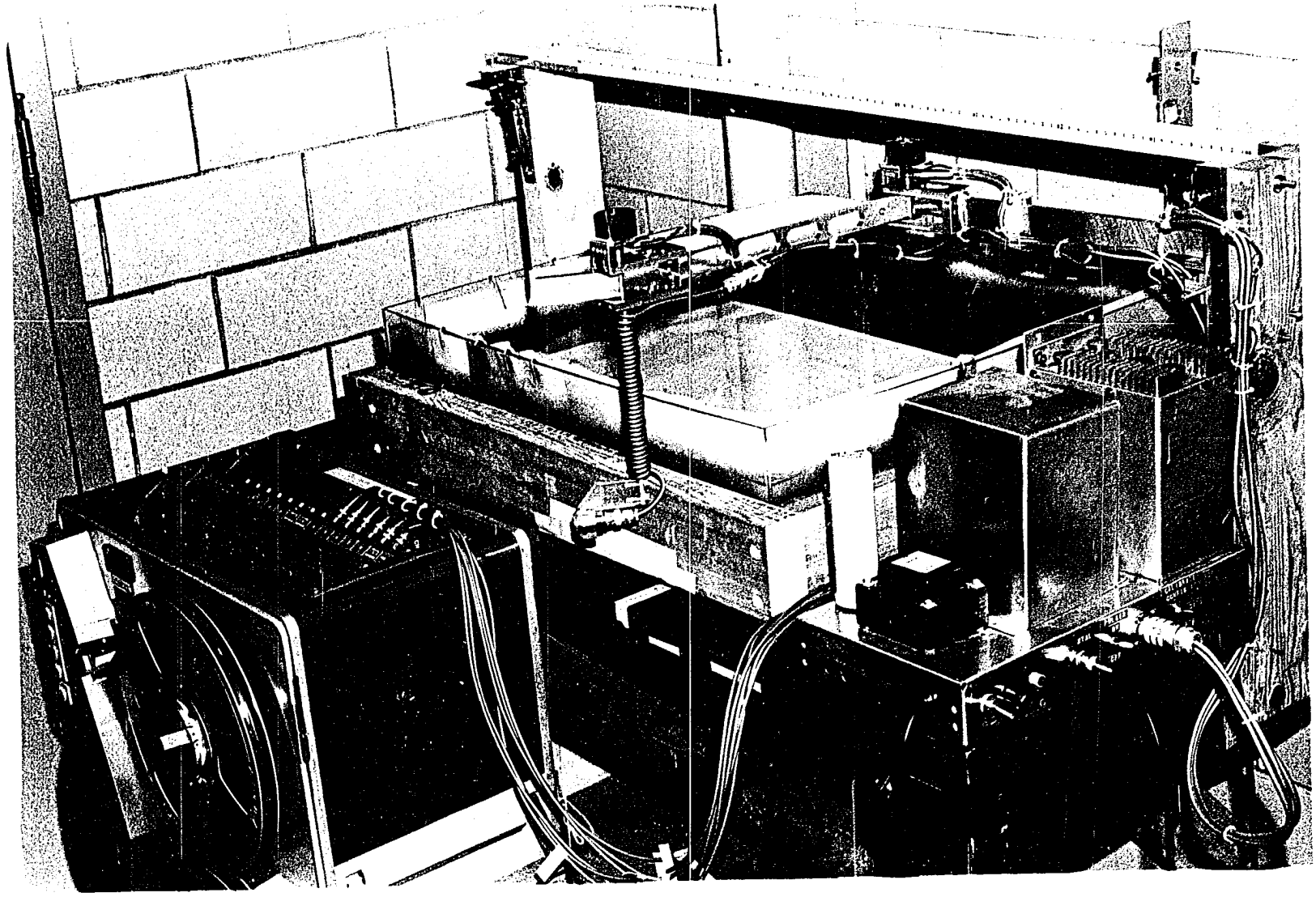

Figure 15. Data acquisition system.

T = time interval between generation of the outgoing pressure wave and reception of the returning pressure wave.

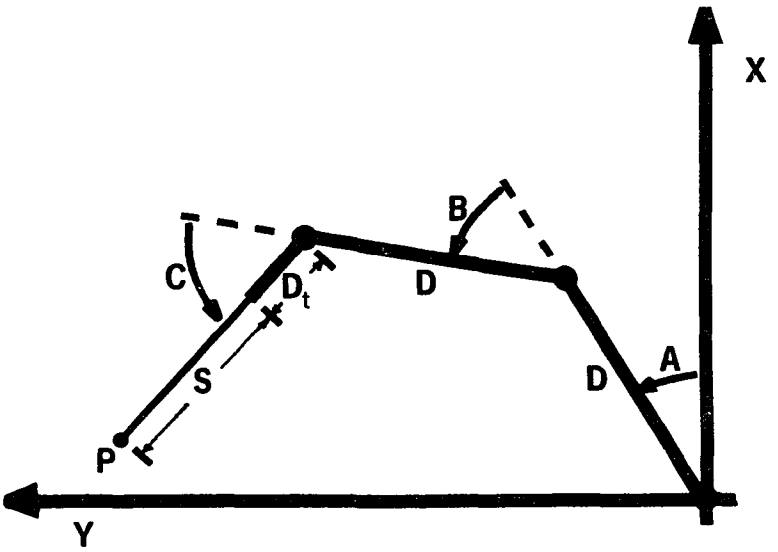

Figure 16. Rectilinear coordinate system.

The three voltages corresponding to the angles of the arm's sections were recorded on three separate channels of a 7 track, analog instrumentation tape recorder. It is by means of this tape recorder that data normally used to create low quality echograms were inputted into the computer.

The transducer was pulsed by an electronic circuit such that an outgoing pressure wave was repetitively generated in the water. The electronic circuit also amplified voltages from the transducer to detect returning pressure waves. These echoes were used to generate short voltage pulses which were recorded on one channel of the tape recorder. The time interval between the generator pulse and each echo pulse was the time

required by the propagating pressure wave to travel to the target and return.

The data recorded on analog magnetic tape was played back into a small digital computer at a tape speed equal to one-eighth of the original recording speed. The echoes return to the transducer in such short times that the computer could not accurately measure them without some means of time expansion. If the computer detects a voltage pulse at the output of the one tape channel, it records on magnetic tape a number that corresponds to the time interval between that echo and its generator pulse. For every echo the computer also records three numbers corresponding to the three voltages of the other analog tape channels containing angular data. All the numerical data on the small computer's digital tape was transferred to another digital tape that could be read by the large IBM System/360 computer. Then the large computer was used to construct the likelihood function from the data on digital tape and to generate the processed echogram.

B. Mechanical System

The transducer's supporting arm was constructed from two aluminum beams having a 6 mm x 21 mm cross-section. The length of each of the first two aluminum sections measured from pivot centers is 315 mm. The two outer pivots were machined to give angles B and C a range of 330° total rotation. The first, or reference pivot was allowed 200° of rotational freedom. Each of the three pivots has ball bearings to support a rotating aluminum pin on which the next section of the arm is mounted. Each of the pins are also directly connected to linear potentiometers (Helipot, Model 3351, 10KΩ, 0.5%, infinite resolution type) to electrically monitor angular rotation of

the pins (these potentiometers are particularly convenient to use because one of the electrical contacts on the back of the potentiometer is situated on the center line of the mounting shaft, facilitating alignment of the mechanical arm). Excess metal not needed for structural strength in the second section of the arm was removed so that the droop of the arm is decreased when angle B is in the region of 90°. The first pivot is attached to a vertical, wooden post via an aluminum plate that allows minor adjustments in the orientation of the transducer's scanning plane. Also attached to the aluminum mounting plate is a thin, taut steel wire that passes 4 mm above the electrical contacts of the potentiometers and passes through the center line of the first pivot. This thin wire was used as the reference location of the X-axis. The wire is positioned in a plane parallel to the transducer's scanning plane and passes through the center line of the pivot of angle A. The wire is supported at the other end of the water tank by another wooden post. A meter stick is also positioned just above the reference wire and slightly to the side. The wire and meter stick were used in calibration of the system.

The water tank was constructed of clear 3/16 inch thick plexiglass sheets and was surrounded by a wooden frame for strength. The inside walls of the tank are lined with 1/2 inch thick foam rubber which acts as a sound absorber. The water is a low-loss medium for transport of ultrasonic waves while plexiglass is a nearly perfect reflector. The effect of the foam rubber is to severely attenuate these waves when they reach the tank boundaries so that unwanted reflections do not introduce erroneous data. Graph paper (10 div/cm) is located below the clear bottom of the tank and was used both in calibration and in positioning target objects. The axis

of the graph paper was aligned with the suspended reference wire by means of a hanging plumb.

The ultrasonic transducer used was manufactured by Nortec Corporation (Model: G - Z - 7 - 2.250) and has a natural resonant frequency at 2.25 MHz. The diameter of the flat radiating surface is 14.5 mm. The transducer is held by a piece of plexiglass machined such that ultrasonic pressure waves returning to the transducer are not reflected by the holder back in the direction of the target. The radiating surface of the transducer is held by the plexiglass section at 60 mm from the center of the last pivot, angle C. The transducer's holder is mounted on the long pin of angle C such that the center line of the transducer is placed 200 mm below the center line of the arm's aluminum sections. A short plexiglass beam is also positioned on the same pin at the level of the aluminum sections such that the direction of the transducer can be controlled by hand without reaching into the water bath. The center line of the transducer is positioned approximately 50 mm below the water's surface. The transducer is connected to the electronic system by means of a coaxial cable.

C. Electronic Recording System

The schematic of the electronic system which is the pulser and receiver of the transducer is shown in Fig. 17. This circuit repetitively shock excites the transducer with a 300 ns, 80 V pulse. The pulse repetition rate was set at 448 Hz by adjusting the labeled potentiometer. This rate was chosen for compatibility with a digital filter described later.

The following is a description of all the events that occur in the time period between any two pulses. Before the transducer is pulsed a

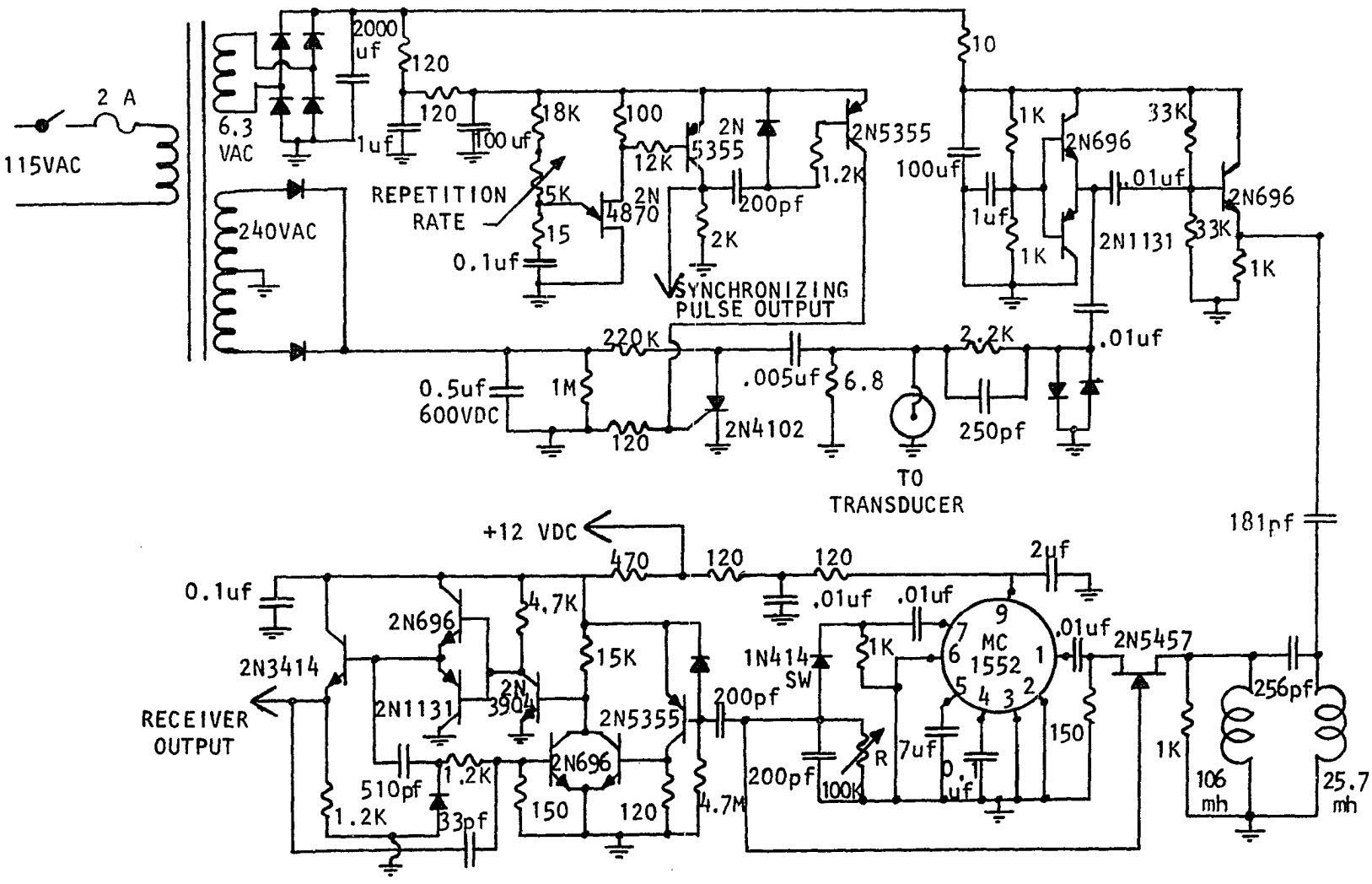

Figure 17. Schematic of transducer's pulser and receiver.

10 μs, 8 V synchronizing pulse is produced. The synchronizing output is fed into Channel 2 (Ch. 2) of the analog tape recorder. The purpose of the synchronizing pulse is to initiate the computer sampling for the actual generator pulse which marks the initiation of the propagating waves away from the transducer. At the end of the synchronizing pulse the silicon controlled rectifier is fired and the transducer is pulsed. The output from the transducer is clipped, fed through a high pass filter and then amplified. The output is clipped to prevent the 80 V pulse from overloading the high gain amplifier. The signal is passed through a high pass filter (4th order Butterworth with 3 db point at 1 MHz) to remove the effects of unwanted vibrations in the transducer at lower frequencies. The amplifier is operated in an automatic gain control (AGC) mode. The field effect transistor at the input of the amplifier acts as a variable resistor and controls the gain of the circuit. For very small signals the gain of the amplifier is 40 db. During the period of time between the shock excitation of the transducer and the return of the first echo the gain of the amplifier is 40 db. When an echo arrives at the transducer the first part of the signal is fully amplified until the gain has adjusted. The amplified is rectified and filtered. As this rectified voltage grows more negative the gain of the amplifier is reduced to -20 db. The AGC can fully react in one microsecond. The gain then begins to increase again at a rate dependent on the setting of R. The negative change in the rectified AGC voltage is used to trigger a monostable generator which generates a 2.4 μs, 8 V pulse. This pulse is the output of the receiver and signifies that an echo of detectable magnitude has returned to the transducer. Thus, a pulse is generated at the receiver output at the excitation of the

transducer (generator pulse) and at the return of each echo (echo pulse). The output from the receiver is fed into Ch. 1 of the analog tape recorder.

Based on this generator-transducer-receiver system just described, an ultrasonic beam is defined around the transducer's center line for a particular test target. The beam for the system of Fig. 17 is shown in Fig. 18 where the target is a 2.38 mm (3/32 inch) diameter aluminum rod that lies in a plane perpendicular to the transducer's center line.

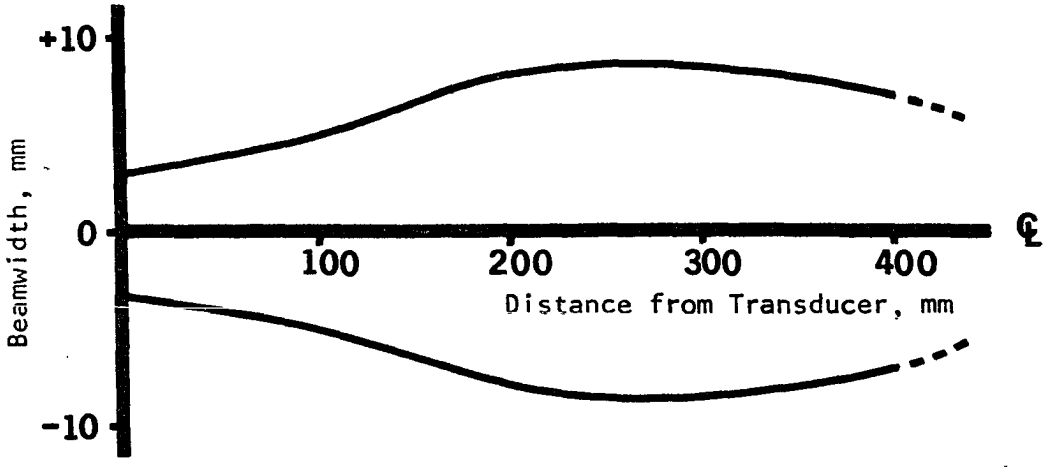

Figure 18. Ultrasonic beam of generator-transducer-receiver system.

The schematic for the circuit that monitors the orientation of the transducer is shown in Fig. 19. The position potentiometers labeled A, B and C monitor respectively the three angles of the transducer's supporting arm. To preserve linearity each of the voltages from the potentiometers is sensed by a high input resistance amplifier (5 MΩ). Each of the amplifiers are used as voltage sources for the analog tape recorder as shown in Fig. 19. A control voltage is also recorded on Ch. 6 of the analog tape recorder indicating the mode of operation of the data acquisition device. A +12 VDC level indicates that the data being taken either corresponds to

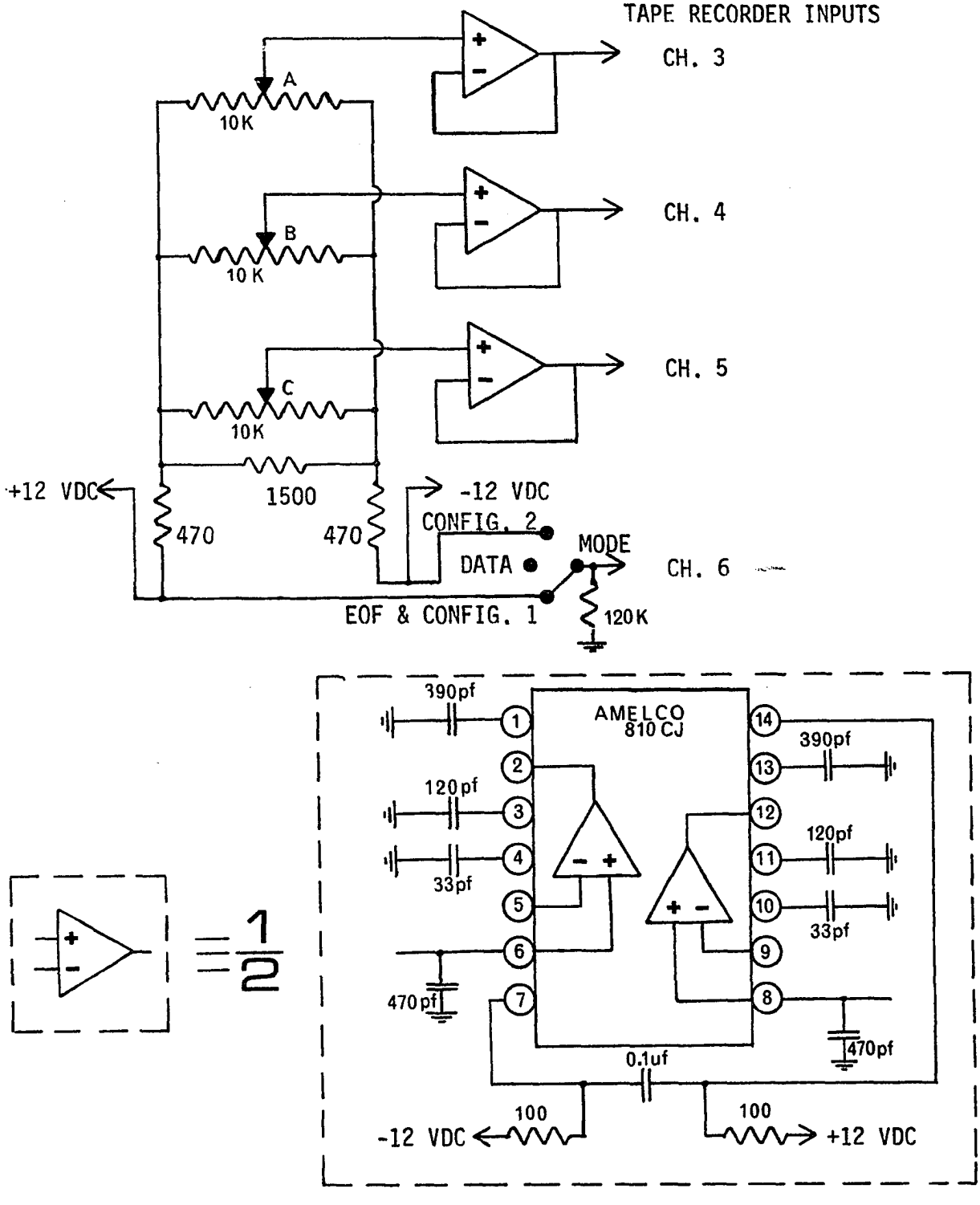

Figure 19. Schematic of circuit for monitoring and recording angular positions of transducer's supporting arm.

one of two calibration modes or to the end of data file (EOF) on analog tape, depending on the order of occurrence. A zero level corresponds to the process of compound scanning. A -12 VDC level corresponds to the other calibration mode. The level recorded on Ch. 6 of the tape can be selected by the operator on a three-position switch located on the front panel of the electronic chasis.

The Ampex Instrumentation Tape Recorder (Model FR-1300) was used to record the six channels of information from the electronic circuits. The mode of operation of each of the 6 recording channels was picked by using the appropriate plug-in modules. Direct record plug-in modules were used used in Channels 3, 4, 5, and 6. All data was recorded at a tape speed of 60 inches/second (IPS). The FM record modules were calibrated with non-standard input voltages at 60 IPS. The principle of calibration is to allow full voltage range recording for each of the angle monitoring voltages while maintaining maximum linearity. Since the voltage from the amplifier monitoring angle A varies only over a ± 4 VDC range while moving the transducer anywhere within the water tank, the FM recording module of Ch. 3 was adjusted such that a +4 VDC level causes a +40% deviation from center frequency and a -4 VDC level causes a -40% frequency deviation. Record modules for Channels 4, 5 and 6 are similarly adjusted such that ± 5.2 VDC, ± 6.0 VDC, and ± 12 VDC each cause $\pm 40\%$ frequency deviation respectively. One-half inch Ampex Corporation instrumentation tape (Model 1.0-741) was used.

D. Experimental Procedure

Before collecting data the mechanical system was calibrated. The alignment of the graph paper's axis below the water tank with the reference wire was checked with a plumb. The position of the meter stick was set so that distances from the center line of the reference pin (pivot of angle A) along the direction of the reference wire were easily measured. The tape unit was allowed to run for at least two hours before recording data eliminating the effects of thermal transients.

The transducer's supporting arm was then held stationary in 4 calibration positions while calibration data was recorded. More specifically, the center line of the pivot of angle C was held directly below the reference wire at a distance of 315 mm from the reference pivot of angle A by two aluminum tubes arising from the transducer's supporting arm near the pivot of angle C and inserting at the periphery of the water tank. Since the length of each of the first two sections of the arm is 315 mm, angles A and B are forced to be either +60° and -120°, or -60° and +120°. While the arm is held in this position, angle C is varied by hand such that the transducer's beam was centered along the direction of the reference wire and directed away from the reference pivot of angle A. With the supporting arm in this position the angles A, B and C were forced to be either +60°, -120°, +60°, or -60°, +120°, -60°. With the mode switch on the front panel of the electronics chasis set to Configuration 1, 100 units of analog tape were recorded for each of the two possible fixed orientations. The process was repeated with the pivot of angle C located directly below the reference wire and 571 mm away from the reference pivot. The transducer's beam was centered along the direction of the reference wire, but

directed towards the reference pivot. With the arm fixed in this position the angles A, B and C were forced to be either +25°, -50°, -155° or -25°, +50°, +155°. With the mode switch set to Configuration 2, 100 units of analog tape were recorded for each of these two possible orientations. After the calibration data was taken, the mode switch was set to Data. The tape unit was started in the record mode and the transducer was moved in a compound scanning manner. Variations in angle C at fundamental frequencies up to 1 Hz are acceptable. When the scanning process was finished, the mode switch on the electronic's chasis was set to EOF, and the tape unit was stopped. The data acquisition phase was completed.

E. Electronic Play-back System

The recorded data on analog magnetic tape was then played back into a Digital Equipment Corporation PDP-12 computer. The tape speed during reproduction was reduced to 7 1/2 IPS. All of the reproduce channels contain modules that operate in the same mode as their respective record channels. The FM reproduce modules are set to operate at the 7 1/2 IPS tape speed. These FM modules are also calibrated in a non-standard manner. Each of the four FM reproduce modules are calibrated such that a +40% frequency deviation from the specified center frequency at 7 1/2 IPS yields a +2 VDC output and a -40% frequency deviation yields a -2 VDC output. Each output is filtered by a passive, RC low-pass network whose zero-frequency gain is 1/2. The purpose of this calibration is to provide a full range of voltage swing to the computer's analog-to-digital converter (ADC) to minimize quantizing error. The range of the ADC is ±1 VDC. The maximum 2 VDC signal from the FM reproduce module of the tape unit is reduced to 1 VDC

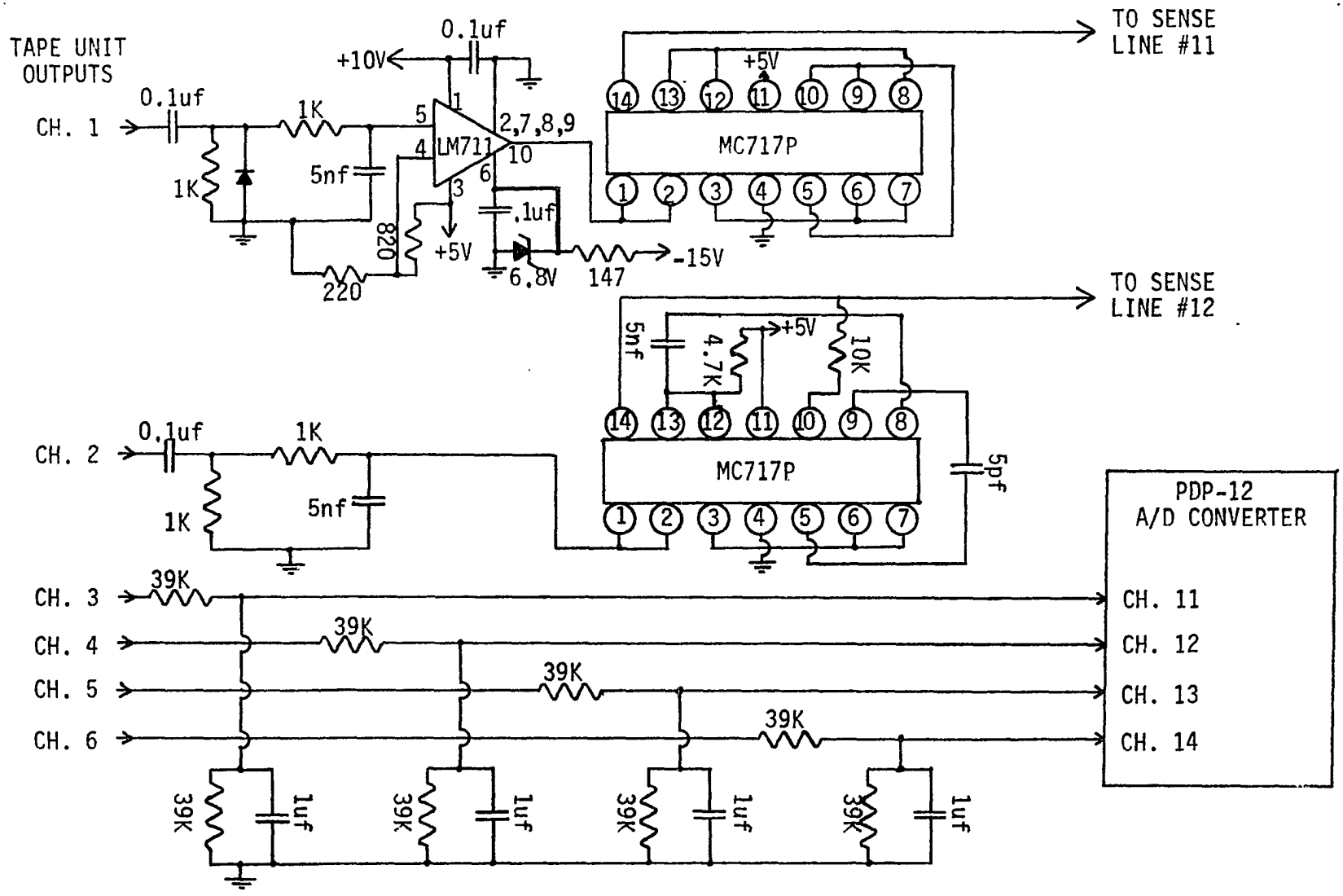

Figure 20. Schematic of circuit for connecting analog tape unit to PDP-12 computer.

by the RC filter network. There is one minor exception in that the FM reproduce module of Ch. 6 was adjusted to give a +60 mv output for 0% deviation.

The electronic circuit used to interface the computer with the six reproduce modules of the tape recorder is shown in Fig. 20. The passive filter is shown in the lower section of the figure. The direct reproduce module of Ch. 1 is filtered to obtain a noise-free, zero based signal. This signal is then processed by a comparator (LM711, National Semiconductor Corporation) which serves as a level detector. The signal from the comparator is shaped and used to control the voltage of the computer's Sense Line 11. During a pulse from Ch. 1 Sense Line 11 is held at 5 VDC. When the output from Ch. 1 is zero the sense line is held near 0 VDC. The pulses on Sense Line 11 correspond to the time expanded pulses from the receiver. The output adjustment on the reproduce module of Ch. 1 was set to cause the sense line pulses to be 20 μs in duration. The signal from the direct reproduce module of Ch. 2 is filtered and used to generate a 40 μs, 5 V pulse on the computer's Sense Line 12. The pulses on Sense Line 12 correspond to the time expanded synchronizing pulses.

F. Computerized Sampling and Data Formating

Since the analog instrumentation tape unit was used as a means of time expansion of data, significant noise was added to the data. The tape unit introduced sinusoidal noise into the outputs of the FM reproduce modules principally at three frequencies: 10KHz, 14 Hz and 7 Hz. The high frequency noise was easily removed by passive filtering. Since the highest

frequency component of the angular data signal was approximately 0.5 Hz, a low-pass filter was used to remove the 7 and 14 Hz components from the total signal. Since low frequency analog filters also introduce time delays, a digital filter (moving, weighted average filter) was used to remove the noise from the three FM channels. Digital filters can be constructed to operate without creating time delays, and can easily be implemented in the computer. The frequency response curve for the digital filter used is shown in Fig. 20. The sampling frequency, f_s, is equal to the synchronizing pulse frequency (56 Hz). Let g(t) be the filtered signal and f(t) be the noisy signal. Then

$$g(t) = [f(t-15T) + 2f(t-14T) + 3f(t-13T) + 6f(t-12T) + 9f(t-11T) + 14f(t-10T) + 20f(t-9T) + 26f(t-8T) + 34f(t-7T) + 42f(t-6T) + 51f(t-5T) + 58f(t-4T) + 65f(t-3T) + 70f(t-2T) + 73f(t-T) + 76f(t) + 73f(t+T) + 70f(t+2T) + \ldots + f(t+15T)]/1024$$

where $T = 1/f_s = 17.8$ millseconds

This filtering function has the frequency response curve shown in Fig. 21, where 28 Hz is its folding frequency.

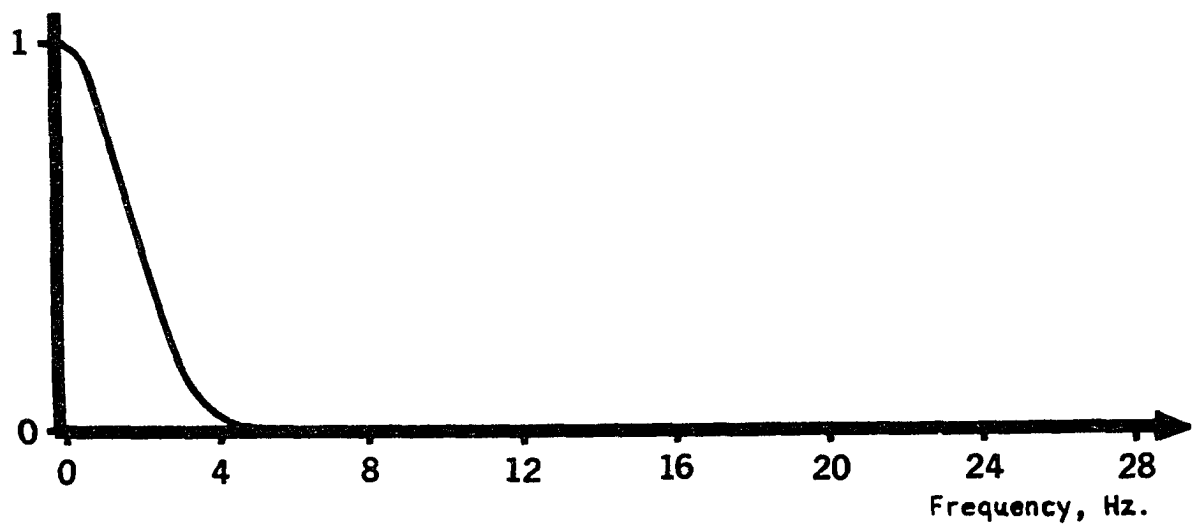

Figure 21. Frequency response of digital filtering function.

The PDP-12 computer is used to digitize and format the data from the analog tape unit. The PDP-12 has a 16 channel multiplexer and a ± 1 V, 10-bit ADC under program control. Only four channels of the ADC are used as shown in Fig. 20. This computer also has 4096 addresses of 12-bit words in core memory and two digital magnetic tape units for additional permanent storage. The digital magnetic tape (Linc tape) has 131,072 addresses of 12-bit words for storage purposes. The program which inputs and formats the analog tape data is called DATAIN.

The following paragraphs are a description of the operation of DATAIN. Channel 14 of the ADC is sampled to determine if the data on the other channels of the analog tape unit corresponds to a calibration mode or to the compound scanning mode. If the data on analog tape was collected in the calibration mode, 63 samples of each of the other three channels (11, 12, and 13) are taken at a sampling rate of 7/8 Hz and are stored in core. In the calibration mode the values of the three angles were held constant. Thus, the only variation in the voltages to the three ADC channels is due to the noise of the tape unit. The low sampling rate is used to ensure that many cycles of the noisy signals are included in each of the three data sets. Later in the computation process with the larger computer, each set of 63 samples will be averaged to obtain one representative value for each of the known angles. After the sampling process is finished the data which has been accumulated in core is transferred to Linc tape. The computer's operation is terminated until it is manually restarted at the beginning address of the program. This process is repeated for each of the four calibration orientations of the transducer's supporting arm. The numbers are stored in core and on Linc tape in the following format: N,

A_1, B_1, C_1, N, A_1, B_1, C_1, . . . where N is a number used only for punctuation purposes. Then it is always known that the number immediately following N corresponds to the value of angle A, and likewise for angles B and C. In the calibration modes N is equal to 1025, 1026, 1027, or 1028 depending on the orientation of the arm. In the data mode N is equal to 1024. These are the decimal equivalents of the octal numbers used in the actual program.

If the data on the analog tape was collected in the compound scanning mode, the computer is then directed to wait for the synchronizing pulse on Sense Line 12. The computer samples this sense line every 5 μs to find the beginning of the synchronizing pulse. After the pulse is sensed, the computer waits for the generator pulse to occur on Sense Line 11. After the occurrence of the generator pulse the computer continues to sample Sense Line 11 at a rate of 50,520 Hz checking for the occurrence of echo pulses and counting the number of sample periods expired since the generator pulse was first detected. Each time an echo pulse is sensed, the number stored in the counter of expired sample periods is also stored in the next sequential data address in core. After a given number of samples are taken on Sense Line 11, the sampling process stops. All echoes returning between this time and the next generator pulse are ignored. The punctuation number, 1024, is stored in the next sequential address and the next three addresses are left vacant so that the computed numbers corresponding to the three angles of A, B and C at the time of the generator pulse can be substituted later by the digital filter routine. Channel 14 of the ADC is sampled again to determine if the compound scanning process has terminated. If the process has not terminated, the digital filtering phase is

entered. The three noisy ADC channels of 11, 12 and 13 are sampled and stored in the storage area of the filter. These numbers roughly correspond to the three angles of A, B and C at the time of the generator pulse and are used to compute the filtered numbers corresponding to the angles of A, B and C for previous generator pulses. These computed numbers are returned to the appropriate vacant addresses in the data core. Then the computer returns to wait for the next synchronizing pulse and the whole process is repeated. When nearly 1024 addresses in the computer's data core are filled, a new set of 1024 addresses is used for storage while the contents of the previously filled set are transferred to Linc tape for permanent storage. When the new set is filled, the old set of addresses is used for storage while the contents of the new set are transferred to Linc tape. The flow chart for DATAIN, the set of instructions for DATAIN and a typical example of a sequence of numbers stored on Linc tape by DATAIN corresponding to both calibration and scanning data are all shown in Appendix A.

Although the analog tape's data has been digitized and formated onto Linc tape, an additional step must be accomplished. The larger IBM System/360 computer cannot read Linc tapes. The data on the tape must be transferred to an IBM compatible tape. A Digital Equipment Corporation LINC-8 computer having an IBM compatible, 7 track, incremental tape recorder was used to translate the Linc tape. The Linc tapes generated on the PDP-12 are read into core in the LINC-8. The LINC-8 computer then converts the octal numbers into BCD (Binary Coded Decimal) format and writes them on the IBM compatible, incremental tape recorder. Each octal number is converted into a signed, four digit, coded decimal number on incremental tape.

After every 200 numbers are written, an interrecord gap (IRG) is generated. Thus, one block of numbers on the incremental tape may be read on the IBM System/360 computer using FORTRAN IV programing language under the format of 200I5. The incremental tape recorder was set to write at a bit density of 556 BPI. Odd parity was also used. To use the incremental tape recorder with the LINC-8 computer, the basic operating program of the small computer, PROGOFOP, was modified. Appendix B lists the changes that were made to the standard PROGOFOP routine after it was loaded into core. The transfer of data from Linc tape to IBM compatible, 7 track tape was accomplished by IBMTAP, which was loaded into core by the modified PROGOFOP routine. A flow chart of IBMTAP and a listing of the set of mnemonic instructions is given in Appendix B.

G. Computerized Data Processing

Subsequently the 7 track, incremental tape was processed according to a FORTRAN IV program by the IBM System/360 computer. Appendix C contains a generalized flow chart and the listing of the main FORTRAN program and control cards. The punctuation numbers in the data tape were used to identify the mode in which the data was taken during the acquisition process. Guided by these punctuation numbers, the computer first computes the calibration constants from the calibration data for the known angles. Using this data, a three-segment, piecewise-linear approximation to the functional relationship between the quantized numbers and the angular values associated with those numbers is constructed for angles A, B and C. Then when a sequence of numbers is encountered in the data tape corresponding to data taken in the compound scanning mode, the assumed position of the target is

calculated using equations (1) and (2) where the values for A, B and C are determined by using the previously constructed piecewise-linear approximations. The value used for D is 315 mm and the value used for D_t is 60 mm. The value for S is determined from equation (3)

where $$T = T_r/8 \quad (4)$$

where T_r = time for echo pulse to return during reproduction on tape unit with tape speed reduced by one-eighth.

But $$T_r = nT_s \quad (5)$$

where T_s = time interval between samples made by the computer on the reproduced output of the receiver.

n = number stored in data sequence on digital tape which is the number of samples taken between the generator pulse and the echo pulse.

and $$T_s = 1/f_s$$

where f_s = sampling rate on reproduced output of receiver. (6)

Combining (3), (4), (5), and (6) yields

$$S = \frac{vn}{16f_s} = \frac{(1.5\ 10^6)\ n}{(16)\ (50{,}520)}$$

or $$S = 1.85\ n \quad (7)$$

Combining (1), (2), and (7)

$$X = 315 \cos(A) + 315 \cos(A+B) + (60+1.85n) \cos(A+B+C) \quad (8)$$

$$Y = 315 \sin(A) + 315 \sin(A+B) + (60+1.85n) \sin(A+B+C) \quad (9)$$

If the droop of the mechanical arm appears to be significant, then it is possible to modify (8) and (9) to account for this effect - see Appendix D.

Using equations (8) and (9) it is possible to calculate from the sequence of numbers stored on the data tape the assumed position of the target which caused an echo to return to the transducer within the required time. For each target position calculated, the contents of the corresponding word in core should be incremented by one to generate the desired likelihood function, i.e. using FORTRAN IV.

$$\text{ARRAY (I, J)} + \text{ARRAY (I, J)} + 1.0 \quad (10)$$

where

$$I = (X-KONST + 100)/2 \quad (11)$$

$$J = Y/2 + 50 \quad (12)$$

where where KONST = the measured distance from the reference pin of angle A to the approximate center of the object under ultrasonic investigation.

Thus, as Y varies over the range [-98,100], J varies over the range [1,100] and as X varies over the range (KONST-98, KONST+100], I also varies over the range [1,100]. In the actual program the values of I and J are integral, and are picked to be the integers closest to the corresponding values of X and Y. In the main program the computer continuously calculates the assumed positions of the object and increments the appropriate addresses in core until the end of the data on the data tape is encountered. Then depending on the presence or absence of a "GO TO 104" statement in the main

program, the computer either plots the processed echogram or the isometric drawing of the likelihood function. The decision theory used in plotting the processed echogram is the same as that discussed in Chapter 4. Both types of plotting routines are called from the main program as subroutines. At the Iowa State University Computation Center, the subroutine used in plotting the processed echograms is called SIMPLOTTER. The subroutine used in plotting the likelihood distribution, f(I, J), is called THREED and is inputted to the computer as an object deck.

V. EXPERIMENTAL RESULTS AND CONCLUSIONS

Figures 22 through 36 show the computer drawings representing likelihood distributions and processed echograms of several experimental targets. A reference mark in the upper right hand corner of each likelihood distribution indicates the orientation of the coordinate system as shown in Fig. 22. Each unit grid on the X-Y plane represents a distance of 2 mm. The absolute positions of the targets in the water bath are given by their coordinates on the processed echograms. All regions processed were 200 mm x 200 mm.

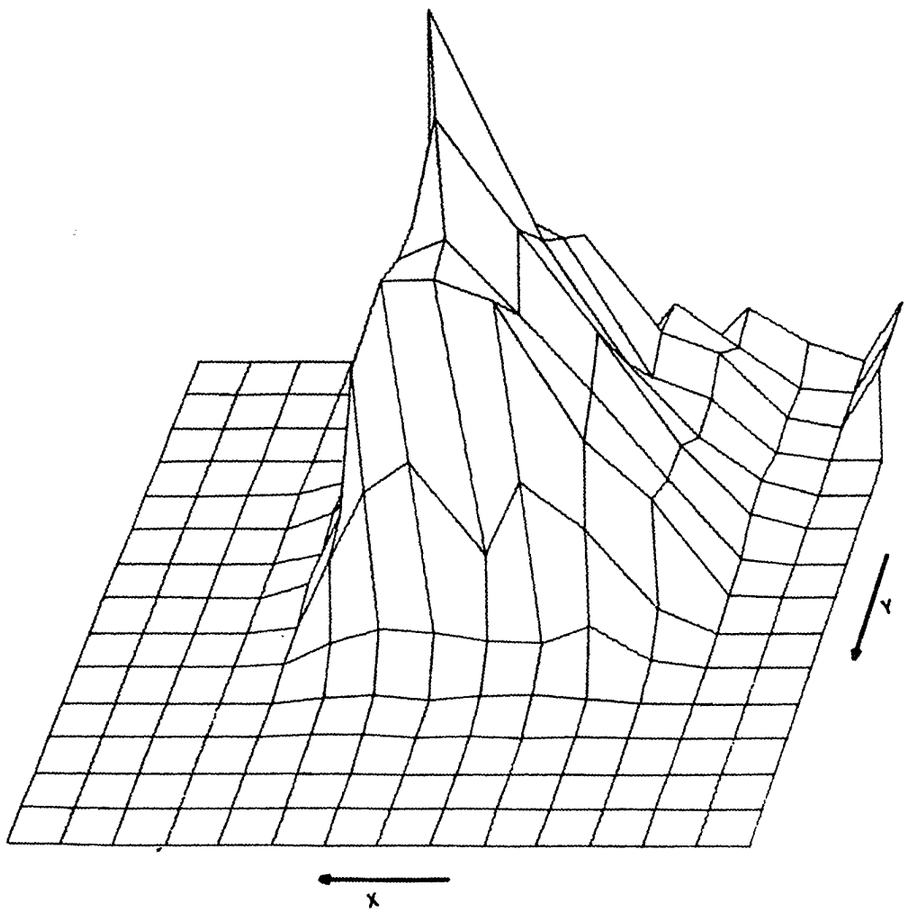

Figure 22. Likelihood distribution with no spacial smoothing for ultrasonic cross-section of a single 2.38 mm diameter aluminum rod.

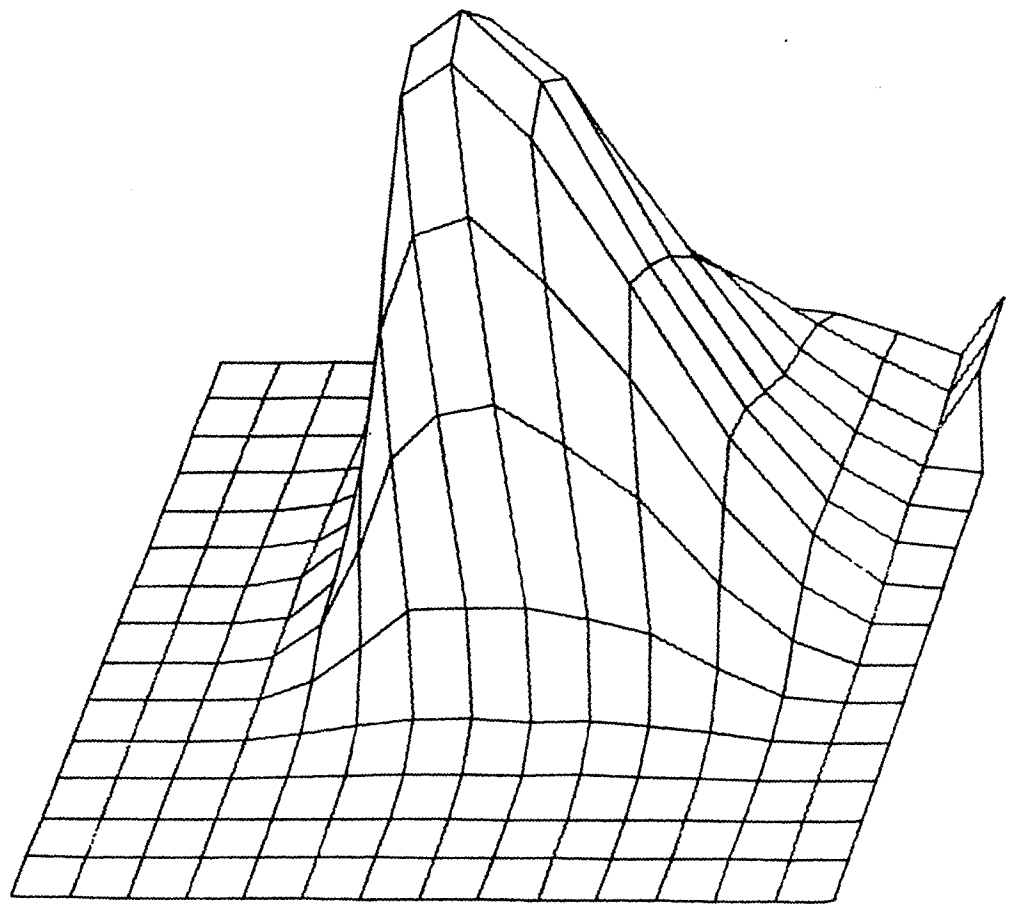

Figure 23. Likelihood distribution of Fig. 22 with spacial smoothing to reduce effects of randomized angular quantization error and analog tape speed variations.

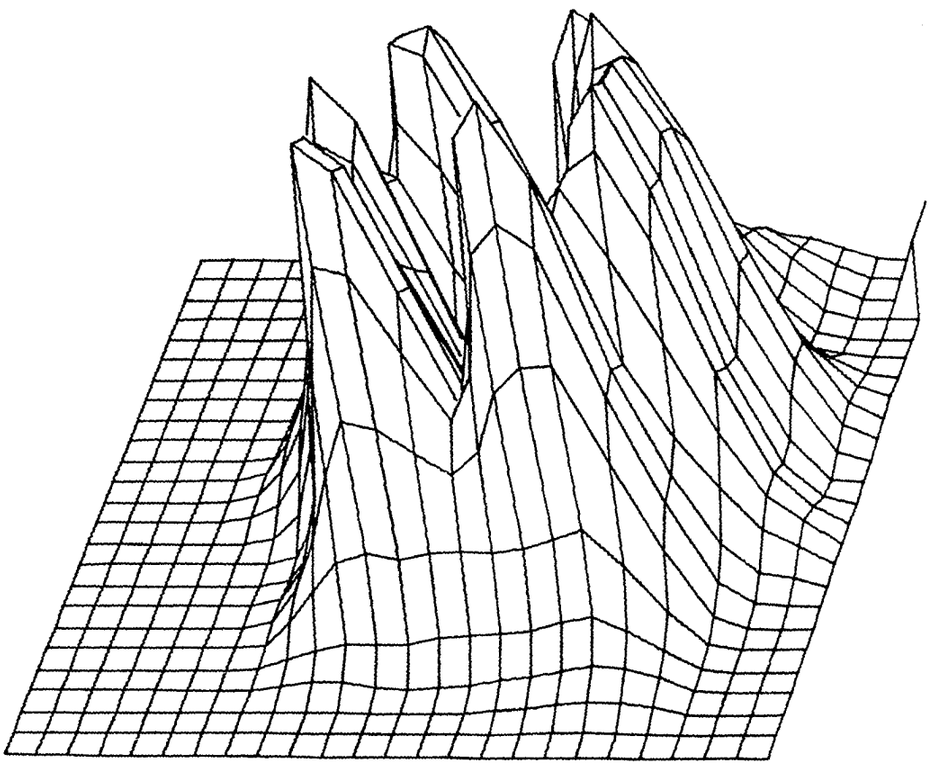

Figure 24. Smoothed likelihood distribution for ultrasonic cross-section of six 2.38 mm diameter, parallel aluminum rods arranged in a pattern shown by the circles of Fig. 27.

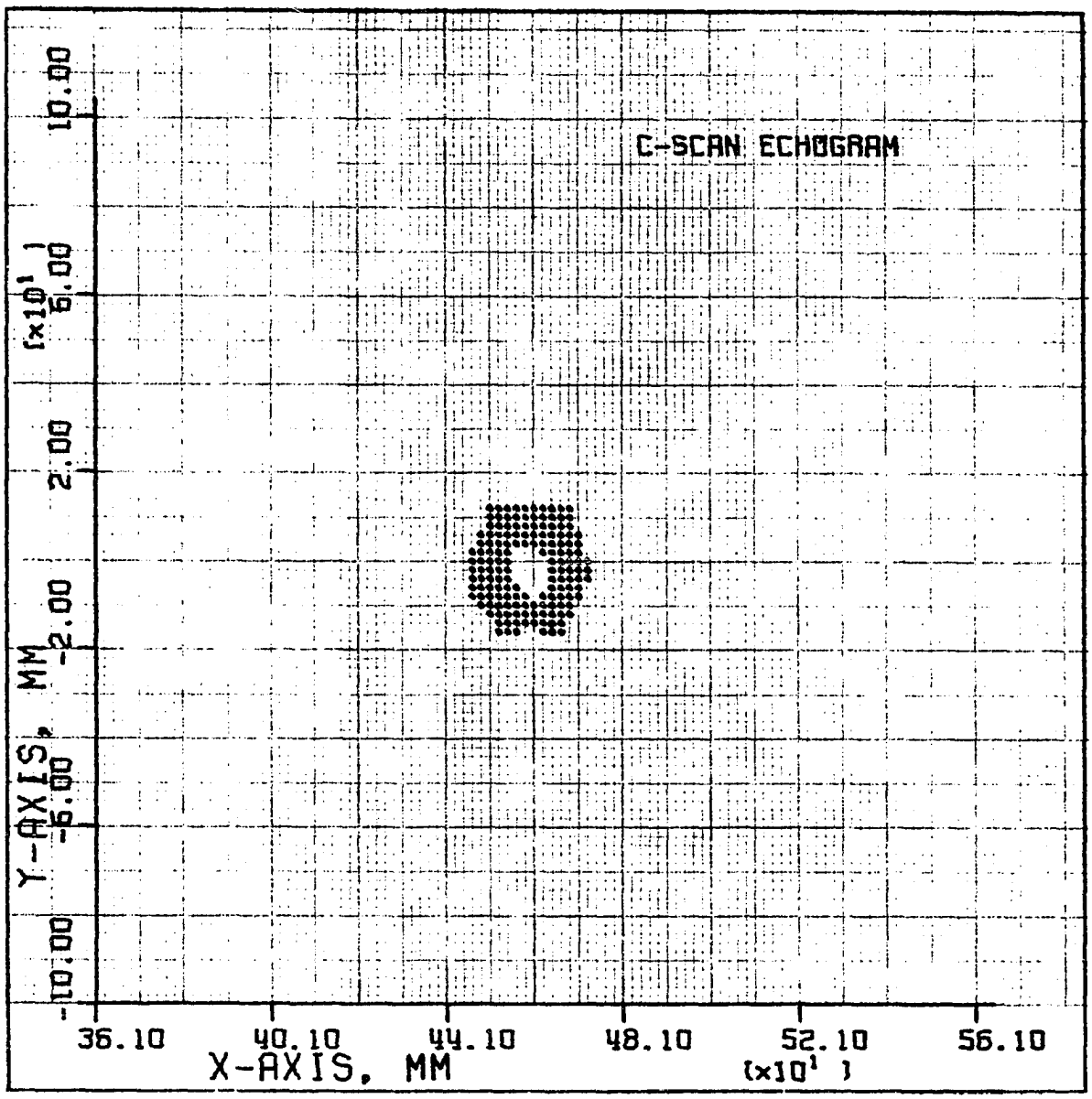

Figure 25. Ultrasonic echogram simulating the effect of image saturation with the distribution of Fig. 24 for the 6 rods by plotting all points in the 200 mm x 200 mm region that have values for the distribution greater than $f_m/3$, where f_m is the distribution's maximum value (threshold = $f_m/3$).

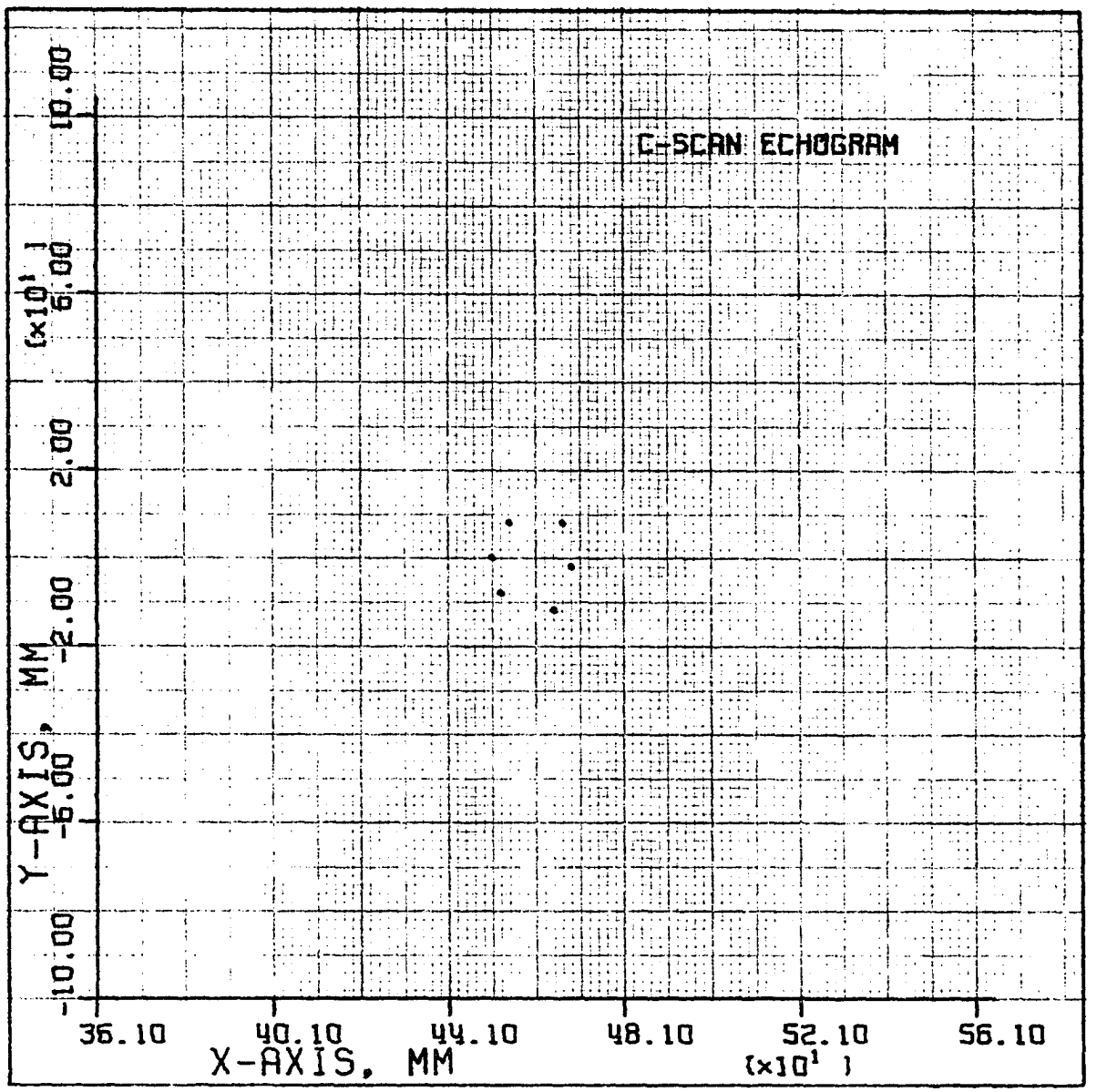

Figure 26. Processed echogram constructed by using peak detection theory on distribution of Fig. 24 for 6 rods (threshold = $f_m/3$).

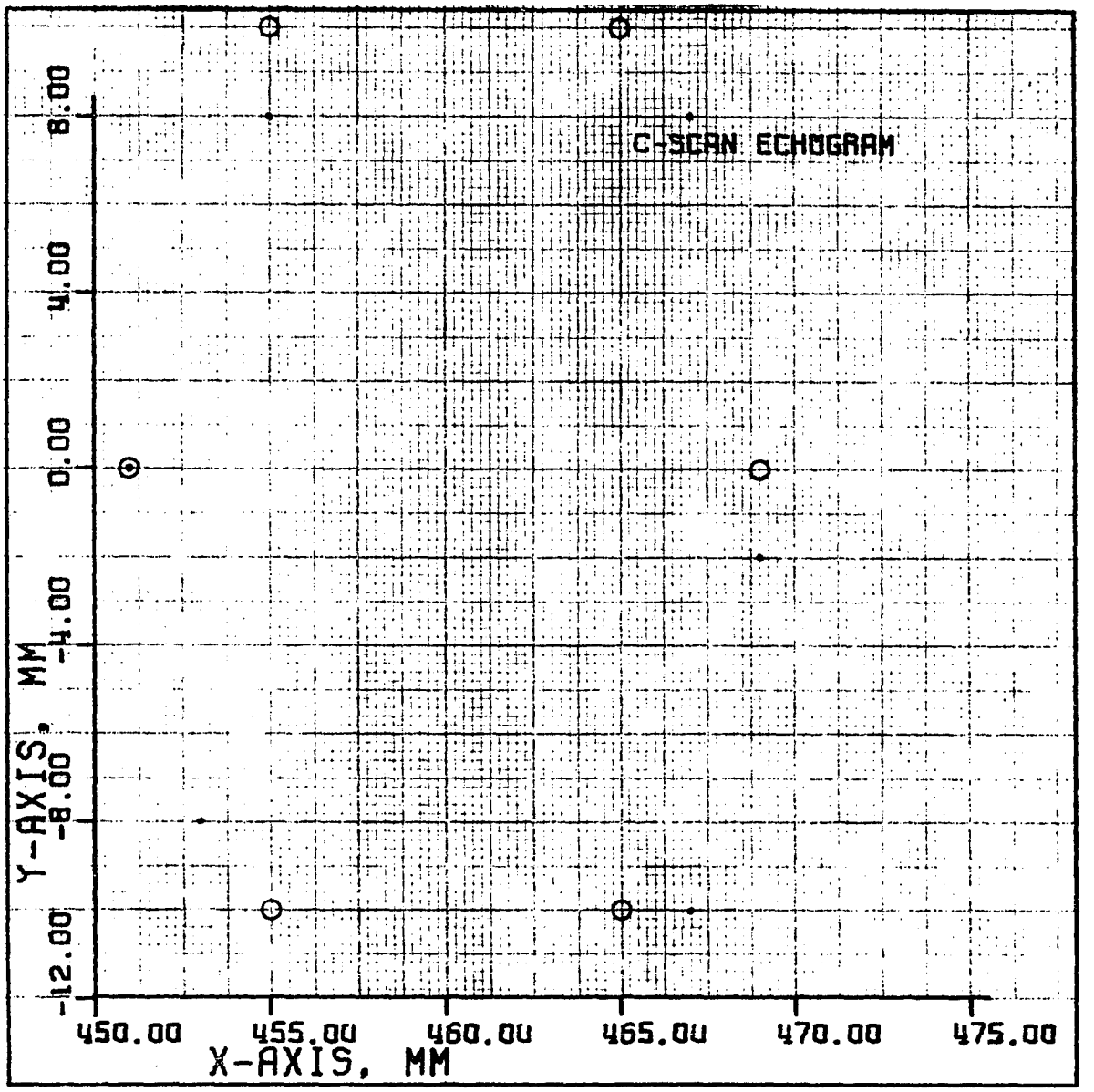

Figure 27. Points show processed echogram of distribution similar to Fig. 24 with larger scale factor. Circles show actual locations of 2.38 mm diameter aluminum rods.

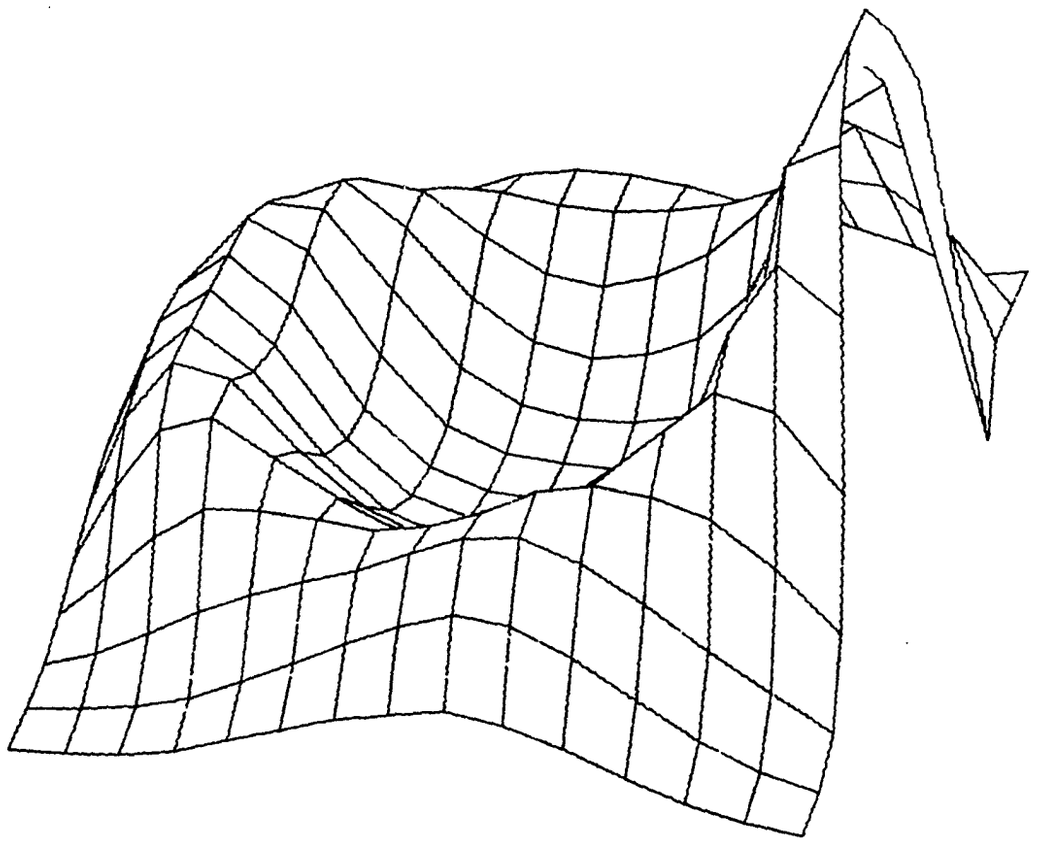

Figure 28. Small region from total smoothed likelihood distribution for ultrasonic cross section of an air filled, 25.4 mm OD plexiglass tube with 1.59 mm wall thickness.

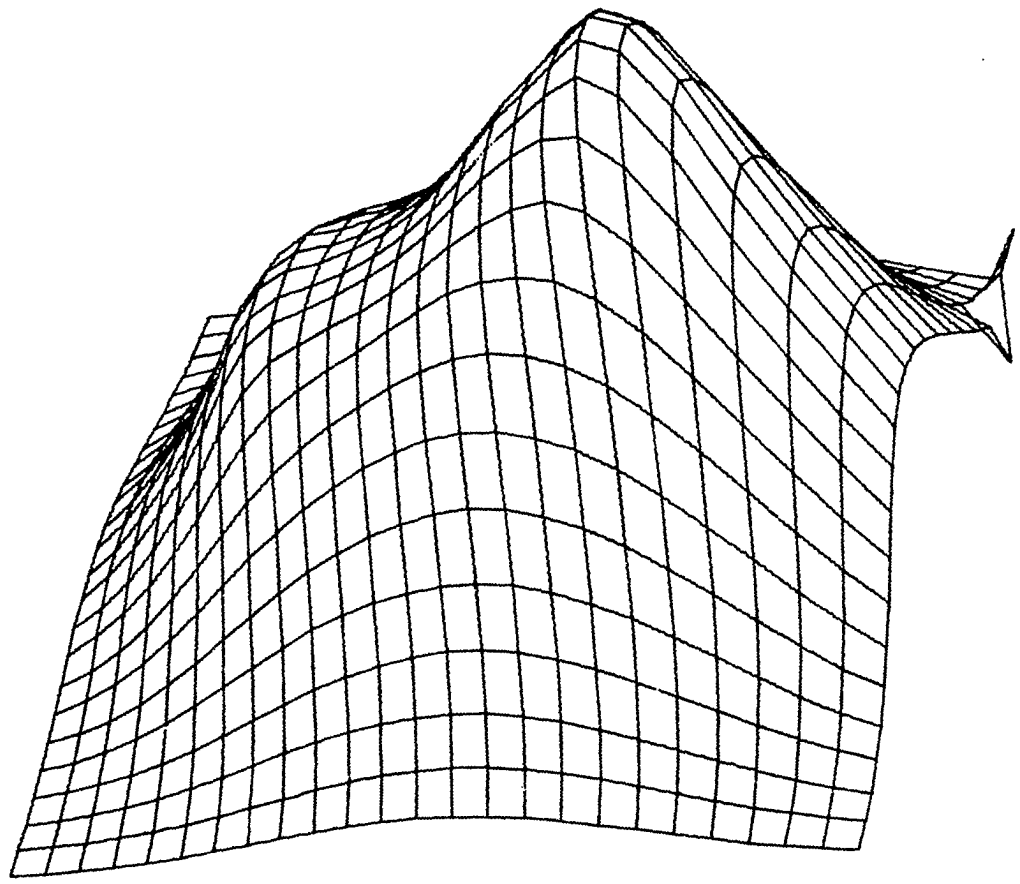

Figure 29. Likelihood distribution constructed from identical data used for Fig. 28 with too much spacial smoothing.

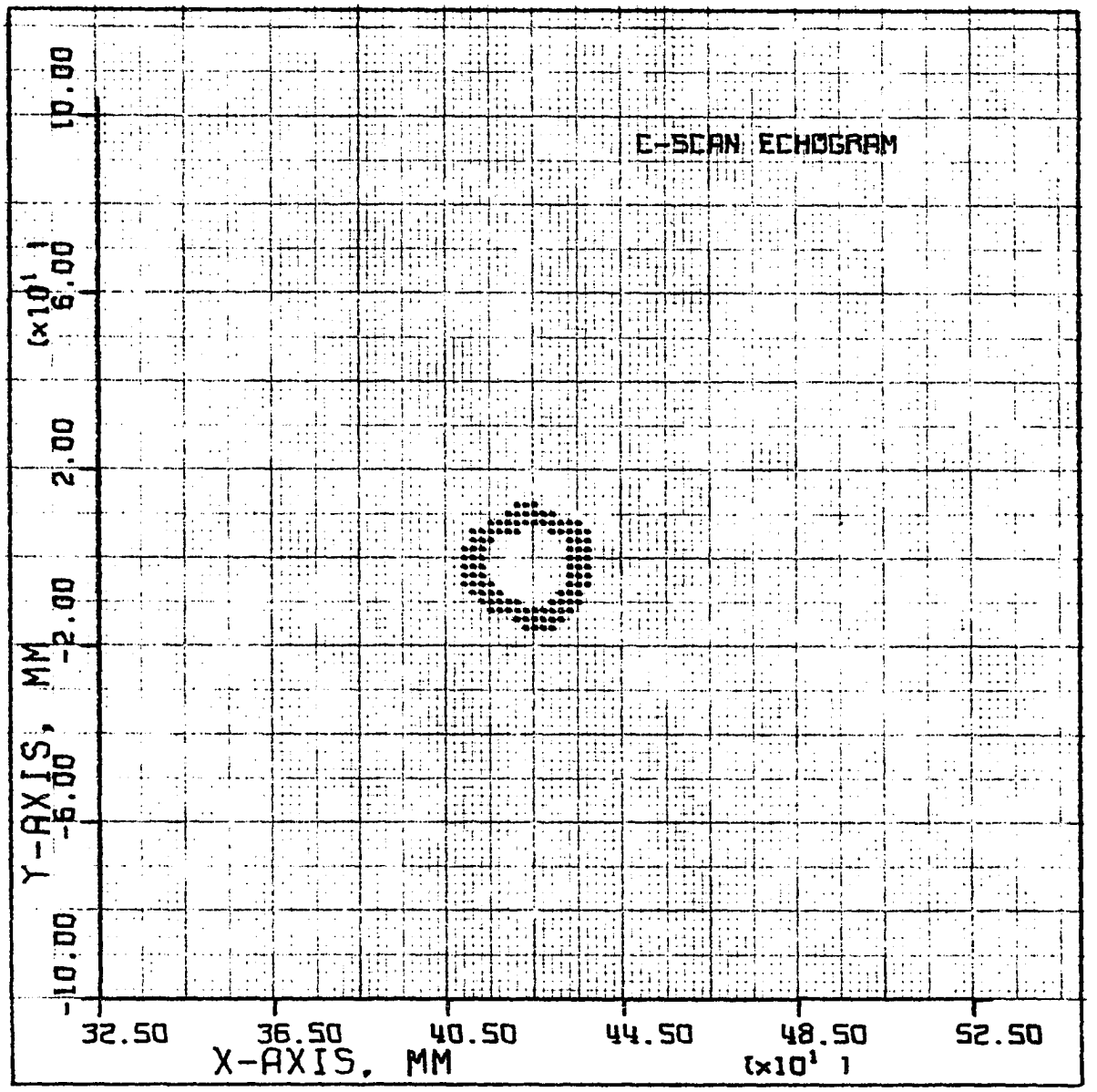

Figure 30. Ultrasonic echogram simulating effect of image saturation with the distribution of Fig. 28 for plexiglass tube (threshold = $f_m/32$).

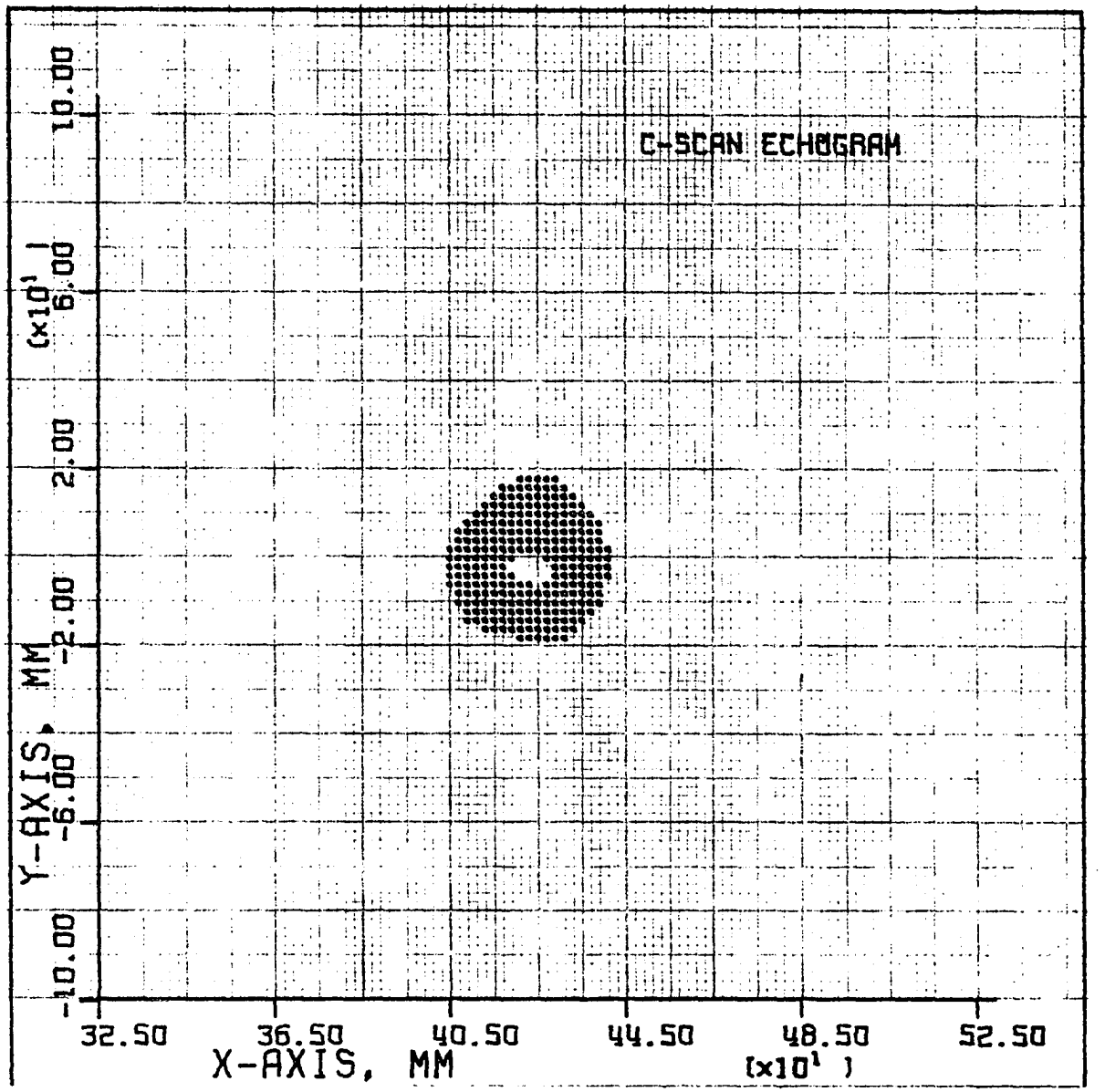

Figure 31. Ultrasonic echogram simulating effect of image saturation with the distribution of Fig. 28 for plexiglass tube (threshold = $f_m/64$).

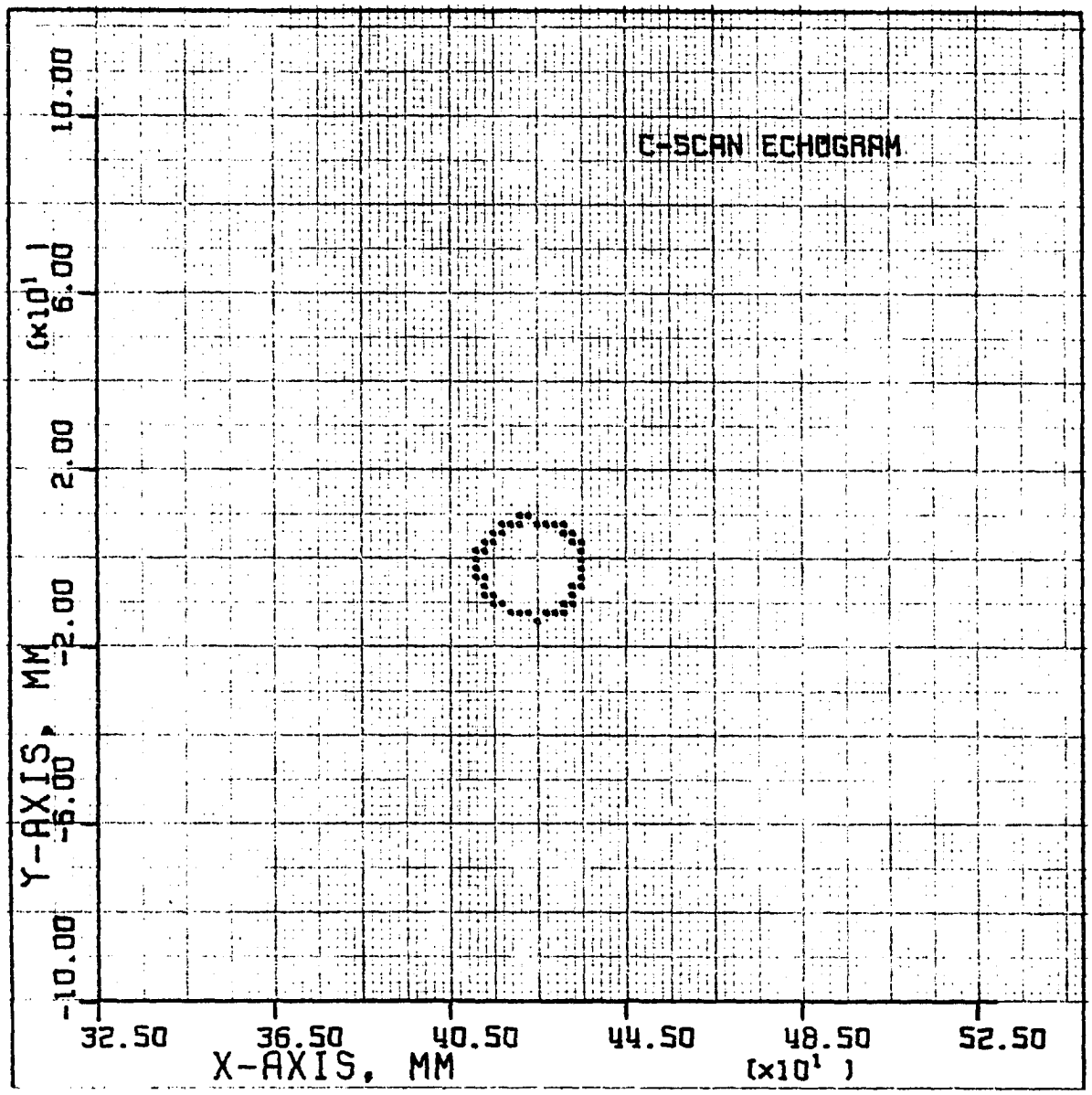

Figure 32. Processed echogram constructed by using ridge detection theory on the distribution of Fig. 28 for plexiglass tube (threshold = $f_m/64$).

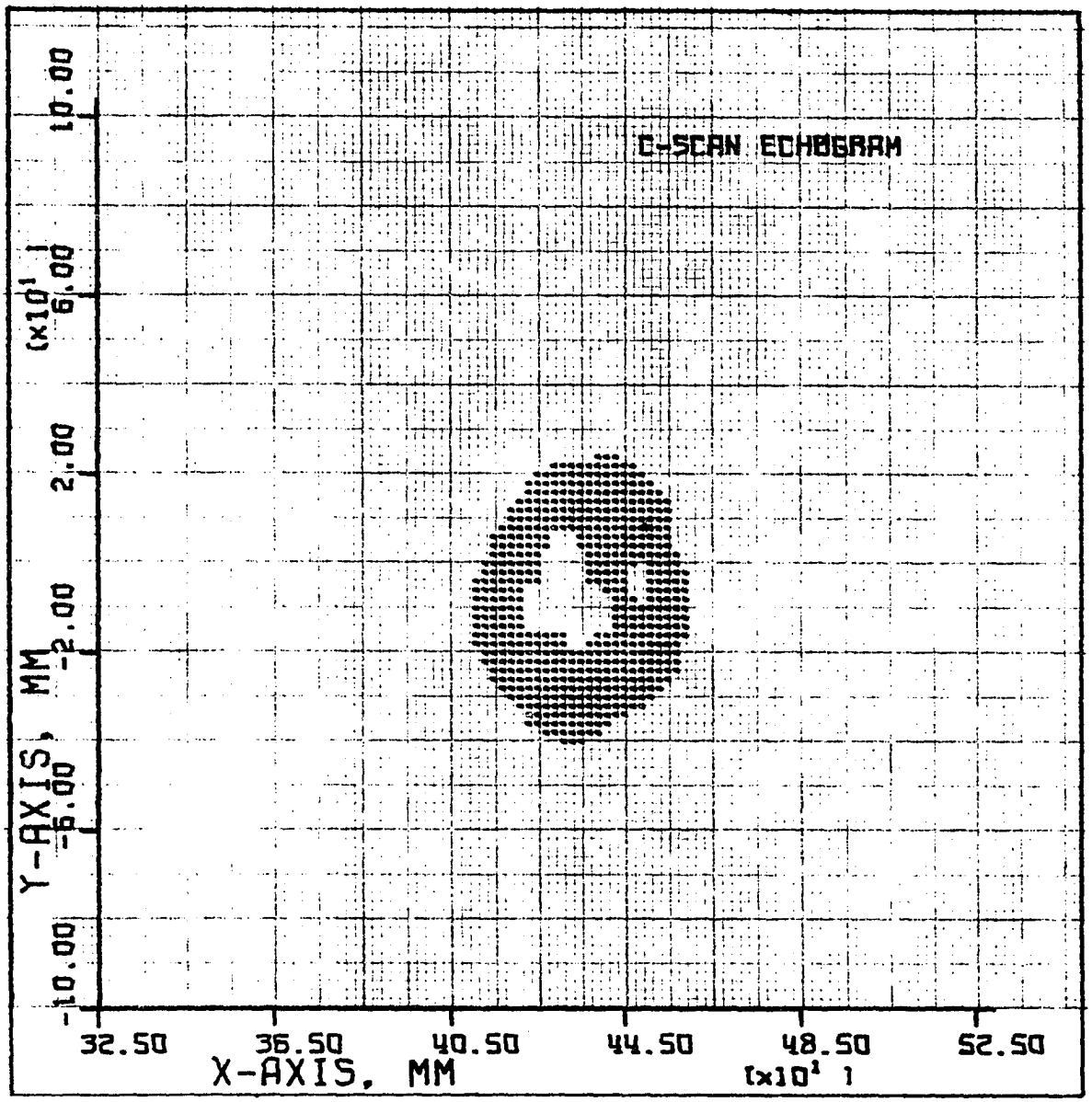

Figure 33. Echogram simulating effect of image saturation for the ultrasonic cross section of the right arm at a level of 25 mm above the wrist with dorsal surface of the arm pointing in the direction of increasing X (threshold = $f_m/16$).

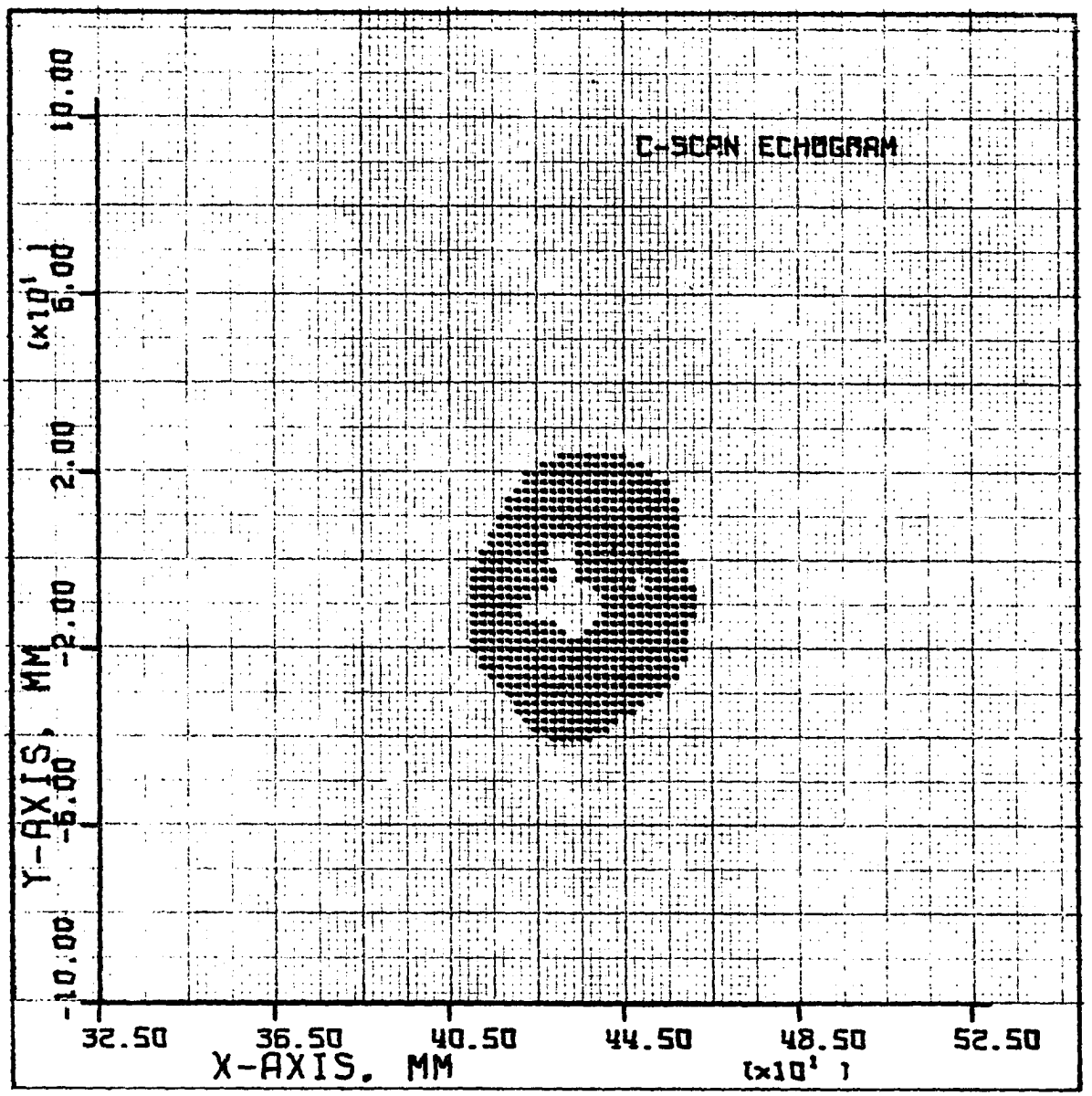

Figure 34. Echogram simulating effect of image saturation for the same arm as in Fig. 33 (threshold = $f_m/32$).

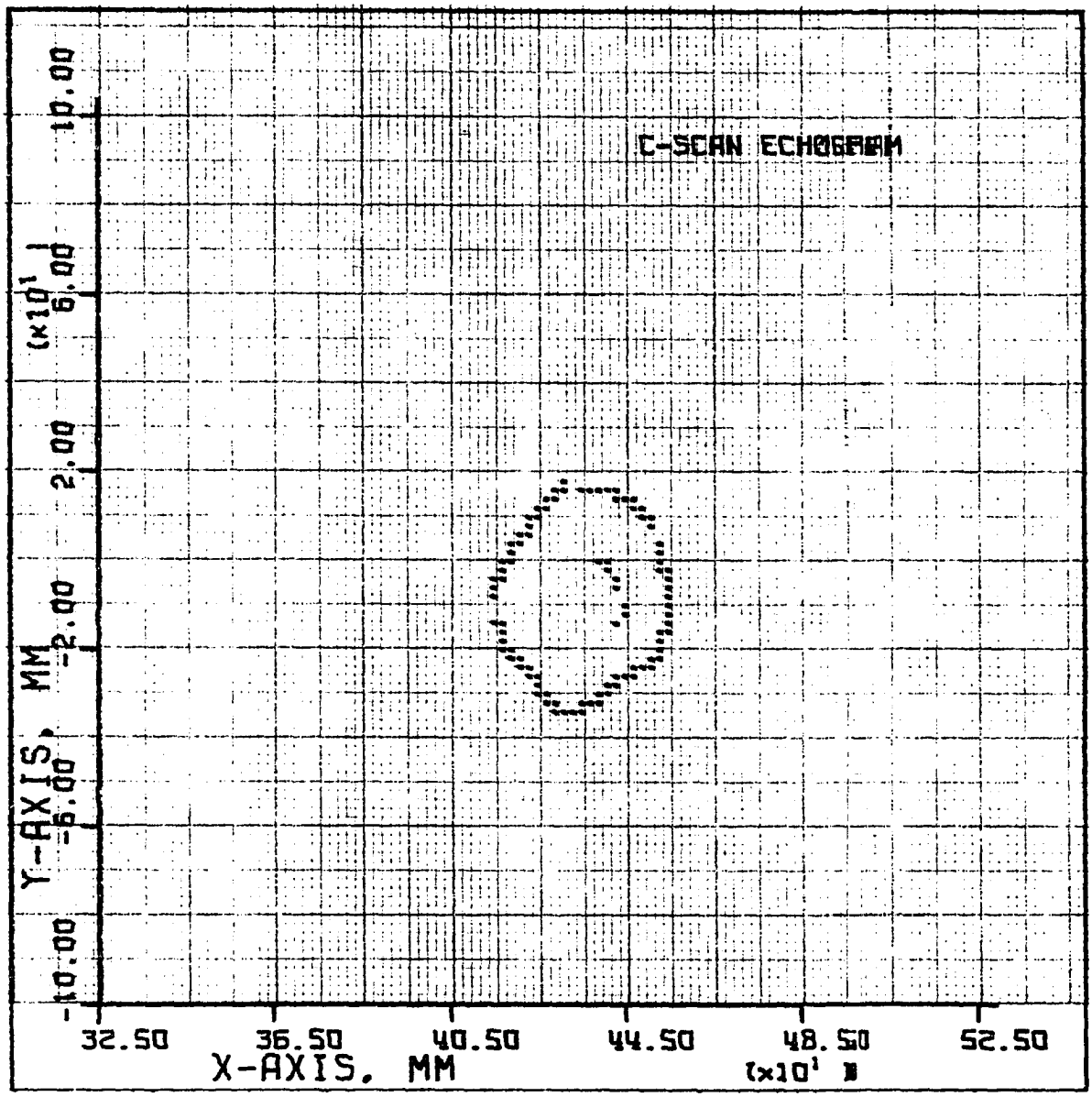

Figure 35. Processed echogram of the same arm as in Fig. 33 showing part of the outlines of the Radius and Ulna bones (threshold = $f_m/16$).

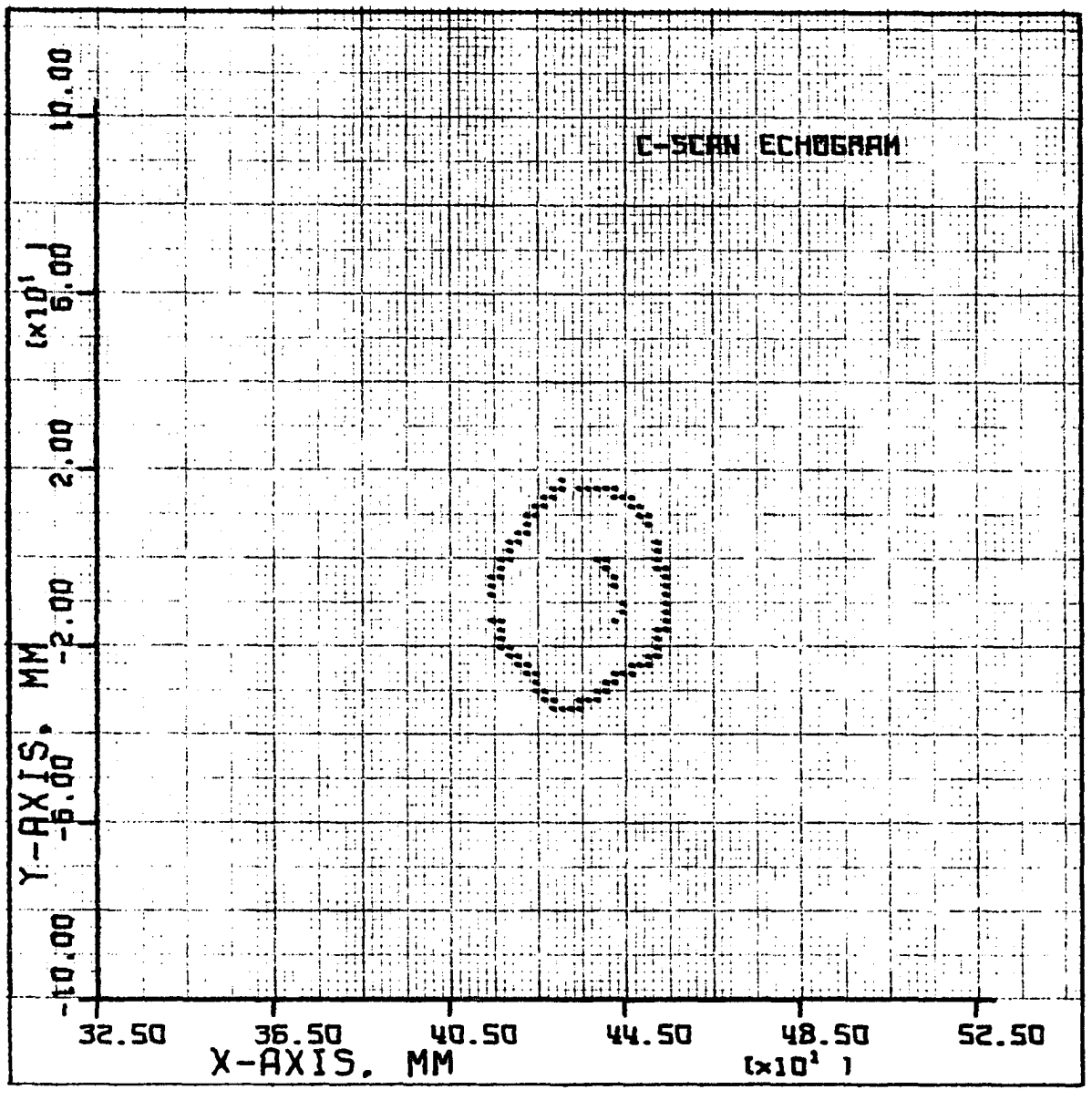

Figure 36. Processed echogram of the same arm as in Fig. 33 (threshold = $f_m/32$).

The pseudo three-dimensional drawing of the two-dimensional likelihood functions show no saturation. Thus, they contain all of the information from the scanning process. This isometric means of presentation is useful because it allows the diagnostician to make complex decisions about the configuration of the target. As an option, the computer program can also generate a processed echogram based on a given decision set. A distinct improvement in resolution is seen in Figures 26, 32 and 35 by using a very elementary decision set. However, the smoothness of boundaries in these processed echograms suffer from the effect of spacial quantization defined by equations (13) and (14), where X and Y are determined from the given integral values of I and J. This effect could be reduced by decreasing the basic quantized intervals for both axes, or by using a more sophisticated plotting routine to plot an interpolated, smooth line based on the supplied points.

In general, the processed echograms also lack the errors associated with multiple reflections between the transducer and any given boundary. Specifically, while recording the data used to generate Fig. 32, many multireflections between the transducer and the cylinder were observed by monitoring the receiver. Yet, the tendency of multireflections to create pseudo targets on the echograms is not apparent in Figs. 30, 31 and 32 due to the thresholds used. The ease of picking the threshold is implied from Figs. 35 and 36.

It is not desirable to have the resolution of the system limited by the graphics display. Typically, the resolution of present systems is limited by the diameter of the intensified dot on the CRT display. How-

ever, this system has the ability to scan a large region and to plot any segment of it with any desired scale factor. As shown in Fig. 27, only the interesting portion of the entire region is plotted.

Ideally, the resolution of any system not limited by image saturation is dependent only on its axial resolution as shown by the theory used to generate Fig. 7. However, it is obvious that the system's resolution cannot exceed the basic spacial quantizing interval. If the associated distances assigned by equations (11) and (12) along the X- and Y-axis between grid points shown in Fig. 16 are only 2 mm, it would be impossible to resolve two small targets separated by 0.5 mm. Likewise, it would be wasteful to pick the constants of equations (11) and (12) such that the spacial quantization interval between grid points is 0.5 mm while the system's axial resolution is 5 mm. Another factor influencing the system's overall resolution is the accuracy in detecting the actual position and direction of the transducer. If the ADC used to convert the monitored voltages of the angular position potentiometers is a 10-bit converter and the full range of some particular angle is 330°, then it is possible for the ADC to miss the correct digitized value by $330°/2^{10}$, or approximately 0.3°. This maximum angular error in radians is multiplied by the length of the arm's section to obtain the maximum possible error in determining the end position of that section. Since the digital filter uses 31 samples to form a weighted average, the quantization error in conversion is decreased by at least a factor of 4. It is then possible to assume a 12-bit ADC is used on an unfiltered, noiseless voltage signal. On this basis it is possible to miscalculate the position of a target lying 140 mm away from the trans-

ducer by a maximum of e_m where

$$e_m = \left[315 \left[\frac{200}{2^{12}}\right] + 315 \left[\frac{200}{2^{12}} + \frac{330}{2^{12}}\right] + 200 \left[\frac{200}{2^{12}} + \frac{330}{2^{12}} + \frac{330}{2^{12}}\right]\right] \frac{3.14}{180}$$

or

$$e_m = 1.71 \text{ mm}$$

It is obvious that no matter how small the axial resolution is made, this system's resolution cannot be made significantly better than 1.7 mm.

The tendency of spacial smoothing on the likelihood distribution to degrade the system's resolution is shown by comparing Figures 28 and 29. However, the difference between the distributions of Fig. 22 and Fig. 23 shows the necessity of spacial smoothing to compensate for the effects of random errors. Notice that in this case the effects of random error displaced the position of the distribution's maximum a distance of 2 mm along the direction of the Y-axis. In addition, distributions similar to Fig. 22 lacking compensation for the random errors may contain many erroneous maxima that confuse the decision process for generating processed echograms. The analog tape unit and the ADC were the two probable sources of this random error. The speed of the analog tape unit varied randomly about 1% due to the hunting action of the phase-lock control system. While its effect in the FM modules was nearly removed by filtering their signals, the effect in the direct record modules of varying the time interval between the generator pulse and its echo pulses was not removed. This uncompensated source of error was probably the major factor causing the distribution of Fig. 23 to have a larger variance than that predicted in Fig. 12.

The actual experimental resolution of the system can be inferred from the distribution of Fig. 24. The separation of the two peaks closest to the viewer is 12 mm. It also appears that these two subdistributions could

be moved 4 mm closer to each other without losing the two distinct peaks. Any closer positioning of these two subdistributions would result in a distribution with one peak instead of two. Thus the minimum separation between peaks is 8 mm. However the positions of the peaks represent the positions of the centers of rods. Since an 8 mm separation of peaks corresponds to a (8 - 2.38) mm separation between rods, the system's resolution is approximately 6 mm. Although two small targets must be separated by 6 mm to be resolved, it appears from Fig. 27 that the error in locating the position of a resolvable target is less than $2\sqrt{2}$ or 2.8 mm.

Note that the theory is based on the assumptions that the transducer's beamwidth is very large and that all targets possess vertical symmetry. Often the structure of an organism approaches vertical symmetry within the limited volume scanned by the beam. But with the restriction of vertical symmetry removed azimuthal resolution again becomes important because objects out of the scanning plane influence the resulting distribution. If along with removing the restriction of vertical symmetry the use of uniform, three-dimensional compound scanning is adopted, the theory derived in Chapter III is again relevant and the system's resolution becomes independent of beamwidth. It is important to note that this computerized system can be modified into a system that constructs a three-dimensional likelihood function and plots a processed echogram from any particular plane of the three-dimensional region. Although the size requirements of computer memory increase, such a system is entirely feasible.

Since it may appear to some readers that the total system is hopelessly complex, they should note that the system was constructed with equipment in the University's inventory. The purpose of such a design is to test the

concept in as inexpensive manner as possible. However, now that the concept has been shown to be valuable, any future use of similar systems requires that the equipment for the total system be redesigned to include the most effective and efficient equipment available. It is definitely desirable to remove the instrumentation tape recorder from the system and eliminate the associated errors and the need of a digital filter.

A suggested system that would be simple and highly accurate is shown in Fig. 37. A small digital controller regulates the operation and sequencing of the subsystems. The controller first causes the acoustic pulse

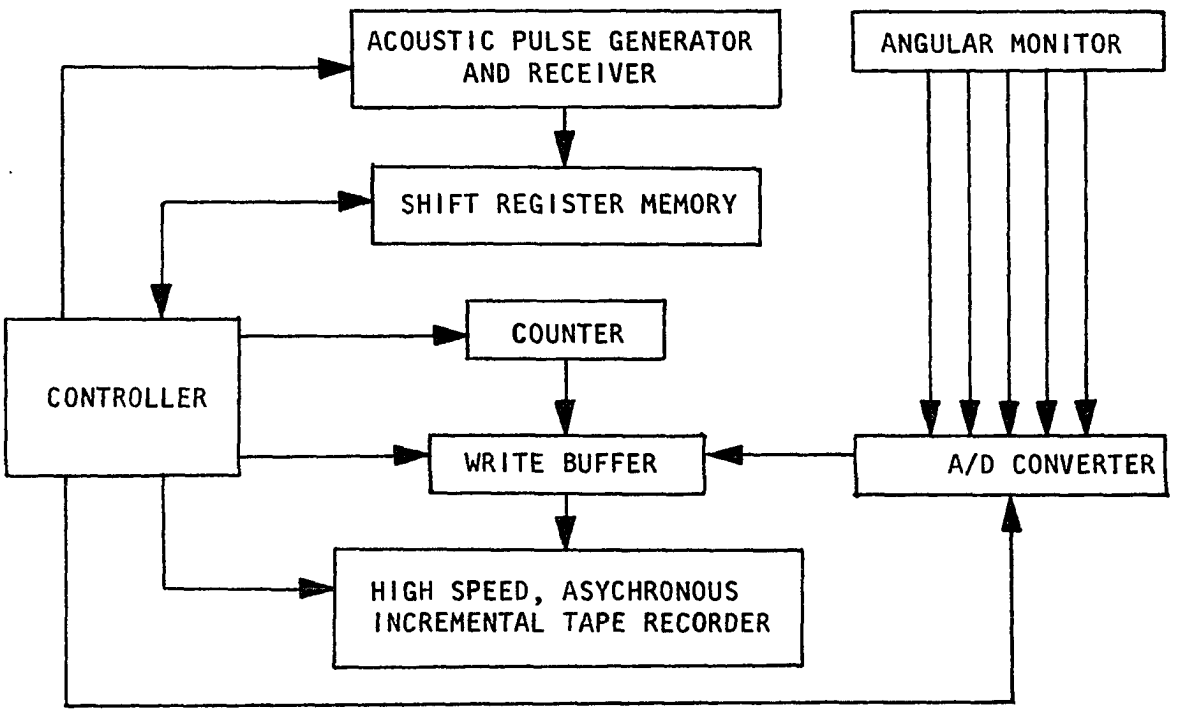

Figure 37. Block diagram of simplified system.

generator to electrically stimulate the ultrasonic transducer. At the same time, a digital shift register used for time expansion of echo pulses is driven at a high clock frequency (e.g. 5 MHz). When echo pulses appear at the receiver's output they are entered into the shift register. The acoustic pulse generator and receiver circuit could be nearly identical to Fig. 17. The high frequency clock of the shift register stops when the register is full. Then a lower frequency clock empties the shift register and drives a counter. If a pulse stored in the shift register appears at the output, the number in the counter which corresponds to the time taken for the acoustic pressure wave to reflect from a target and return is written on the IBM compatible tape recorder. This process continues until the shift register is completely emptied. A punctuation number is then recorded to indicate the end of the echos' trip-time data. The angular voltages corresponding to the transducer's direction and position are converted to digital numbers and sequentially recorded on tape. The controller then causes the acoustic generator to again stimulate the transducer and the whole process repeats. The controller also causes inter-record gaps to be recorded on tape when necessary. By this means an IBM digital data tape is generated.

Note that the high sampling rate on the receiver's output makes it possible to improve the axial resolution of the system by a factor of ten above the axial resolution of the system described in Chapter IV. Considering the cost and the simplicity of such a system, its implementation is entirely feasible.

In conclusion, the general manner of constructing ultrasonic echograms described herein shows promise of maturing C-scan diagnostic ultrasound from its present experimental state to a more significant and useful state. The basic theory which has accumulated authenticity from the similarity of Figures 12 and 23 indicates that the system's resolution is limited only by its axial resolution. Experimentally there was a definite increase in resolution due to processing.

VI. LITERATURE CITED

1. R. Warwick, J. Pond, B. Woodward and C. Connolly, IEEE Trans. on Sonics and Ultrasonics 17, 158 (1970).

2. J. A. Kennedy and R. Muenow, IEEE Trans. on Sonics and Ultrasonics 14, 47 (1967).

3. P. S. Green, in Acoustical Holography, edited by A. F. Metherell (Plenum Press, New York - London, 1971), p. 173.

4. T. G. Brown, Ultrasonics 6, 118 (1967).

5. J. Stone, IEEE Trans. on Sonics and Ultrasonics 18, 86 (1971).

6. J. R. Frederick, Ultrasonic Engineering, (John Wiley and Sons Inc., New York, 1965).

7. J. Krautkramer and H. Krautkramer, Ultrasonic Testing of Materials, (Springer - Verlag New York Inc., New York, 1969).

8. W. J. Garrett and D. E. Robinson, Ultrasound in Clinical Obstetrics, (Charles C. Thomas Publishing, Springfield, Illinois, 1970).

9. F. R. Castella, in Acoustical Holography, edited by A. F. Metherell (Plenum Press, New York - London, 1971), p. 247.

10. W. E. Kock, Electronics, 80 (Oct. 12, 1970).

11. W. M. Brown and L. J. Porcello, IEEE Spectrum, 54 (Sept., 1969).

12. G. Kossoff, D. E. Robinson and W. J. Garrett, IEEE Trans. on Sonics and Ultrasonics 12, 31 (1965).

13. D. E. Robinson, G. Kossoff and W. J. Garrett, Ultrasonics 4, 186 (1966).

14. F. L. Thurstone, IEEE Trans. on Sonics and Ultrasonics 17, 154 (1970).

15. IBM Systems Reference Library File No. 5360-25, GC 28-6515-7, Oct., 1968.

16. G. Baum, J. Acoustical S. A. 48, 1407 (1970).

17. A. J. Hall, Ultrasonics 8, 211 (1970).

18. F. L. Thurstone and W. M. McKinney, Ultrasonics 4, 25 (1966).

19. D. D. Lobdell, IEEE Trans. on Sonics and Ultrasonics 15, 202 (1968).

VII. ACKNOWLEDGEMENTS

I especially want to thank the Biomedical Engineering Program under the motivating leadership of Dr. Neal Cholvin, Professor and Chairman, for providing me with the financial assistance that made possible my doctoral studies at Iowa State University. I also wish to thank Professor David Carlson for proposing the problem and his helpful suggestions and criticisms at times of despair.

I also want to thank Gratia, my wife, who has willingly and incessantly labored at menial jobs to help support us through these times. In addition to serving as the typist for this dissertation, she has also been a constant source of motivation to me.

VIII. APPENDIX A: PROGRAM DATAIN

A. Flow Chart

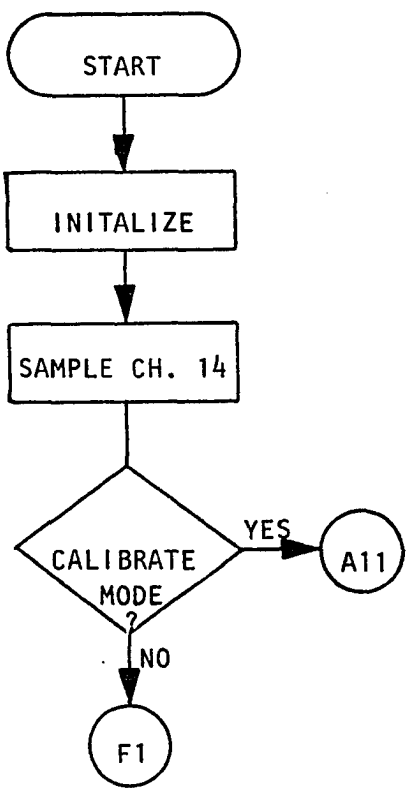

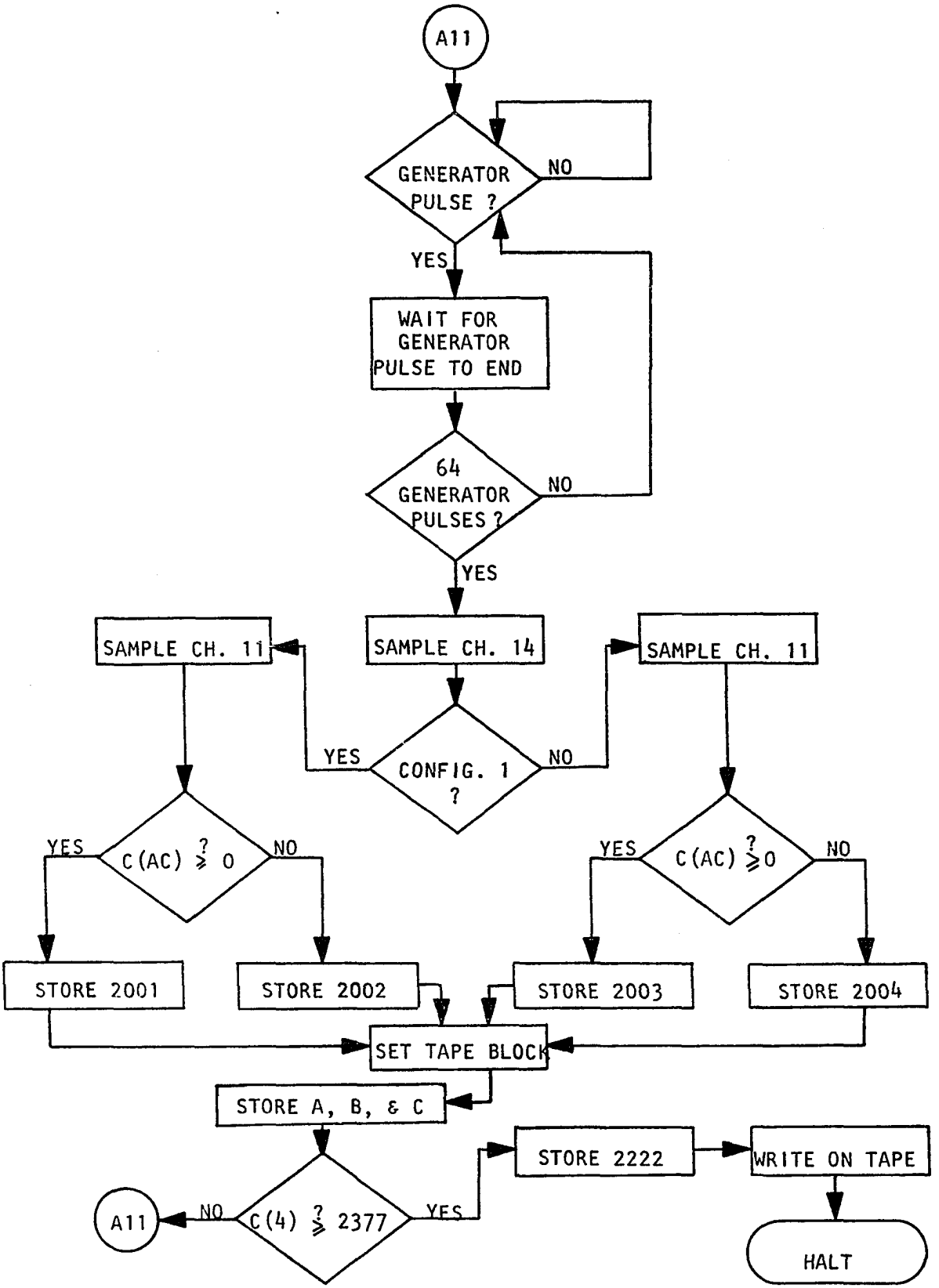
A11
GENERATOR PULSE ?
NO
YES
WAIT FOR GENERATOR PULSE TO END
64 GENERATOR PULSES ?
NO
YES
SAMPLE CH. 11
SAMPLE CH. 14
SAMPLE CH. 11
YES
CONFIG. 1 ?
NO
YES
C(AC) ≷ 0
NO
YES
C(AC) ≷ 0
NO
STORE 2001
STORE 2002
STORE 2003
STORE 2004
SET TAPE BLOCK
STORE A, B, & C
STORE 2222
WRITE ON TAPE
A11
NO
C(4) ≷ 2377
YES
HALT

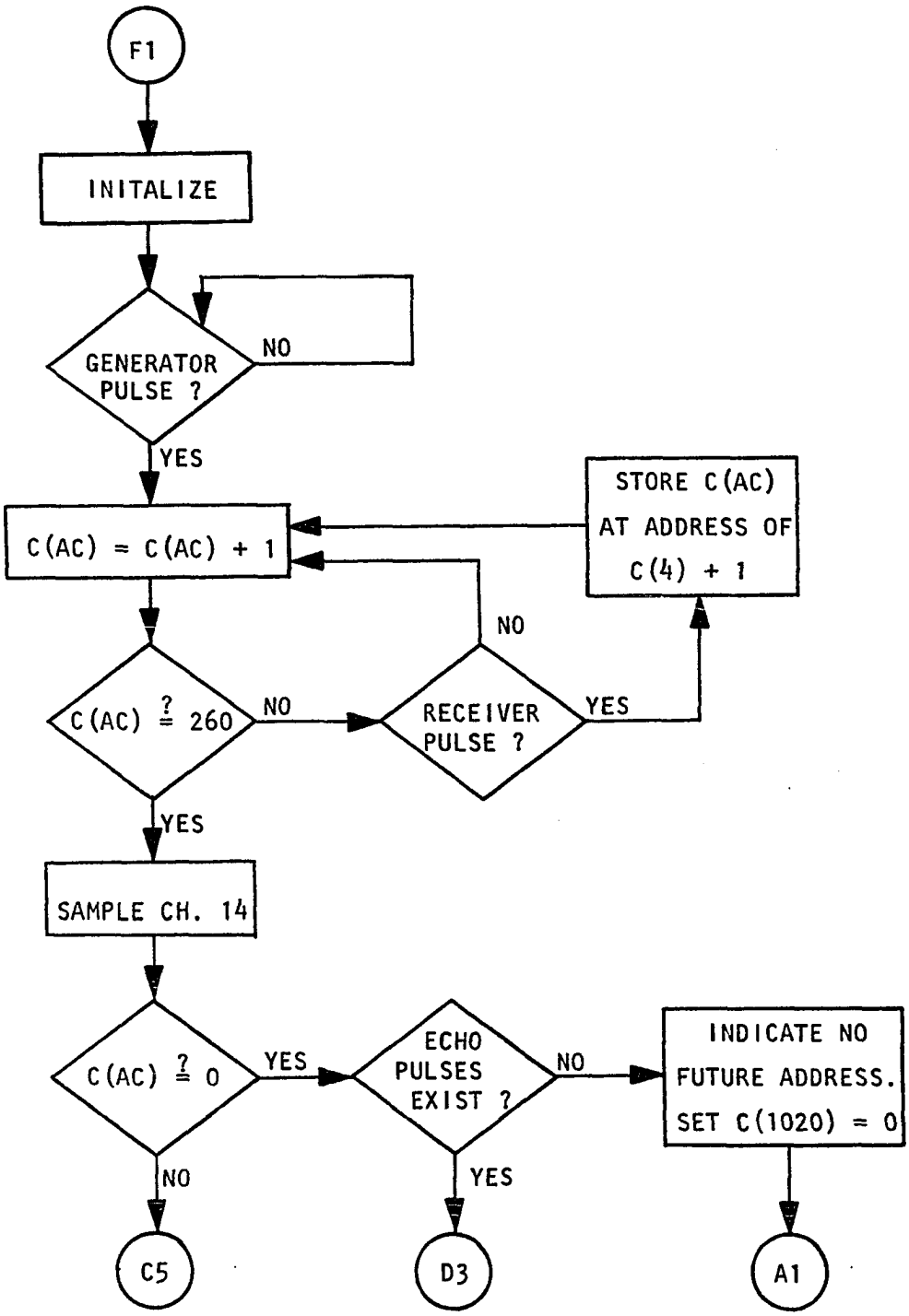
F1
INITALIZE
GENERATOR PULSE ?
NO
YES
C(AC) = C(AC) + 1
STORE C(AC) AT ADDRESS OF C(4) + 1
C(AC) ≟ 260
NO
RECEIVER PULSE ?
NO
YES
YES
SAMPLE CH. 14
C(AC) ≟ 0
YES
ECHO PULSES EXIST ?
NO
INDICATE NO FUTURE ADDRESS. SET C(1020) = 0
NO
YES
C5
D3
A1

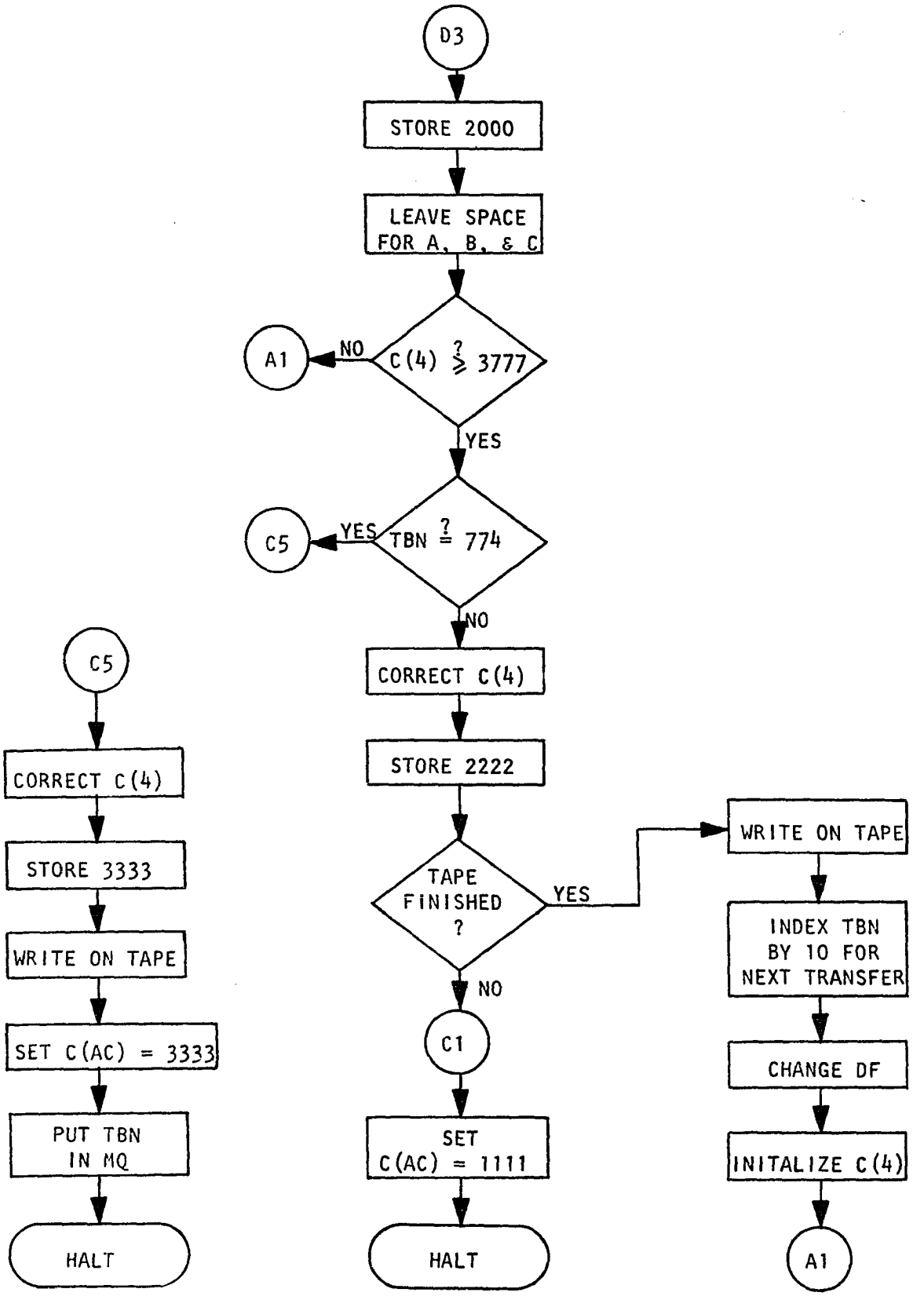
D3
STORE 2000
LEAVE SPACE FOR A, B, & C
C(4) ? ≷ 3777
NO
A1
YES
TBN ? = 774
YES
C5
NO
CORRECT C(4)
STORE 2222
TAPE FINISHED ?
YES
WRITE ON TAPE
INDEX TBN BY 10 FOR NEXT TRANSFER
CHANGE DF
INITALIZE C(4)
A1
NO
C1
SET C(AC) = 1111
HALT
C5
CORRECT C(4)
STORE 3333
WRITE ON TAPE
SET C(AC) = 3333
PUT TBN IN MQ
HALT

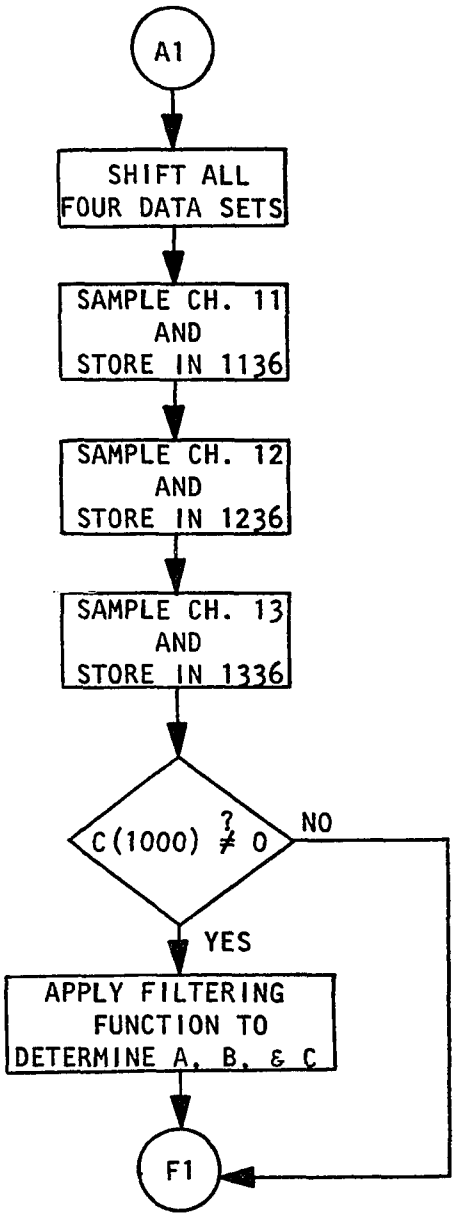
A1
SHIFT ALL FOUR DATA SETS
SAMPLE CH. 11 AND STORE IN 1136
SAMPLE CH. 12 AND STORE IN 1236
SAMPLE CH. 13 AND STORE IN 1336
C(1000) ? ≠ 0
NO
YES
APPLY FILTERING FUNCTION TO DETERMINE A, B, & C
F1

B. DATAIN Source Listing

```
/     29 FEB 72
/
          CHK U
          0004
          STD
          JMP .-1
          LDF 0
          CLR
          BSE I
          0010
          AXO
          LDA I
          3014
          STC B5
          ADD B5
          STC C3
/
/FILTER INITIALIZATION
/
          SET I 1
          -37
          LDA I
          777
          STC E5
G1,       SXL 12
          JMP .-1
          SET I 2
E5,       NOP
          CLR
          STA I 2
          LDA
          2
          ADA I
          100
          STC 2
          SAM 11
          STA 2
          LDA
          2
          ADA I
          100
          STC 2
          SAM 12
          STA 2
          LDA
          2
          ADA I
          100
          STC 2
          SAM 13
          STA 2
          LDA I
          1
          ADD E5
          STC E5
          XSK I 1
          JMP G1
/
/END OF FILTER INITIALIZATION
/
          SET I 4
          3777
          SAM 14
          BCL I
          0177
          AZE
          JMP A11
/
/SAMPLE PERIOD ON SENSE
/LINES IS APPROXIMATELY
/20 MICROSECONDS.
/
F1,       CLR
          SXL 12
          JMP .-1
          SXL 11
          JMP .-1
          LDA I
          1
          NOP
          NOP
          NOP
          NOP
          NOP
          NOP
          NOP
          NOP
          NOP
          NOP
          NOP
A6,       NOP
          NOP
```

```
        NOP
A2,     ADA I
        0001
        SAE I
C6,     260
/
/C(C6) IS THE TIME WINDOW
/FOR REFLECTIONS.  260
/CORRESPONDS TO 386 MICRO-
/SECONDS OR 290 MM DISTANT
/REFLECTING POINT.
/
        SKP
        JMP A3
        SXL 11
        JMP A6
        STA I 4
        JMP A2
A3,     SAM 14
        JMP C2
C5,     LDA I
        3
        ADD E4
        STC 4
        LDA I
        3333
        STA I 4
        STD
        JMP .-1
        WCG U
C3,     3004
        STD
        JMP .-1
        CLR
        ADD C3
        BCL I
        7000
        SCR 14
        LDA I
        3333
        HLT
C2,     BCL I
        0177
        AZE I
        JMP B1
        JMP C5
A11,    SET I 1
        -100
        SXL 12
        JMP .-1
        SET I 2
        -40
        NOP
        XSK I 2
        JMP .-2
        XSK I 1
        JMP .-10
        SAM 14
        BCL I
        0177
        APO I
        JMP B2
        SAM 11          /CONFIG 2
        APO
        JMP BB1
        LDA I
        2003
        STA I 4
        JMP B0
BB1,    LDA I
        2004
        STA I 4
        JMP B0
B2,     SAM 11          /CONFIG 1
        APO
        JMP BB2
        LDA I
        2001
        STA I 4
        JMP B0
BB2,    LDA I
        2002
        STA I 4
        JMP B0
B0,     BCL I
        7770
        STC B7
        SAM 11
        STA I 4
        SAM 12
        STA I 4
        SAM 13
        STA I 4
        CLR
        BSE I
        2372
        COM
        ADD 4
        APO
        JMP A11
```

```
        CLR
        BSE I
        2222
        STA I 4
        CLR
        BSE I
        0020
        AXO
        CLR
        TMA
        WRC U
B7,     0001
        CLR
        ADD B7
        HLT
B1,     CLR
        ADD 4
        SAE I
B4,     3777
        JMP D3
        CLR
        STC 1020
        JMP A1
D3,     LDA I
        2000
        STA I 4
        CLR
        ADD 4
        STC 1020
        STA I 4
        STA I 4
        STA I 4
        CLR
        ADD 4
        STC B4
        CLR
        BSE I
        3750
        COM
        ADD 4
        APO
        JMP A1
        CLR
        ADD B5
        SAE I
        3774
        JMP B3
        JMP C5
B3,     LDA I
        3
        ADD E4
        STC 4
        LDA I
        2222
        STA I 4
        STD
        JMP C1
        WCG U
B5,     3004
D2,     CLR
        ADA I
        0010
        ADD B5
        STC B5
        ADD B5
        STC C3
        ADD B5
        BCL I
        7767
        AZE I
        JMP .+3
        LDF 0
        JMP A7
        LDF 1
A7,     SET I 4
        3777
        LDA I
        3774
        STC E4
/
/INITIALIZE POINTER FOR
/ADDRESS.
/
        JMP A1
C1,     CLR
        BSE I
        1111
        HLT
/
/DIGITAL FILTER FOR
/ANGLES A, B, & C.
/
A1,     LDA I
        777
        STC E1
        ADD E1
        ADA I
        1
        STC E2
        LDA I
```

```
        5077
/
/EQUAL TO 1077, BUT SETS
/FRACTIONAL MULTIPLICATION.
/
        STC E3
        SET I 5
        -4
F10,    SET I 1
E1,     NOP
        SET I 2
E2,     NOP
        SET I 3
        -36
        LDA I 2
        STA I 1
        XSK I 3
        JMP .-3
        LDA I
        100
        ADD E1
        STC E1
        LDA I
        1
        ADD E1
        STC E2
        XSK I 5
        JMP F10
/
/ADDRESS INFO IS PASSED TO
/1020 WHICH IS CONTINUOUSLY
/SHIFTED TO LOCATION 1000
/BY ABOVE INSTRUCTION LIST.
/C(1000)=0 INDICATES THERE
/WERE NO REFLECTIONS.
/OTHERWISE, C(1000) IS
/ADDRESS OF ANGULAR DATA
/IN CORE FOR THAT ECHO TRAIN.
/
        SAM 11
        STC 1136
        SAM 12
        STC 1236
        SAM 13
        STC 1336
        LDA
        1000
        AZE I
        JMP F1          /RETURN
        STC E4
        SET I 13
E4,     NOP
        SET I 14
        -3
F2,     SET I 10
E3,     NOP
        CLR
        STC 1402
        STC 1403
        LDA I
        1
        MUL I 10
        JMP DBLADD
        LDA I
        2
        MUL I 10
        JMP DBLADD
        LDA I
        3
        MUL I 10
        JMP DBLADD
        LDA I
        6
        MUL I 10
        JMP DBLADD
        LDA I
        11              /9 IN
/                       DECIMAL
        MUL I 10
        JMP DBLADD
        LDA I
        16              /14
        MUL I 10
        JMP DBLADD
        LDA I
        24              /20
        MUL I 10
        JMP DBLADD
        LDA I
        32              /26
        MUL I 10
        JMP DBLADD
        LDA I
        42              /34
        MUL I 10
        JMP DBLADD
        LDA I
        52              /42
        MUL I 10
        JMP DBLADD
```

```
LDA I
63
MUL I 10
JMP DBLADD
LDA I
72
MUL I 10
JMP DBLADD
LDA I
101
MUL I 10
JMP DBLADD
LDA I
106
MUL I 10
JMP DBLADD
LDA I
111
MUL I 10
JMP DBLADD
LDA I
114
MUL I 10
JMP DBLADD
LDA I
111
MUL I 10
JMP DBLADD
LDA I
106
MUL I 10
JMP DBLADD
LDA I
101
MUL I 10
JMP DBLADD
LDA I
72
MUL I 10
JMP DBLADD
LDA I
63
MUL I 10
JMP DBLADD
LDA I
52
MUL I 10
JMP DBLADD
LDA I
42
MUL I 10
JMP DBLADD
LDA I
32
MUL I 10
JMP DBLADD
LDA I
24
MUL I 10
JMP DBLADD
LDA I
16
MUL I 10
JMP DBLADD
LDA I
11
MUL I 10
JMP DBLADD
LDA I
6
MUL I 10
JMP DBLADD
LDA I
3
MUL I 10
JMP DBLADD
LDA I
2
MUL I 10
JMP DBLADD
LDA I
1
MUL I 10
JMP DBLADD
CLR
LDA
1402
SCR 14
LDA
1403
SCR 7
/
/4*C(AC)/1024 AFTER QAC
/INSTRUCTION.
/
APO
JMP NEG
QAC
QLZ I
JMP F5
```

/51

/58

/65

/70

/73

/76

```
          ADA I
          1
          JMP F5
NEG,      CAC
          BSE I
          4000
          CLZ
          JMP F5
          ADA I
          -1
F5,       SAE I
          2000
          JMP .+3
          ADA I
          1
          SAE I
          2222
          JMP .+3
          ADA I
          1
          SAE I
          3333
          JMP .+3
          ADA I
          1
          STA I 13
          LDA I
          100
          ADD E3
          STC E3
          XSK I 14
          JMP F2
          JMP F1
/
/
          *1500
DBLADD,   STC 1401
          LDA
          0
          STA I
RETURN,   NOP
          CAC
          LZE
          COM
          STC 1400
          LDA
          1401
          SCR I 1
          STC 1401
          ADD 1400
          LZE I
          JMP .+5
          BSE I
          4000
          STC 1400
          JMP .+4
          BCL I
          4000
          STC 1400
          SET I 6
          1400
          SET I 7
          1402
          CLR
          LDA 6
          LAM 7
          LDA I 6
          LAM I 7
          STC 1404
/
/C(AC)=0, AND LINK BIT
/IS UNCHANGED.
/
          SET I 7
          1402
/RETURN   LAM 7
          STC 1404
          LAM I 7
/
/SUM IS NOW IN 1403 AND 1402
/
          CLR
          ADD RETURN
          STC 0
END,      JMP 0
```

C. Example of Data Formated by DATAIN

```
1025  0246 -0342  0167  1025  0245 -0342  0167
1025  0244 -0342  0166  1025  0246 -0342  0168
1025  0242 -0343  0164  1025  0244 -0342  0165
1025  0244 -0342  0165  1025  0244 -0342  0165
1025  0245 -0342  0167  1025  0245 -0342  0167

1026 -0220  0353 -0147  1026 -0220  0353 -0147
1026 -0220  0354 -0147  1026 -0219  0355 -0146
1026 -0220  0354 -0146  1026 -0219  0355 -0146
1026 -0221  0352 -0147  1026 -0220  0353 -0147
1026 -0220  0354 -0146  1026 -0220  0354 -0147

1027  0108 -0144 -0392  1027  0108 -0144 -0392
1027  0109 -0144 -0392  1027  0110 -0144 -0392
1027  0109 -0144 -0392  1027  0110 -0143 -0391
1027  0112 -0142 -0390  1027  0109 -0144 -0392
1027  0111 -0143 -0390  1027  0109 -0144 -0392

1028 -0087  0147  0410  1028 -0086  0148  0412
1028 -0086  0149  0413  1028 -0087  0148  0411
1028 -0088  0147  0410  1028 -0087  0148  0411
1028 -0087  0148  0412  1028 -0088  0147  0410
1028 -0088  0147  0410  1028 -0087  0147  0411

0056  0065  1024  1263 -1450  0279
0056  0060  1024  1263 -1450  0278
0056  0060  1024  1262 -1450  0278
0055  0059  0064  1024  1262 -1451  0277
0004  1024  1261 -1451  0276
0055  1024  1261 -1451  0276
0056  0060  1024  1260 -1451  0275
0056  1024  1259 -1451  0274
0056  0060  1024  1259 -1452  0274
0056  0060  1024  1259 -1452  0273
0056  0060  1024  1258 -1452  0273
0056  1024  1258 -1452  0272
0056  0060  1024  1258 -1452  0272
0056  1024  1258 -1452  0272
0056  0060  1024  1258 -1452  0272
0056  0060  1024  1258 -1452  0271
0056  1024  1258 -1452  0271
0056  0060  1024  1258 -1452  0270
0056  1024  1258 -1452  0270
0056  1024  1258 -1452  0270
0052  0056  1024  1258 -1452  0269
0052  0056  1024  1257 -1452  0269
0052  0056  1024  1257 -1452  0268
0052  0056  1024  1257 -1452  0268
```

IX. APPENDIX B: PROGRAM IBMTAP

A. Flow Chart

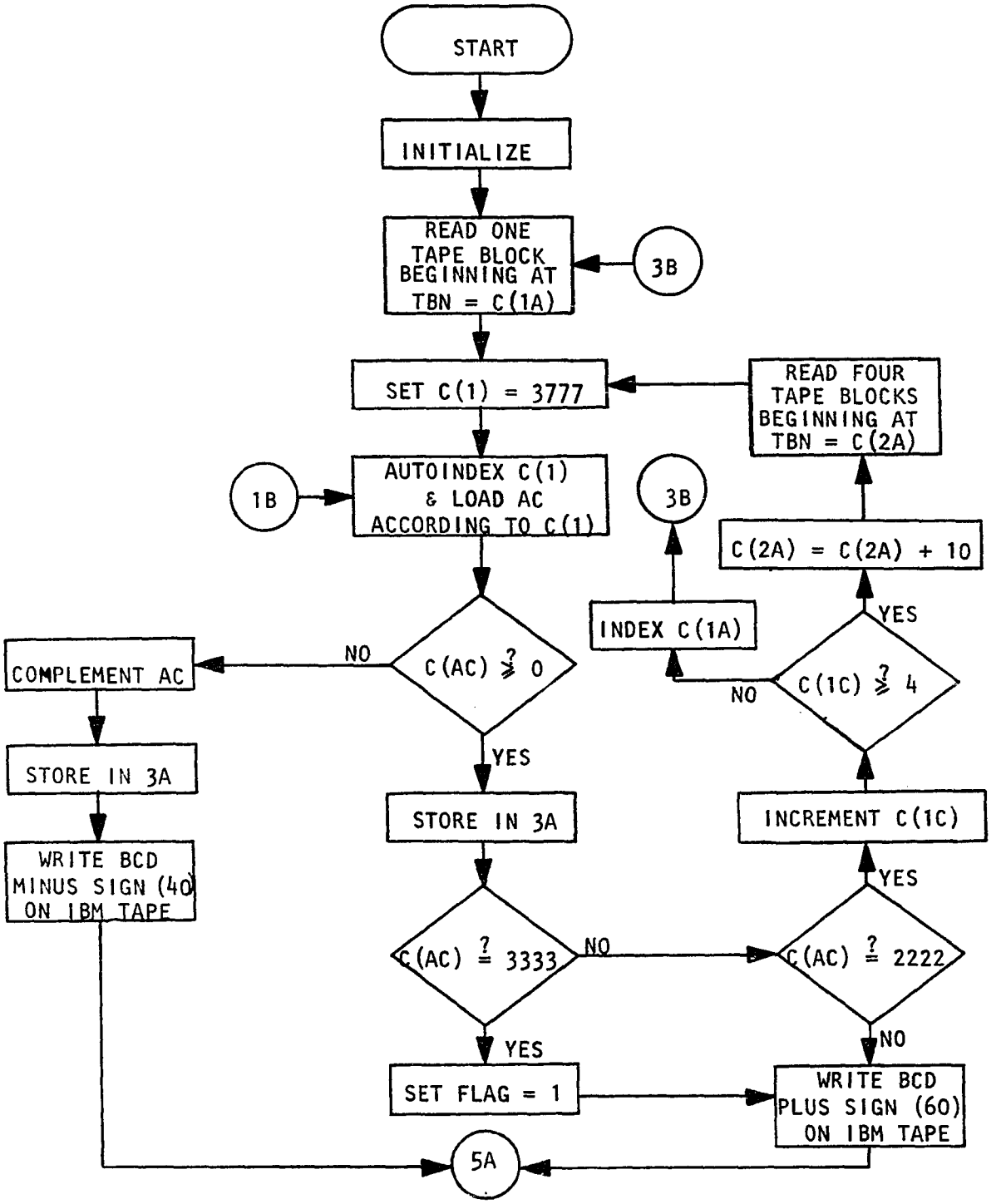

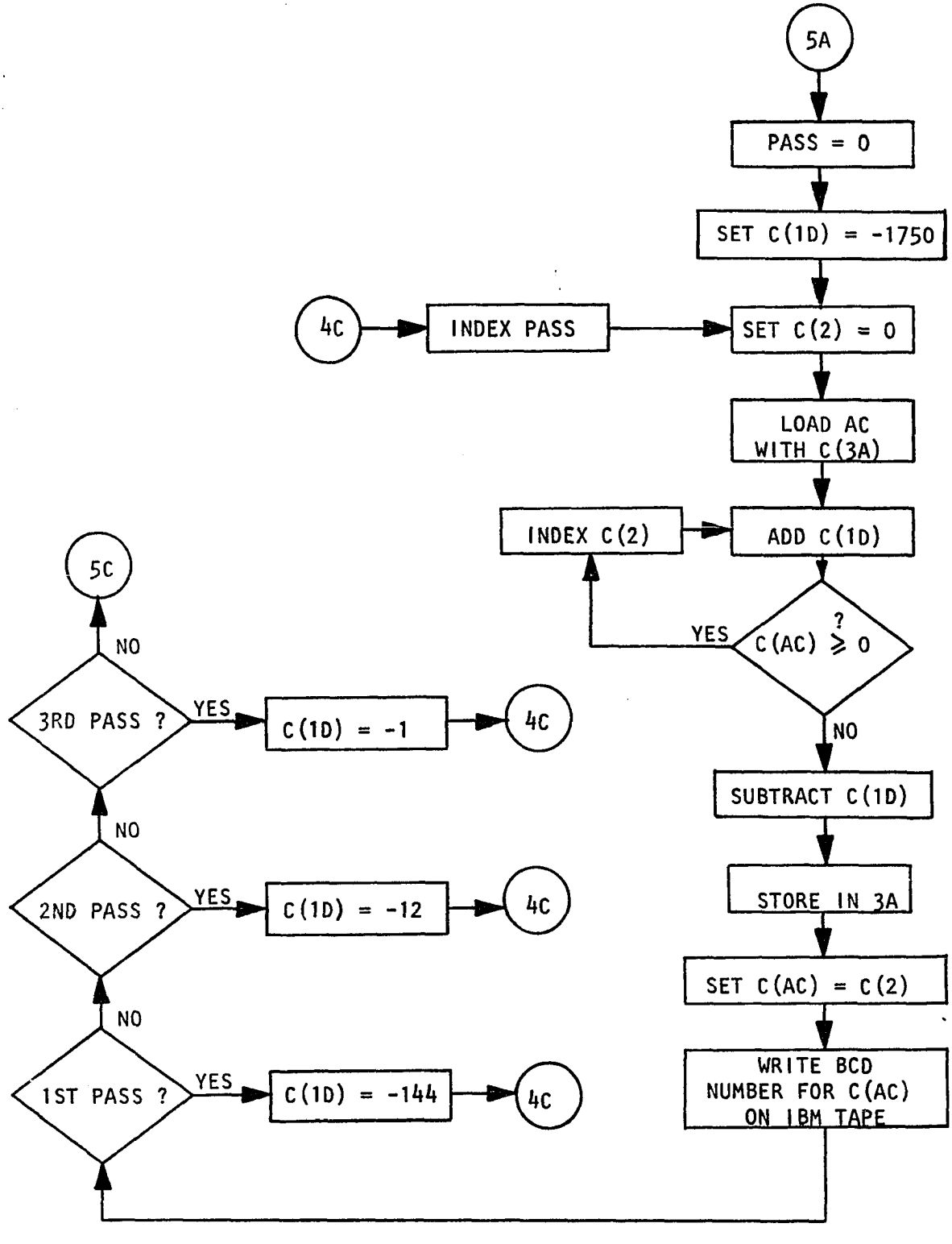
5A
PASS = 0
SET C(1D) = -1750
4C
INDEX PASS
SET C(2) = 0
LOAD AC WITH C(3A)
INDEX C(2)
ADD C(1D)
YES
C(AC) ≥ ? 0
NO
SUBTRACT C(1D)
STORE IN 3A
SET C(AC) = C(2)
WRITE BCD NUMBER FOR C(AC) ON IBM TAPE
5C
NO
3RD PASS ?
YES
C(1D) = -1
4C
NO
2ND PASS ?
YES
C(1D) = -12
4C
NO
1ST PASS ?
YES
C(1D) = -144
4C

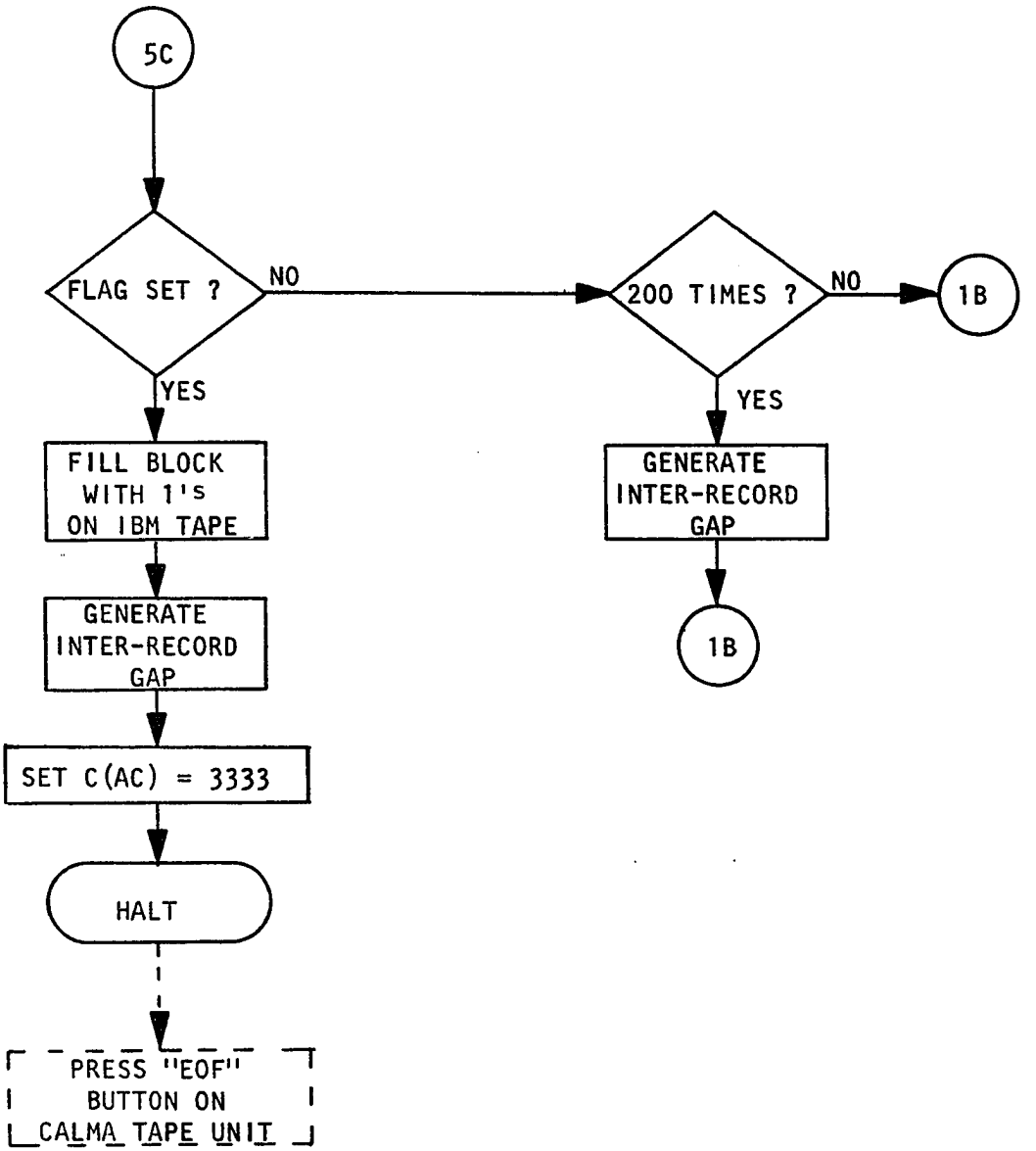
5C
FLAG SET ?
NO
200 TIMES ?
NO
1B
YES
YES
FILL BLOCK WITH 1's ON IBM TAPE
GENERATE INTER-RECORD GAP
GENERATE INTER-RECORD GAP
SET C(AC) = 3333
1B
HALT
PRESS "EOF" BUTTON ON CALMA TAPE UNIT

B. IBMTAP Source Listing

```
[ RUN ONLY WITH MODIFIED
[ PROGOFOP
[  20 JAN 1972
[ C. MEYER
[
     LDA i
     3004
     STC 2A
     LDA i
     4001
     STC 1A
     SET i 3
     -310
[-200 DECIMAL
[FORMAT 20015
     LDA i
     7777
     STC 7A
[INITIALIZE FLAG TO
[-0
     CLR
     STC 1C
#3B RDE u
#1A 4001
#2B SET i 1
     3777
#1B LDA i 1
     APO i
     JMP 4A
     COM
     STA i
#3A 0
[CONTENTS OF 3A IS
[OCTAL NUM TO BE
[CONVERTED TO DEC
     LDA i
     40
[BCD MINUS SIGN
     EXC 16
     JMP 5A
#4A STC 3A
     ADD 3A
     SAE i
     3333
     JMP 6A
     STC 3A
     LDA i
     1
     STA i
#7A 0
[FLAG TO +1
#7B LDA i
     60
[BCD CODE FOR +
     EXC 16
     JMP 5A
#6A SAE i
     2222
     JMP 7B
     LDA i
#1C 0
[PASS COUNTER OF
[MAIN ROUTINE
     ADA i
     1
     STC 1C
     ADD 1C
     BCL i
     0003
     AZE
     JMP P+6
     LDA i
     1
     ADD 1A
     STC 1A
     JMP 3B
#2D LDA i
     10
     ADD 2A
     STC 2A
     RCG u
#2A 3004
     JMP 2B
#5A CLR
[CONVERT OCTAL TO
[DECIMAL
     STC 2C
     LDA i
     -1750
     STA i
#1D 0
#3C SET i 2
     0
     CLR
     ADD 3A
     ADD 1D
     AZE i
     JMP P+3
     APO
     JMP P+3
     XSK i 2
     JMP P-6
```

```
     COM
     ADD 1D
     COM
     STC 3A
     CLR
     ADD 2
     AZE
     JMP P+3
     LDA i
     12
[BCD CODE FOR 0
     EXC 16
     LDA i
#2C  0
[PASS COUNTER OF
[CONVERTER
     AZE
     JMP P+5
     LDA i
     -144
     STC 1D
     JMP 4C
     SAE i
     1
     JMP P+5
     LDA i
     -12
     STC 1D
     JMP 4C
     SAE i
     2
     JMP 5C
     LDA i
     -1
     STC 1D
#4C  LDA i
     1
     ADD 2C
     STC 2C
     JMP 3C
#5C  CLR
     ADD 7A
     APO
     JMP 6C
     XSK i 3
     JMP P+2
     JMP P+15
     SET i 4
     -4
     LDA i
     60
[BCD CODE FOR +
     EXC 16
     LDA i
     1
[BCD CODE FOR 1
     EXC 16
     XSK i 4
     JMP P-2
     XSK i 3
     JMP P-13
     LDA i
     2000
[IRG GENERATOR
     EXC 16
     LDA i
     3333
     HLT
#6C  XSK i 3
     JMP 1B
     SET i 3
     -310
     LDA i
     2000
[IRG GENERATOR
     EXC 16
     JMP 1B
```

C. Modifications to PROGOFOP

Address	New Contents
0067	0120
0120	7200
0121	7200
0122	6701
0123	5122
0124	6171
0125	1130
0126	6706
0127	5520
0130	2000
1474	4467

X. APPENDIX C: FORTRAN PROGRAM

A. Flow Chart

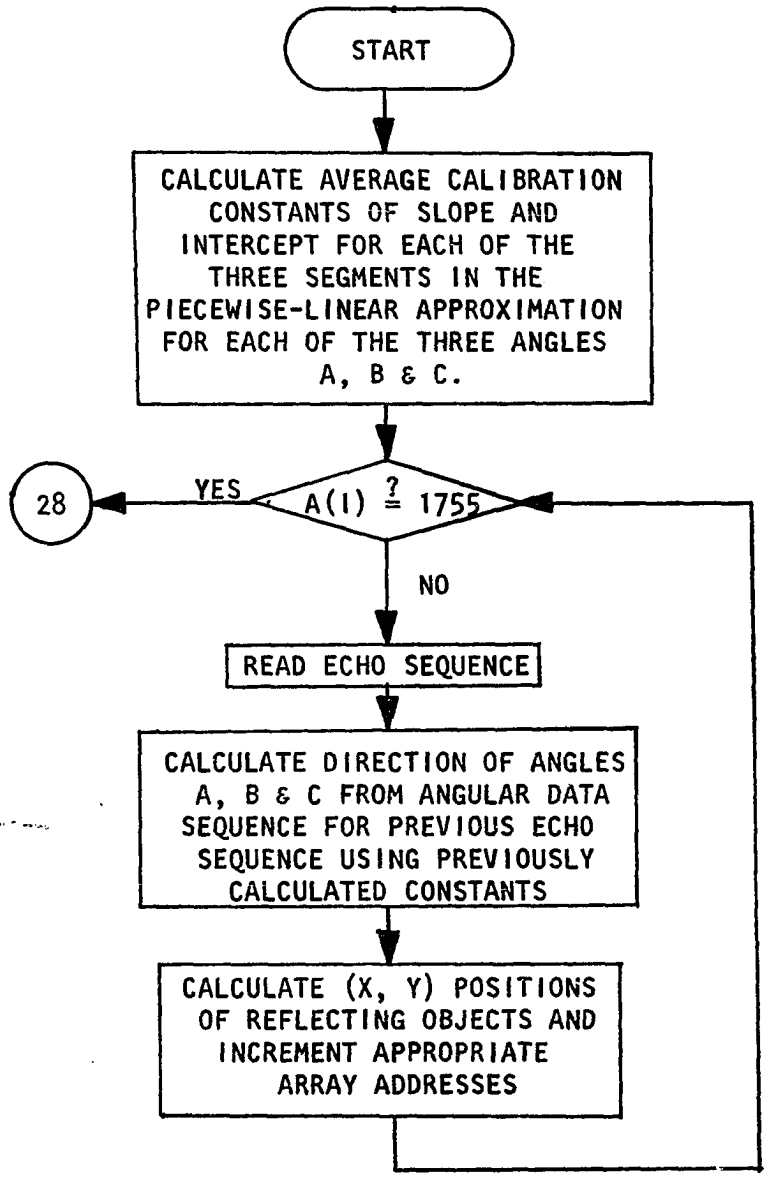

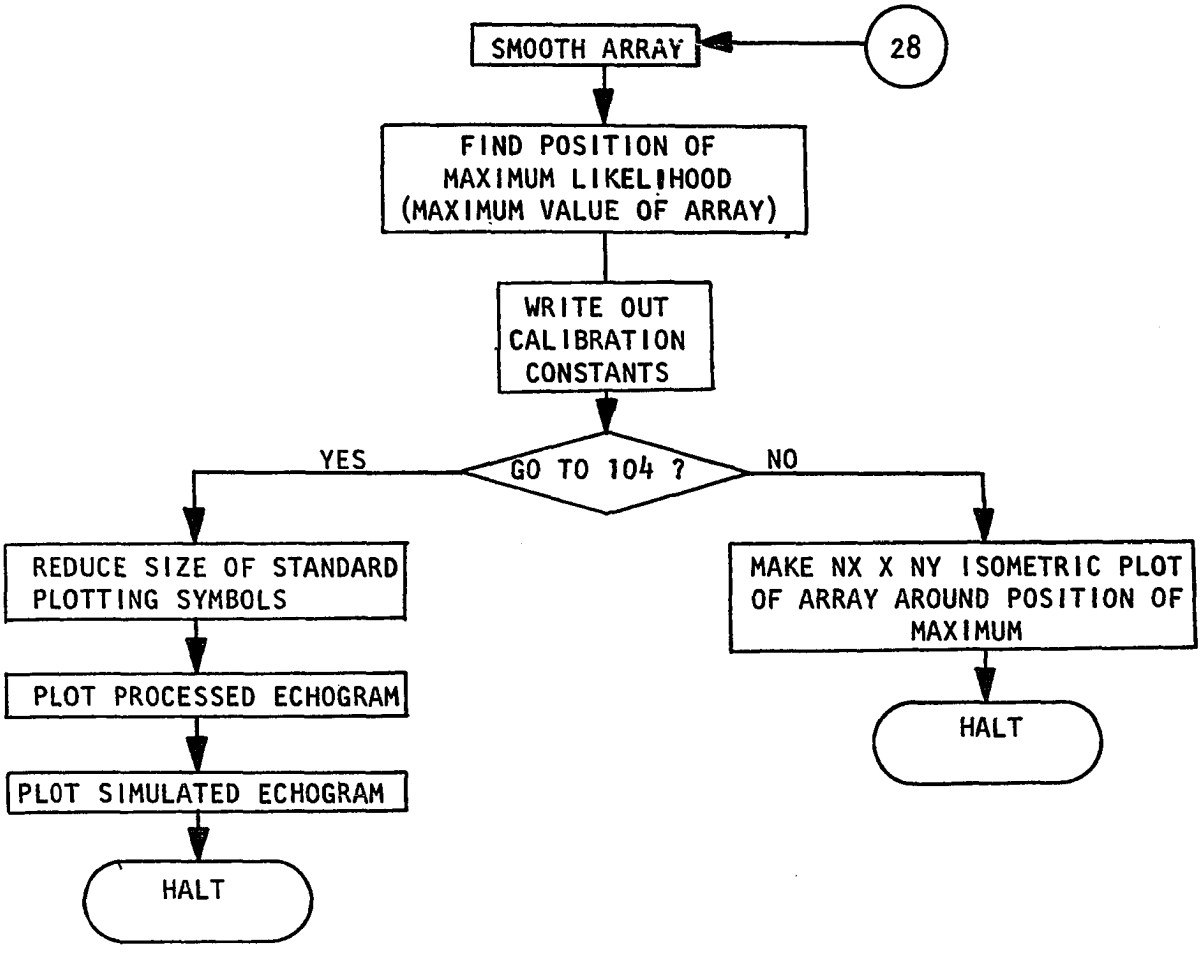
SMOOTH ARRAY
28
FIND POSITION OF MAXIMUM LIKELIHOOD (MAXIMUM VALUE OF ARRAY)
WRITE OUT CALIBRATION CONSTANTS
GO TO 104 ?
YES
NO
REDUCE SIZE OF STANDARD PLOTTING SYMBOLS
PLOT PROCESSED ECHOGRAM
PLOT SIMULATED ECHOGRAM
HALT
MAKE NX X NY ISOMETRIC PLOT OF ARRAY AROUND POSITION OF MAXIMUM
HALT

B. FORTRAN Source Listing

```
//E227MMMM JOB 'I4435,TI=6,RE=128K',CMEYER,TIME=3
//S1   EXEC  FORTG,PARM.LKED='HIAR,MAP,LIST,LET',REGION.GO=(128K,50K),   X
// TIME.GO=2,PARM.GO='PLOT ON TYPE 00 PAPER'
//FORT.SYSIN  DD  *
       COMMON ANGA , ANGB , HV , D                                          3D004
       COMMON $L , $M , $N , CX , CY , CZ , QX , QY , QZ , $D               3D005
C                                                                           3D006
      COMMON/BULK/ARRAY
      INTEGER NX/25/,NY/25/
      DIMENSION CA(25,25)
C
C                        NX AND NY MUST BE ODD AND .LT. 70 FOR RE.GO=128K
C
      INTEGER UPPER  / 100 /,  LOWER  /  1  /
      REAL ADEG/110./,  BDEG/45.0/
C                                                                           3D010
      REAL DATE(7)/7*'    '/,  PARM(11)/11*'    '/                         3D012
C                                                                           3D013
      REAL*4 M11, M12, M13, M21, M22, M23, M31, M32, M33
      REAL*4 K11, K12, K13, K21, K22, K23, K31, K32, K33
      REAL*4 CC(4,3), PI, THETAI(3)
      DIMENSION ARRAY(100,100),BB(100,100),XC(100),YC(100),SL(4)
      INTEGER*4 I,J,M,B(5),K,A(200),N(4),P,L,C(4,3),DS,IANG(3),IX,IY,
     +XMID,YMID,KONST,XMIN,XMAX,YMIN,YMAX,IANG2(3),O
      REAL*4 NN(4), DD(30), ANG(3)
      DATA PI/3.14159265359/
      DO 37 I=1,100
      DO 37 J=1,100
   37 ARRAY(I,J)=0
      DO 62 L = 1, 3
   62 IANG2(L) = 0
C
C                        DETERMINE CALIBRATION CONSTANTS
C
   91 DO 3 M=1,2
      DO 3 J=1,3
    3 C(M,J)=0.0
```

```
      B(1)=1025
      B(2)=1026
      B(3)=1027
      B(4) = 1028
      B(5)=1024
      K=1
      DO 72 I = 1, 4
   72 N(I) = 0
    4 READ (8,5) (A(P),P=1,200)
    5 FORMAT (200I5)
      I=0
    6 I=I+1
      IF (I.EQ.201) GO TO 4
      IF (A(I).EQ.B(K)) GO TO 7
      IF (A(I).EQ.B(K+1)) GO TO 8
      GO TO 6
    7 N(K)=N(K)+1
      DO 9 L=1,3
   12 I=I+1
      IF (I-201) 10,11,11
   11 READ (8,5) (A(P), P=1,200)
      I=0
      GO TO 12
   10 C(K,L)=C(K,L)+A(I)
    9 CONTINUE
      GO TO 6
    8 IF (A(I).EQ.1024) GO TO 13
      K=K+1
      GO TO 7
   13 DO 17 K=1,4
      NN(K)=N(K)
      DO 17 L=1,3
      CC(K,L)=C(K,L)
   17 CC(K,L)=CC(K,L)/NN(K)
      M11 = 35. / ( CC(1,1) - CC(3,1) )
      K11 = 60. - CC(1,1) * M11
      M12 = 50. / ( CC(3,1) - CC(4,1))
```

```
      K12 = 25. - CC(3,1) * M12
      M13 = 35. / ( CC(4,1) - CC(2,1) )
      K13 = -25. - CC(4,1) * M13
      M21 = 70. / ( CC(2,2) - CC(4,2) )
      K21 = 120. - CC(2,2) * M21
      M22 = 100. / ( CC(4,2) - CC(3,2) )
      K22 = 50. - CC(4,2) * M22
      M23 = 70. / ( CC(3,2) - CC(1,2) )
      K23 = -50. - CC(3,2) * M23
      M31 = 95. / ( CC(4,3) - CC(1,3) )
      K31 = 155. - CC(4,3) * M31
      M32 = 120. / ( CC(1,3) - CC(2,3) )
      K32 = 60. - CC(1,3) * M32
      M33 = 95. / ( CC(2,3) - CC(3,3) )
      K33 = -60. -CC(2,3) * M33
   16 READ (5,39)    KONST
   39 FORMAT ( I10)
      RKONST = KONST
   22 I=I+4
C
C                          BUILD ARRAY
C
   27 IF (A(I).EQ.1755) GO TO 28
      J=0
   29 J=J+1
      DD(J)=A(I)
      I=I+1
      IF (I.NE.201) GO TO 30
      READ (8,5) (A(P),P=1,200)
      I=1
   30 IF (A(I).NE.1024) GO TO 29
      JSET = J
      DO 31 K=1,3
      I=I+1
      IF (I.NE.201) GO TO 32
      READ (8,5) (A(P),P=1,200)
      I=1
```

```
   32 IANG(K)=A(I)
   31 CONTINUE
C
C                          IGNOR REPETITIOUS DATA
C
      IF ( IANG(1) .NE. IANG2(1) ) GO TO 61
      IF ( IANG(2) .NE. IANG2(2) ) GO TO 61
      IF ( IANG(3) .NE. IANG2(3) ) GO TO 61
      GO TO 34
   61 DO 63 L = 1,3
   63 IANG2(L) = IANG(L)
C
      DO 33 K=1,3
      ANG(K) = IANG(K)
   33 ANG(K)= ANG(K) / 4.0
      IF (ANG(1) .GT. CC(3,1))  THETA(1) = M11 * ANG(1) + K11
      IF (ANG(1) .LE. CC(3,1))  THETA(1) = M12 * ANG(1) + K12
      IF (ANG(1) .LT. CC(4,1))  THETA(1) = M13 * ANG(1) + K13
      IF (ANG(2) .GT. CC(4,2))  THETA(2) = M21 * ANG(2) + K21
      IF (ANG(2) .LE. CC(4,2))  THETA(2) = M22 * ANG(2) + K22
      IF (ANG(2) .LT. CC(3,2))  THETA(2) = M23 * ANG(2) + K23
      IF (ANG(3) .GT. CC(1,3))  THETA(3) = M31 * ANG(3) + K31
      IF (ANG(3) .LE. CC(1,3))  THETA(3) = M32 * ANG(3) + K32
      IF (ANG(3) .LT. CC(2,3))  THETA(3) = M33 * ANG(3) + K33
      DO 18 J = 1, 3
   18 THETA(J) = THETA(J)  * PI / 180.
      XONE=315. *COS(THETA(1))+315. *COS(THETA(1)+THETA(2))
     +    + 1.4 * SIN(THETA(2)) * SIN(THETA(1))
      YONE=315. *SIN(THETA(1))+315. *SIN(THETA(1)+THETA(2))
     +    - 1.4 * SIN(THETA(2)) * COS(THETA(1))
      XX=COS(THETA(1)+THETA(2)+THETA(3))
      YY=SIN(THETA(1)+THETA(2)+THETA(3))
      SLOPE = YY / XX
      DO 34 K=1,JSET
      X = ( 60.  +1.8557 * DD(K) ) * XX + XONE
      Y = ( 60.  +1.8557 * DD(K) ) * YY + YONE
      Y = Y/2.0 + 50.
```

```
      X = ( X - RKONST + 100.0 ) / 2.0
      IX=X
      RX=IX
      R=X-RX
      IF (R.LT.0.5) GO TO 35
      IX=IX+1
   35 IY=Y
      RY=IY
      R=Y-RY
      IF (R.LT.0.5) GO TO 36
      IY=IY+1
   36 CONTINUE
      IF (IX.GT. 99) GO TO 34
      IF (IX.LT.2) GO TO 34
      IF (IY.GT. 99) GO TO 34
      IF (IY.LT.2) GO TO 34
      ARRAY(IX,IY)=ARRAY(IX,IY)+1.0
   34 CONTINUE
      I=I+1
      IF (I.NE.201) GO TO 27
      READ (8,5) (A(P),P=1,200)
      I=1
      GO TO 27
C
C                          TRANSFER SLOW CORE TO FAST CORE
C
   28 DO 40 I=1,100
      DO 40 J=1,100
   40 BB(I,J)=ARRAY(I,J)
C
C                          DIGITAL FILTER
C
      K = 1
      LOWER = K + 1
      UPPER = 100 - K
      DO 56 I = LOWER, UPPER
      DO 56 J = LOWER, UPPER
```

```
      SUM = 0.0
      IMAX = I + K
      IMIN = I - K
      JMAX =  J + K
      JMIN = J - K
      DO 95 IX = IMIN, IMAX
      DO 95 IY=JMIN, JMAX
      SUM = SUM + BB(IX,IY)
   95 CONTINUE
      ARRAY(I,J) = SUM / 9.0
   56 CONTINUE
      DO 57 I = LOWER, UPPER
      DO 57 J = LOWER, UPPER
   57 BB(I,J) = ARRAY(I,J)
      DO 112 I = 3, 98
      DO 112 J = 3, 98
  112 ARRAY(I,J) = ( 8.*BB(I,J)+BB(I+1,J+1)+BB(I+1,J)+BB(I+1,J-1)
     + +BB(I,J+1)+BB(I,J-1)+BB(I-1,J+1)+BB(I-1,J)+BB(I-1,J-1)) / 16.0
      DO 107 I = 3, 98
      DO 107 J = 3, 98
  107 BB(I,J) = ARRAY(I,J)
      LOWER = 4
      UPPER = 97
   55 CONTINUE
C
C                          FIND MAXIMUM
C
      ZMAX = 0.0
      DO 41 I = LOWER, UPPER
      DO 41 J = LOWER, UPPER
      IF (BB(I,J).LT.ZMAX ) GO TO 41
      ZMAX =BB(I,J)
      XMID = I
      YMID = J
   41 CONTINUE
      XMID = 50
      YMID = 50
```

```
      IREAL = 2*XMID + KONST - 100
      JREAL = 2*(YMID - 50)
      WRITE (6,21)
   21 FORMAT (1H1)
      WRITE (6,19) M11, M12, M13, M21, M22, M23, M31, M32, M33
   19 FORMAT (1H0, E15.8,5X,E15.8,5X,E15.8)
      WRITE ( 6, 84 )
   84 FORMAT (1H0)
      WRITE (6,19) K11, K12, K13, K21, K22, K23, K31, K32, K33
      WRITE ( 6,48) IREAL, JREAL
   48 FORMAT (1H0,'PLOT CENTERED AT (', I4, ',', I4, ')' )
      GO TO 104
C
C          PREPARE TO PLOT 3-D DISPLAY OF NX X NY REGION CENTERED AT (KONST,0)
C
      IMAX = XMID + (NX-1) / 2
      IMIN = XMID - (NX-1) / 2
      IF (IMAX.GT.100) GO TO 42
      IF (IMIN.LT.  1) GO TO 43
      GO TO 44
   42 XMID = 100 - (NX-1) / 2
      GO TO 44
   43 XMID = 1 + (NX-1) / 2
   44 JMAX = YMID + (NY-1) / 2
      JMIN = YMID - (NY-1) / 2
      IF (JMAX .GT. 100) GO TO 45
      IF (JMIN .LT.  1) GO TO 46
      GO TO 47
   45 YMID = 100 - (NY-1) / 2
      GO TO 47
   46 YMID = 1 + (NY-1) / 2
   47 XMIN= 2 * (XMID - (NX-1) / 2 ) + KONST - 100
      XMAX = XMIN + 2*(NX-1)
      YMIN = 2 * (( YMID - (NY-1) / 2 ) - 50 )
      YMAX = YMIN + 2 * (NY-1)
      WRITE (6,49) XMIN, XMAX, YMIN, YMAX
   49 FORMAT (1H0,'GRAPHED REGION = ( (X,Y) |',I4,' .GE. X .LE. ',I4,
```

```
     +' , ',I4,' .GE. Y .LE. ',I4,')')
C
      DO 50 II= 1,NX
      DO 50 JJ= 1,NY
      I = II + XMID - ( (NX-1)/2 + 1 )
      J = JJ + YMID - ( (NY-1)/2 + 1 )
   50 CA(II,JJ) =BB(I,J)
C
C           FIND MINIMUM OF REGION TO BE GRAPHED
C
      ZMIN = 0.0
      DO 51 I= 1,NX
      DO 51 J= 1,NY
      IF (CA(I,J).GE. ZMIN) GO TO 51
      ZMIN =CA(I,J)
   51 CONTINUE
      WRITE (6,53) ZMAX, ZMIN
   53 FORMAT (1HO, 'GRAPHED MAXIMUM = ',F6.1, 20X, 'GRAPHED MINIMUM = ',
     +F6.1)
C
C                       CREATE INDEX MARK ON DISPLY
C
      DO 52 J=1,3
   52 CA(1,J)= ZMIN + (ZMAX - ZMIN) / 8.0
      CA(1,4) = ZMIN
C
C                       DISPLAY 3-D REGION
C
      CALL LABEL (DATE,PARM,NPARM)                                    3D014
      ANGA = ADEG * PI / 180.0                                        3D016
      ANGB = BDEG * PI / 180.0                                        3D017
      HV = 10.0                                                       3D018
      CALL THREED (CA,NX,NY,3)
      CALL ENDPLT                                                     3D030
      WRITE (6,54) DATE
   54 FORMAT (1HO, 7A4)
      STOP
```

```
  104 CONTINUE
      WRITE (6,125) ZMAX
  125 FORMAT (1HO, 'GRAPHED MAXIMUM =', F6.1 )
C
C                          REDUCE THE SIZE OF SYMBOLS TO BE PLOTTED
C
      CALL ORIGIN (  .02, 0.0, 5 )
C
C                          PICK COORDINATES TO BE PLOTTED
C
      XSF = 40.0
      YSF = XSF
      XMINA = RKONST - 100.0
      THRESH = ZMAX / 32.0
      M = 0
      L = 0
      DO 102 I = LOWER , UPPER
      DO 102 J = LOWER , UPPER
      IF ( BB(I,J) .LT. THRESH ) GO TO 102
C
C                          PLOT POINTS OF SIGNIFIGANT CREST
C
      SL(1)  = ABS( BB(I+1,J) - BB(I,J) ) + ABS( BB(I-1,J)- BB(I,J) )
     + +ABS( BB(I+2,J) - BB(I+1,J) ) + ABS( BB(I-2,J) - BB(I-1,J) )
      SL(2)  = ABS( BB(I,J+1) - BB(I,J) ) + ABS( BB(I,J-1) - BB(I,J) )
     + +ABS( BB(I,J+2) - BB(I,J+1) ) + ABS( BB(I,J-2) - BB(I,J-1) )
      SL(3) = ABS(BB(I+1,J+1)-BB(I,J))+ABS(BB(I-1,J-1)-BB(I,J))
     + +ABS(BB(I+2,J+2)-BB(I+1,J+1))+ABS(BB(I-2,J-2)-BB(I-1,J-1))
      SL(4) = ABS(BB(I-1,J+1)-BB(I,J))+ABS(BB(I+1,J-1)-BB(I,J))
     + +ABS(BB(I-2,J+2)-BB(I-1,J+1))+ABS(BB(I+2,J-2)-BB(I+1,J-1))
      SMAX = 0.0
      DO 121 NNN = 1, 4
      IF ( SL(NNN) .LT. SMAX ) GO TO 121
      SMAX = SL(NNN)
  121 CONTINUE
      IF ( SL(2) .EQ. SMAX ) GO TO 122
      IF ( SL(3) .EQ. SMAX ) GO TO 123
```

```
      IF ( SL(4) .EQ. SMAX ) GO TO 124
      IF (( BB(I,J).GT.BB(I+1,J)).AND.(BB(I,J).GT.BB(I-1,J))) GO TJ 106
      GO TO 102
  122 IF ((BB(I,J).GT.BB(I,J+1)).AND.(BB(I,J).GT.BB(I,J-1))) GO TO 106
      GO TO 102
  123 IF((BB(I,J).GT.BB(I+1,J+1)).AND.(BB(I,J).GT.BB(I-1,J-1))) GOTO 106
      GO TO 102
  124 IF((BB(I,J).GT.BB(I-1,J+1)).AND.(BB(I,J).GT.BB(I+1,J-1))) GOTO 106
      GO TO 102
  106 L = L + 1
      IF ( L .NE. 101 ) GO TO 103
      M = M + 1
      XSIZE = 0.0
      IF ( M .EQ. 1 ) XSIZE = 5.1
      CALL GRAPH ( 100,XC,YC,1 ,7,XSIZE,5.1,XSF,XMINA,YSF,-100.0,
     + 'X-AXIS, MM;', 'Y-AXIS, MM;', 'C-SCAN ECHOGRAM;', ' ;' )
      L = 1
  103 XC(L) = 2*I + KONST - 100
      YC(L) = (J-50) * 2
  102 CONTINUE
      XSIZE = 5.1
      IF ( M .NE. 0 ) XSIZE = 0.0
      CALL GRAPH (   L,XC,YC,1 ,7,XSIZE,5.1,XSF,XMINA,YSF,-100.0,
     + 'X-AXIS, MM;', 'Y-AXIS, MM;', 'C-SCAN ECHOGRAM;', ' ;' )
  105 CONTINUE
C
C                          PLOT ALL POINTS ABOVE THRESHOLD OF F
C
      M = 0
      L = 0
      DO 202 I = LOWER , UPPER
      DO 202 J = LOWER , UPPER
      IF ( BB(I,J) .LT. THRESH ) GO TO 202
  206 L = L + 1
      IF ( L .NE. 101 ) GO TO 203
      M = M + 1
      XSIZE = 0.0
```

```
      IF ( M .EQ. 1 ) XSIZE = 5.1
      CALL GRAPH ( 100,XC,YC,1 ,7,XSIZE,5.1,XSF,XMINA,YSF,-100.0,
     + 'X-AXIS, MM;', 'Y-AXIS, MM;', 'C-SCAN ECHOGRAM;', ' ;' )
      L = 1
  203 XC(L) = 2*I + KONST - 100
      YC(L) = (J-50) * 2
  202 CONTINUE
      XSIZE = 5.1
      IF ( M .NE. 0 ) XSIZE = 0.0
      CALL GRAPH (   L,XC,YC,1 ,7,XSIZE,5.1,XSF,XMINA,YSF,-100.0,
     + 'X-AXIS, MM;', 'Y-AXIS, MM;', 'C-SCAN ECHOGRAM;', ' ;' )
  205 CONTINUE
      STOP
      END
//LKED.SYSLIB DD
// DD
// DD DSN=SYS1.PLOTLIB,DISP=SHR
//LKED.SYSIN  DD  *
                          (THREED PLOTTING OBJECT DECK GOES HERE)
 HIARCHY  1,BULK
//GO.FT08F001  DD  DSNAME=PSQ.DATAIN,DISP=(OLD,KEEP),                    X
// UNIT=(TAPE7,,DEFER),VOLUME=SER=DATAIN,LABEL=(1,NL),                    X
// DCB=(LRECL=1000,RECFM=FB,BLKSIZE=1000,DEN=1,TRTCH=T)
//GO.PLOTTAPE DD DSNAME=&PLOTTP,DISP=(NEW,PASS),UNIT=(TAPE7,,DEFER),    V9/71 #4
//             VOLUME=(PRIVATE,RETAIN,SER=TPPLOT)      V.9/71 CALCOMP#5
//GO.SYSIN  DC  *
       425
//GO.FT14F001 DD DSNAME=&SM,UNIT=SYSDA,DISP=(NEW,PASS),                  SMPLT1/3
// SPACE=(800,(120,15)),DCB=(RECFM=VS,LRECL=796,BLKSIZE=800)             SMPLT2/3
//SMPLTTR EXEC PLOT,PLOTTER=INCRMNTL
```

XI. APPENDIX D: DROOP EQUATIONS FOR TRANSDUCER'S SUPPORTING ARM

The rotational torque applied to the arm's first section along its long axis is responsible for the rotation, ψ, of that section. The force of gravity acting on the combined mass of Section 2 and the transducer acting at the center of gravity, C_g, produces the torque T.

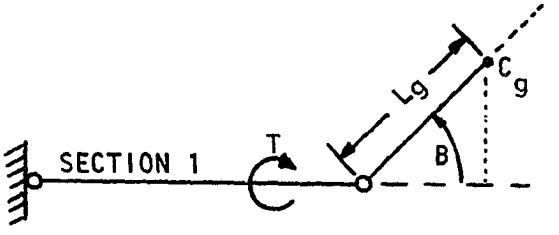

Figure 38. Torque applied on first section by remainder of supporting arm.

Thus $$T = k_1 \text{ SIN } B$$

From Young's Law $$\psi = k_2 T = k_3 \text{ SIN } B \qquad (15)$$

Figure 39 shows the major effect of the angular rotation of the first section on the long pin of angle C. Note that the bottom of the pin is not located below the upper pivot as assumed by equation (10) and (11). A top view of the arm's configuration as shown in Fig. 40 is helpful in determining the actual position of the bottom of the pin with respect to its assumed position.

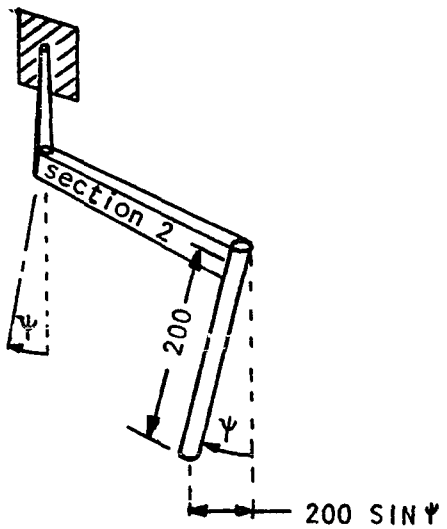

Figure 39. Effect of droop on the pin of angle C.

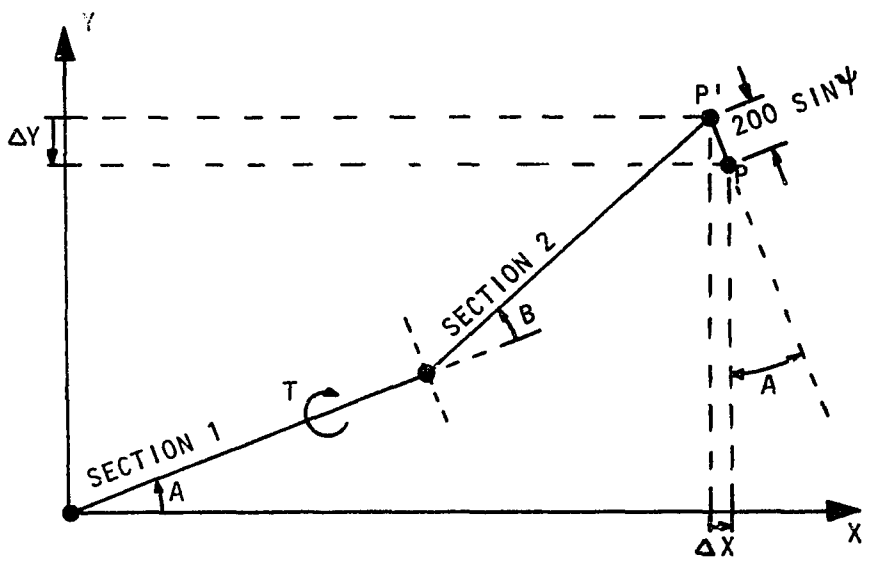

Figure 40. Top view of transducer's supporting arm.

Then $$\Delta X = 200 \text{ SIN } \psi \text{ SIN A} \quad (16)$$

$$\Delta Y = -200 \text{ SIN } \psi \text{ COS A} \quad (17)$$

where $$P_x = P'_x + \Delta X$$

and $$P_y = P'_y + \Delta Y$$

where P is the actual location of the bottom of the pin and P' is the assumed position.

Using (15), (16), and (17)

$$\Delta X = 200 \text{ SIN } (k_3 \text{ SIN B}) \text{ SIN A} \quad (18)$$

$$\Delta Y = -200 \text{ SIN } (k_3 \text{ SIN B}) \text{ COS A} \quad (19)$$

The constant, k_3, is easily determined experimentally. For example, in the following configuration ΔY was measured to be -1.0 mm while A = -45° and B = 90°.

Thus $$-1.0 = -200 \text{ SIN } (k_3) \text{ COS } (-45°)$$

$$\frac{2}{200\sqrt{2}} = \text{SIN } k_3$$

$$0.007 = \text{SIN } k_3$$

Using the fact that the sine of a small angle is equal to that angle

$$k_3 = .007$$

and similarly from (18) and (19)

$$\Delta X = 1.4 \text{ SIN B SIN A}$$

$$\Delta Y = -1.4 \text{ SIN B COS A}$$

Now by adding ΔX to the right side of equation (10) and ΔY to the right side of equation (11) the errors of the supporting arm's droop are compensated.